Earth-Science Reviews 203 (2020) 103145

Contents lists available at ScienceDirect

Earth-Science Reviews

journal homepage: www.elsevier.com/locate/earscirev

Fjords as Aquatic Critical Zones (ACZs)

Thomas S. Bianchi[a,*], Sandra Arndt[b], William E.N. Austin[c,m], Douglas I. Benn[c], Sebastien Bertrand[d], Xingqian Cui[e], Johan C. Faust[f], Katarzyna Koziorowska-Makuch[g], Christopher M. Moy[h], Candida Savage[i,j], Craig Smeaton[c], Richard W. Smith[k], Jaia Syvitski[l]

[a] Department of Geological Sciences, University of Florida, Gainesville, FL 32611-2120, USA
[b] BGeoSys, Department of Geosciences, Environment and Society, Université Libre de Bruxelles, Brussels, Belgium
[c] School of Geography and Sustainable Development, University of St. Andrews, St. Andrews KY16 9AL, UK
[d] Renard Centre of Marine Geology, Ghent University, Krijgslaan 281 S8, 9000 Gent, Belgium
[e] Department of Earth, Atmospheric, and Planetary Sciences, Massachusetts Institute of Technology, Cambridge, MA, USA
[f] School of Earth and Environment, The University of Leeds, LS2 9JT Leeds, UK
[g] Institute of Oceanology Polish Academy of Sciences, ul. Powstańców Warszawy 55, Sopot, Poland
[h] Department of Geology, University of Otago, PO Box 56, Dunedin 9054, New Zealand
[i] Department of Marine Science, University of Otago, Dunedin, New Zealand
[j] Department of Biological Sciences, Marine Research Institute, University of Cape Town, South Africa
[k] Global Aquatic Research LLC, Sodus, New York 14551, USA
[l] CSDMS Integration Facility, INSTAAR, University of Colorado, Boulder, CO 80309-0545, USA
[m] Scottish Association for Marine Science, Scottish Marine Institute, Oban PA37 1QA, UK

A B S T R A C T

In recent decades, the land-ocean aquatic continuum, commonly defined as the interface, or transition zone, between terrestrial ecosystems and the open ocean, has undergone dramatic changes. On-going work has stressed the importance of treating Aquatic Critical Zones (ACZs) as a sensitive system needing intensive investigation. Here, we discuss fjords as an ACZ in the context of sedimentological, geochemical, and climatic impacts. These diverse physical features of fjords are key in controlling the sources, transport, and burial of organic matter in the modern era and over the Holocene. High sediment accumulation rates in fjord sediments allow for high-resolution records of past climate and environmental change where multiple proxies can be applied to fjord sediments that focus on either marine or terrestrial-derived components.

Humans through land-use change and climatic stressors are having an impact on the larger carbon stores in fjords. Sediment delivery whether from accelerating erosion (e.g. mining, deforestation, road building, agriculture) or from sequestration of fluvial sediment behind dams has been seriously altered in the Anthropocene. Climate change affecting rainfall and river discharge into fjords will impact the thickness and extent of the low-salinity layer in the upper reaches of the fjord, slowing the rate of the overturning circulation and deep-water renewal – thereby impacting bottom water oxygen concentrations.

1. Introduction

Anthropogenic activity began to rapidly and expansively change the environment during the global Industrial Revolution (~1850 CE) and greatly intensified during the "Great Acceleration" (~1950 CE). These changes led to the general concept of the Anthropocene (Crutzen and Stoermer, 2000), which has received scrutiny in recent years (e.g., Carrington, 2016). How has this dramatic alteration of our planet surface, recently referred to as Anthroturbation (Zalasiewicz et al., 2014), coupled with climate change affected the biogeochemical gradients and abilities of organisms to adapt in the biosphere? On-going work has stressed the importance of treating Aquatic Critical Zones (ACZs) as a sensitive system needing intensive investigation (Bianchi and Morrison, 2018). Here, ACZs, as the topic of this review, are defined as the land-ocean interfaces where crucial geological, chemical, biological and physical processes operate together to sustain systematic functionalities of aquatic systems.

Of these ACZs, fjords, as a type of system mainly distributed in the mid-high latitudes, receive considerable attention, due to their high vulnerability to anthropogenic pressure and increasing evidence of Holocene climate fluctuations (Shindell et al., 1999; Rysgaard et al., 2003; Iriarte et al., 2010). Fortunately, progressive work in the past decades has allowed us to gather a good understanding of the morphological and sedimentological aspects of fjords (Syvitski et al., 1987). In recent years, geochemical analysis of the sediments and overlying water column has provided us with a better understanding of their significance and contribution to global carbon cycling and climate. Observations suggest that, across all aquatic systems, Fjords represent

* Corresponding author.
E-mail address: tbianchi@ufl.edu (T.S. Bianchi).

https://doi.org/10.1016/j.earscirev.2020.103145
Received 28 August 2019; Received in revised form 3 February 2020; Accepted 27 February 2020
Available online 02 March 2020

carbon cycle hotspots that bury the largest amount of organic carbon per unit area in the world, which makes them a crucial ecosystem in regulating carbon cycle over time (e.g., Smith et al., 2015).

Under suitable conditions, particularly where the effects of sediment bioturbation (Berger and Heath, 1968; Peng et al., 1977; Schiffelbein, 1984; Boudreau, 1998) is minimized, fjord sediment cores have been successfully used to generate high-resolution palaeoclimate records, with temporal resolution reaching sub-decadal scales (e.g. Mikalsen et al., 2001; Faust et al., 2014b). These optimal records are an important archive for evaluating the nature of past changes and allow us to evaluate how fjords have been driven or regulated by climate and environmental changes (e.g. Cage and Austin, 2010; Faust et al., 2016). However, as we discuss in Section 2, large-scale processes (e.g. slumping, turbidity flows) as well as sediment resuspension and bioturbation, can all act to reduce the temporal resolution and should be carefully taken into account when interpreting fjord sediment records.

Fjords lie at the nexus of terrestrial, cryospheric, oceanic and atmospheric interactions within the Earth system and are particularly sensitive to climate change. As such, processes operating within a fjord can furnish significant insight into how the system may respond to environmental forces. For example, fjord records can provide insight into the global or hemispheric-scale mechanisms influencing regional climate change. These records also provide critical context and perspective that can link the changes we observe today, such as polar amplification in Arctic fjords, with the long-term background and range of variability recorded in the geologic record.

Here, we will mainly review in detail three subjects, which include the sedimentological, geochemical, and climatic impacts on fjords. We first discuss the geomorphogenetic characteristics of these systems, how they vary across latitudes, and what impacts they have on water circulation parameters. We then link these physical features to the sources, transport, and burial of organic matter in the modern era and over the Holocene. Finally, we explore how these systems have been impacted by humans through land-use change and climatic stressors and offer some guidance for the management of these - albeit spatially-limited systems, that provide important carbon stores for the planet.

2. Geomorphogenetic and biogeochemical features of fjords

2.1. Formation, geomorphology, and sediment dynamics

2.1.1. Definition

The terms fjord, fiord, fjorthr, loch, and lough apply to deep, mid-high latitude estuaries that have been/are presently being excavated or modified by land-based glacial ice; a subset being shallower, temperate-zone estuaries called fjords (Syvitski et al., 1987; Perillo, 1995). All fjord systems around the world were formed by glacial carving at zones of geological weakness in the crust (e.g. faults), notwithstanding river valleys that eventually became glaciated in the Pleistocene and therefore, have the same essential characteristics. They are sea drowned trough-shaped valleys in latitudes higher than 40 degrees (e.g., Farmer and Freeland, 1983; Syvitski et al., 1987). Principal fjord provinces occur along the coasts of North and South America (above 42° latitude); many sub-Antarctic islands including the Kerguelen Islands and South Georgia, the Russian and Canadian Arctic Archipelagos, Svalbard and other high latitude islands; the southwest coast of New Zealand's South Island; Antarctica; Iceland and Greenland; and northern Europe, including the west coast of Scotland (Syvitski et al., 1987; Cottier et al., 2010) (Fig. 1).

2.1.2. General characteristics

Fjords are immature, non-steady-state systems, evolving and changing over relatively short time scales; sites of net sediment accumulation; and predominantly features of mountainous regions (Fig. 2). They are often long, narrow, deep, and steep-sided inlets, frequently branched and sinuous, but sometimes remarkably straight where an ice flow once followed a major fault. Fjords are the deepest of all estuaries, and may contain one or more submarine sills, which determine many of their distinctive physical and biogeochemical characteristics (Freeland et al., 1980; Perillo, 1995), and are efficient sediment traps because of these characteristics. Fjords elongate the transition regions between the land and open ocean, through a series of strong physical and chemical gradients where fresh and salt waters mix and interact, resulting in a “fjord-type” stratified circulation (Inall et al., 2015; Fraser et al., 2018) and marked physical and biogeochemical vertical gradients (e.g. Austin and Inall, 2002) (Fig. 2). Fjord two-layer circulation is one of the four dominant styles of estuarine circulation, creating high levels of water column stratification (buoyancy set up by inflowing fresh water being more important than tidal mixing processes), and a surface velocity driven by water discharge - where interfacial mixing results in an increased advective component of the landward salt flux (Hansen and Rattray Jr, 1966; Gillibrand et al., 2005; Skarðhamar and Svendsen, 2010). Parameters affecting fjord circulation, sedimentation, biogeochemistry, and biota are diverse (Syvitski et al., 1987; Howe et al., 2010) and can be characterized with certain end-member features (Table 1). The different fjord end-members are differentially in part, controlled by the following dominant physical drivers: (1) glacier dynamics (wet or cold based; floating or tidewater or terrestrial; variations in ice terminus position; sea level history); (2) freshwater delivery of bed load, suspended and dissolved loads; (3) weather and climate: ice-sheet dynamics, sea-ice conditions, thermal stratification, wind events (waves, upwelling, and aeolian transport), terrestrial and marine biomass production; (4) oceanography: 3-dimensional circulation constrained by bottom topography and fluid stratification, and as affected by boundary conditions - discharge, fetch, tides, episodic seiches, internal waves, surface waves and offshore swells, Coriolis effect, shelf-fjord exchanges including deep-water flushing, sea ice dynamics and shelf exchange, ice terminus and icebergs; and (5) slope instabilities: frequency and mass of slope failures (subaerial and submarine) and subsequent gravity flows.

2.1.3. Tidewater glaciers and fjords

The characteristic morphology of fjords is the product of erosion by outlet glaciers over multiple late-Cenozoic glacial cycles. Glacial erosion rates depend on several factors, especially ice velocity, the shear stress at the base of the ice, and substrate properties (Benn and Evans, 2010); the deepest glacial erosion therefore typically occurs in areas of flow acceleration (e.g. down-flow of ice confluences) and where bedrock is weak and well-jointed. Along-flow variations in erosion rates mean that many fjords consist of over-deepened basins separated by shallow sills.

Twenty-five percent of world's fjords currently contain marine-terminating or tidewater glaciers (Syvitski and Shaw, 1995). Flow speeds are very variable depending on climate and catchment characteristics, with the highest velocities occurring in areas of high snowfall, and where ice from large catchments is focused into narrow outlets. Fjord-glacier velocities range from 0.06 km y^{-1} for the Coronation glacier draining the Penny Ice Cap on Baffin Island, to 0.2–0.4 km y^{-1} for Muir glacier in Alaska, to ~1 km y^{-1} for Jorge Montt glacier in Patagonia (Rivera et al., 2012; Moffat, 2014), and over 10 km y^{-1} for Jakobshavn glacier in W. Greenland (Joughin et al., 2014).

Tidewater glaciers terminate in ice cliffs where they lose mass by melting below the waterline (subaqueous melt) and the breakaway of icebergs (calving), collectively known as frontal ablation. In most environments, tidewater glaciers also lose mass by subaerial melting, in the same way as land-terminating glaciers lose mass (Pfeffer, 2007). Subaqueous melt rates depend on fjord-water temperature and tangential water velocities across the submerged ice face, and are particularly high where warm fjord water is entrained by plumes of buoyant meltwater emerging from beneath the ice (Jenkins, 2011; Moffat, 2014; Cowton et al., 2015; Truffer and Motyka, 2016; Khazendar et al., 2019). Melt rates are difficult to determine, but heat budget analyses show that

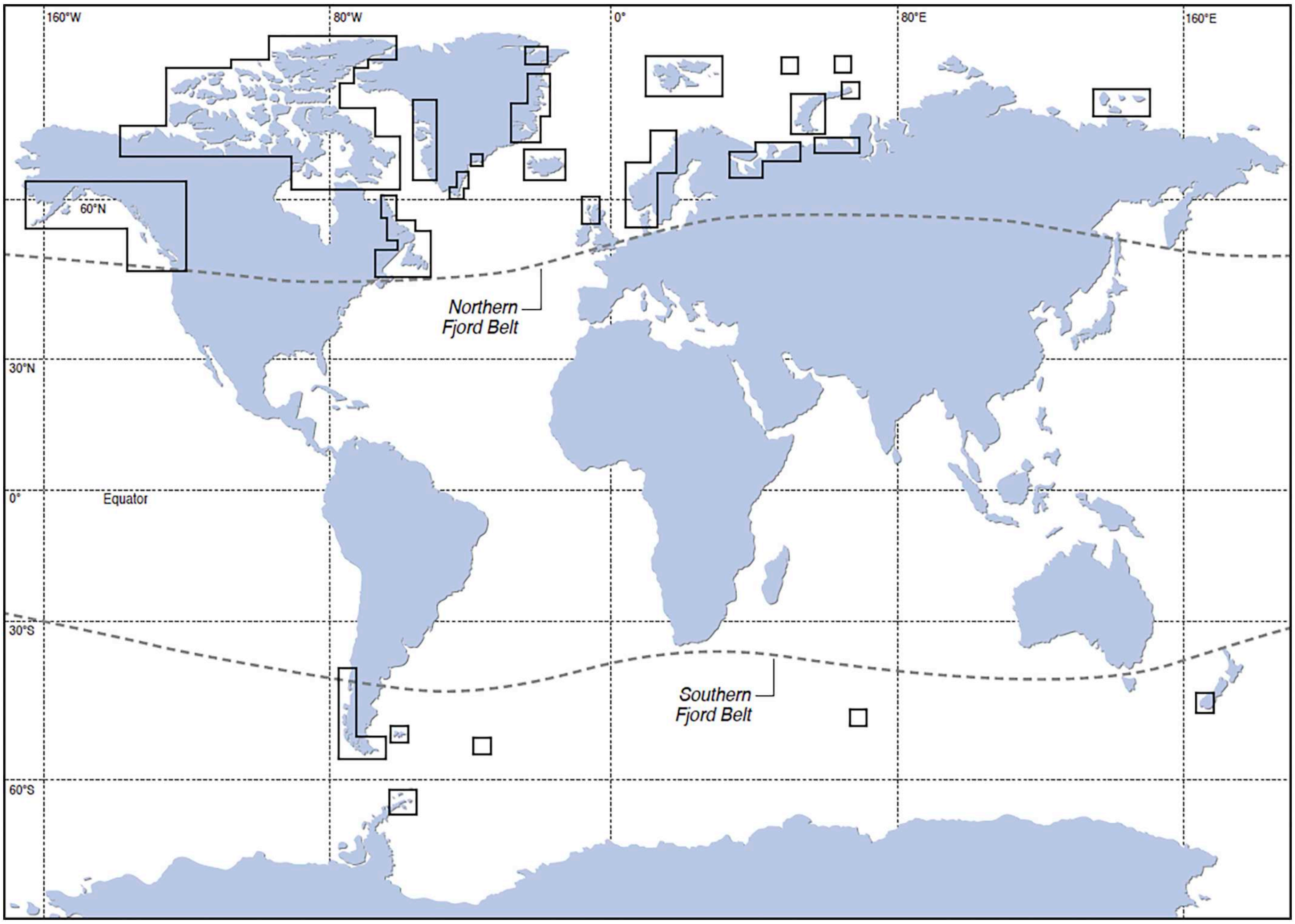

Fig. 1. Global distribution of fjords.

horizontal melt rates may be several meters per day in temperate fjords during the summer months (Rignot et al., 2010; Bartholomaus and Larsen, 2013; Motyka et al., 2013).

Iceberg calving in fjords occurs in response to two main factors. First, terminus instability is encouraged by a down-flow reduction in resistance from the glacier bed or sidewalls (Benn et al., 2007; Benn and Åström, 2018). Consequently, calving is encouraged in locations where glaciers flow into deeper water or by a wider reach of a fjord. Second, subaqueous melting can undermine the subaerial parts of terminal ice cliffs, causing them to collapse (Truffer and Motyka, 2016; How et al., 2019). Importantly, calving events triggered by melt-undercutting may be larger than the melted cavity itself; through this ‘multiplier effect’, calving rates may be several times the subaqueous melt rate (O'Leary and Christoffersen, 2013; Benn and Åström, 2018). At individual glaciers, frontal ablation may occur by a combination of terminus instability and melt-undercutting (e.g., Medrzycka et al., 2016), although in many regions melt-undercutting is the dominant process (Bartholomaus and Larsen, 2013; Luckman et al., 2015).

Changes in the terminus positions of tidewater glaciers (advance and retreat) are governed by the balance between ice velocity and frontal ablation rates. Because calving rates are affected by fjord depth and width, calving losses are lowest where fjords are narrow and/or shallow (Carr et al., 2014). Consequently, glacier termini tend to stabilize at such locations, known as pinning points. In contrast, tidewater glaciers may retreat very rapidly through over-deepening, at rates of several km yr^{-1}. Fjord bathymetry and topography thus exert a strong control over the response of tidewater glaciers to climate change. An initial signal (e.g., an increase in atmospheric or ocean temperatures) may initially have little effect on frontal position if the glacier is located at a pinning point. If contact with the pinning point is lost, however, calving rates can increase rapidly and the glacier can undergo rapid retreat until the front re-stabilizes at the next pinning point. Well-documented examples include Columbia Glacier, Alaska (O'Neel et al., 2005), Marinelli glacier, southern Patagonia (Koppes et al., 2009), and Helheim Glacier, E. Greenland (Howat et al., 2005). The dependence of frontal ablation rates on fjord characteristics means that populations of tidewater glaciers can exhibit asynchronous, non-linear responses to regional climatic or oceanographic signals (Larsen et al., 2016; Motyka et al., 2017).

Glaciers also affect fjords through their impact on local sea-level change. Loss of glacier ice increases mean global sea level by adding mass to the oceans, but within glacierized regions this is typically more than offset by the effect of isostatic rebound. Uplift (and relative sea-level fall) may continue for millennia following deglaciation; consequently, local sea levels are still falling relative to the land along many fjord-head environments in Baffin Island, Labrador, and Norway, while global sea level is presently rising. Because ice loading decreases from the center of an ice mass toward the periphery, there may be significant (10–30 m) differences between post-glacial uplift experienced at the head of a fjord and its outer coast (Overeem and Syvitski, 2010).

2.1.4. The sediment fill of fjords

Being the deepest of all nearshore environments (up to 1300 m), fjords can acquire great thicknesses (up to 800 m) of unconsolidated Late Quaternary sediments (Fig. 3). Such extreme water depths so close to land, point to the erosive power of glaciers that carved the fjords. The

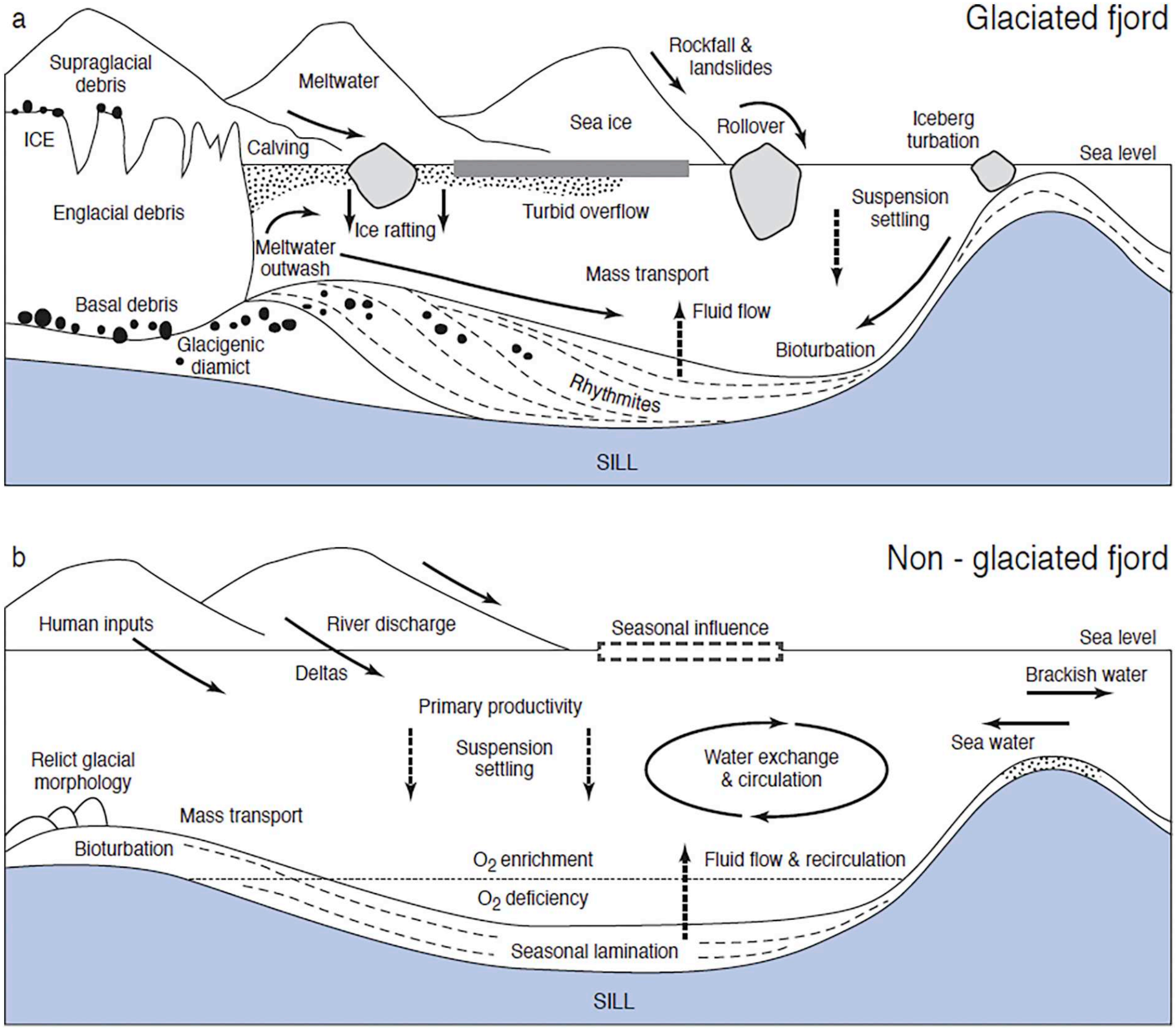

Fig. 2. Principle physical processes within fjord (adapted from Howe, 2010). (a) Glaciated fjords) and (b) Non-glaciated fjords.

Table 1
Characterization of fjord-end-members (see, Syvitski et al., 1987; Howe et al., 2010).

Fjord End-members	Regions	References
High sedimentation fjords with particulates settling through a density-stabilized water column	Knight and Bute Inlets, British Columbia	Farrow et al., 1983; Syvitski et al., 1985
Low sedimentation fjords where detritus settles through intermittently stratified water	Bedford Basin, Nova Scotia	Syvitski et al. (1995)
Well-mixed fjords where circulation is dominated by tide and wave action	Pelorus Sound, New Zealand	Carter, 1976, Makkovik Bay, Labrador: Piper et al., 1983
Polar fjords subject to periglacial processes on land, and influenced by the presence of sea ice through at least part of the year	McBeth Fiord, Baffin Island	Winters and Syvitski, 1992);
Glacial fjords where glaciers (tidewater or floating) control circulation and sedimentation dynamics	Kangerdlugssuaq Fjord, E Greenland; Glacier Bay, Alaska; Disenchantment Bay; Brialmont Cove, Antarctica; Coronation Fiord, Baffin Island	Syvitski et al., 1996, Azetsu-Scott and Syvitski, 1999; Hill et al., 1998; Curran et al., 2004; Domack et al., 1994; Syvitski, 1989
Fjords containing suboxic to anoxic basin waters and marked by temporal and spatial biogeochemical gradients	Resurrection Bay, Alaska; Iddefjord, Norway; Byfjord, Sweden; Loch Etive, Scotland	Burrell, 1988; Engström 1975; Rosenberg et al., 1977; Howe et al., 2002; Nørgaard-Pedersen et al., 2006, Woulds et al., 2016
Fjords overwhelmed by slope instabilities	Saguenay Fiord, Quebec; Rupert Inlet, British Columbia; Itirbilung Fiord, Baffin Island: Hardangerfjorden, Norway	Syvitski and Schafer 1996, Hay et al., 1982; Syvitski and Hein, 1991; Bellwald et al., 2016

significance (R^2 = 0.48) between bedrock depth and the thickness of fjord deposits, suggests a scaling relationship between local ice erosion and subsequent sediment deposition (Fig. 3).

The sediment fill of fjords is strongly influenced by the magnitude of local sea level. Fjords that deglaciated early (ca. 20,000 years ago) are initially affected by regional isostasy, and then by changes in ocean volume (eustasy) (Fig. 2). Fjords that deglaciated more recently (say 5000 years ago) are mostly influenced by isostasy; having largely missed the main eustatic sea level rise of 120 m from about 16 to 8 kyr BP (Overeem and Syvitski, 2010). However, deglaciation after the Last

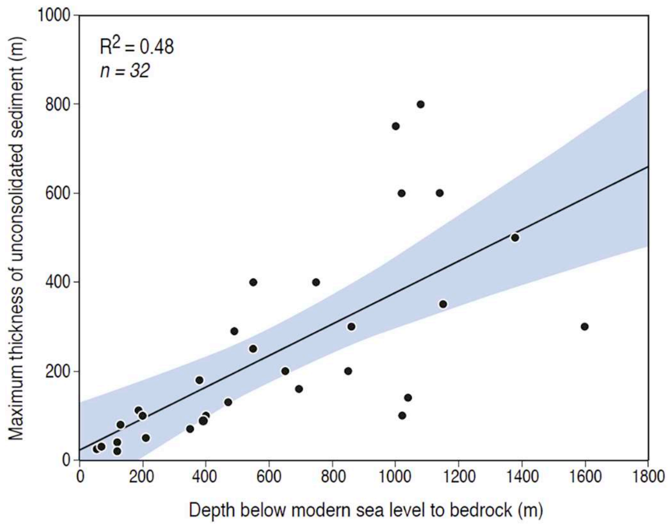

Fig. 3. Relationship between fjord depths (to bedrock) and the maximum thickness of unconsolidated sediment for 32 fjords with 95% confidence intervals (data from Syvitski et al., 1987, Syvitski, 1993, Syvitski and Lee, 1997, Stravers and Syvitski, 1991, Syvitski et al., 1996).

Glacial Maximum (LGM) will have a different combined effect of isostacy/eustasy compared to more recent deglacial retreat. Sediment accumulating in fjords during the paraglacial and postglacial phases reflect not only the duration of sediment input, but also the complexities of global versus local sea level rise (Fig. 2).

Fjord deposits reflect five depositional environments (Syvitski, 1993):

(1) Ice-contact diamicton, with distinct constructional macro-relief, associated with grounding line fans, lodgment till and morainal deposits, including sediment compacted by an advancing tidewater glacier. Modern-day examples include: Prince William Sound, Alaska (O'Neel et al., 2005), and the Kangerdlugssuaq Fjord, Sikussak, E. Greenland (Syvitski et al., 1996; Dowdeswell et al., 2010).
(2) Ice-proximal glacimarine sands and diamicton deposited rapidly some 2 to 50 km from a tidewater ice margin, where deposit length depends on the magnitude of tidewater glacial discharge into the marine environment. Modern examples include Glacier Bay, Alaska (Powell, 1990; Cowan and Powell, 1991), Columbia Fjord, Alaska (Love et al., 2016) with other examples found in Labrador Sea, East Greenland, North Iceland, and the Ross Sea, Antarctica (Andrews and Principato, 2002; Straneo et al., 2010).
(3) Ice-distal glacimarine muds, sometimes varved, along with dropstones that record hemipelagic sedimentation further away from the direct influence of ice front dynamics. In Kangerdlugssuaq Fjord, E. Greenland, the melt emanating from 15+ km^3 y^{-1} (~1000 fairly large) icebergs supplies half of the freshwater delivered to the fjord, and nearly all of the sediment input, with sedimentation rates of 2.4 cm y^{-1} near the iceberg dense head of the fjord, to 0.6 cm y^{-1} 50 km down the fjord (Syvitski et al., 1996; Andrews et al., 1997; Christoffersen et al., 2012).
(4) Paraglacial gravels, sands and muds record the terrestrial ablation of ice sheets and caps, while the fjord valleys offer an oversupply of unconsolidated sediment, made available by uplifted marine and fluvial terraces that rivers cut into, and is transported by excess discharge due an ablating ice mass (Forbes and Syvitski, 1995). Knight and Bute Inlets, British Columbia, represent modern settings where significant ablation of upstream valley glaciers deliver high loads of glacial flour to the fjords (Syvitski and Farrow, 1983; Syvitski et al., 1985). Runoff from Greenland represents 1.1% of the Earth's freshwater flux, yet delivers 8% (~1 Gt y^{-1}) of the modern fluvial export of sediment to the global ocean (~14 Gt y^{-1}); 15% of Greenland's rivers transport 80% of the total sediment load of the ice sheet (Overeem et al., 2017).
(5) Postglacial sands, muds, and gravelly-sandy lags that record modern ocean dynamics and terrestrial conditions outside of the influence of an ice sheet. Many of the fjords of Labrador (Gilbert, 1983), Norway (Aarseth, 1997), Scotland (McIntyre and Howe, 2010; Howe et al., 2010) and New Zealand (Pickrill, 1987; Pickrill et al., 1992) can be considered exemplars.

Importantly, these five depositional environments are not associated with a particular time interval. Modern glacial fjords do not yet receive postglacial sediment and may not for hundreds or thousands of years. Fjords deglaciated during the Pleistocene Epoch, may have received postglacial sediment prior to the start of the Holocene. Ice contact and ice proximal sediments are often localized to former tidewater still-stand positions (Stravers and Syvitski, 1991; Syvitski, 1993). The sediment volume defining each deposit type depends on the energy supplying the sediment, and the duration of a particular environment. In Lake Melville, glacimarine deposits comprise 54% of the basin fill, deposited in 1000 y; postglacial deposits account for 23% of basin fill, deposited in 6000 y (Table 2).

Compared to other coastal and shelf environments, accumulation rates are unusually high in fjords (Syvitski, 1993), in large part due to high inputs of inorganic matter from glaciers and rivers. The highest rates occur during the deglacial period: 4 to 12 cm y^{-1} on average for ice proximal sediments; 2.4 cm y^{-1} for ice distal settings; 0.3–0.8 cm y^{-1} for paraglacial deposits; and 0.1–0.4 cm y^{-1} for postglacial deposits (Table 3). These fjord-averaged accumulation rates mask the spatial and temporal variability unique to each fjord. With few exceptions, glacial meltwater loads are 10-fold larger than sediment fill rates associated with postglacial loads (Table 3). For example, of the 80 to 350 m of sediment fill associated with ten Baffin Island fjords, postglacial sediments deposited during the last 6000 years account for < 10 m of the sediment columns (Syvitski et al., 1990). Yet in comparison, Loch Sunart, a fjord on the west coast of Scotland, has observed sediment depths extending to ~80 m with postglacial sediments representing at least 20 m of that depth in places (Baltzer et al., 2010; Smeaton et al., 2016). Accumulation rates of up to 1 m y^{-1} have been measured in fjords where calving glaciers are currently retreating (Boldt, 2014). Geometry also strongly influences the apparent accumulation rates in fjords (Syvitski, 1993). For example, Lake Melville, is a 38 km wide and 250 km long fjord, with a system-wide depositional rate of 9 Kt km^2 y^{-1} that is 2.7- to 4.4-fold smaller when compared to narrow fjords that accentuate vertical stacking (Table 3).

2.1.5. Sedimentation styles

Given the long, narrow and deep nature of fjords, and the typically thin (well-stratified) surface layer, horizontal and vertical gradients are expanded at the expense of lateral gradients. Certainly, some fjords provide such simple geometry - a single river entering the head of the

Table 2
Late Quaternary, depositional area, sediment volumes and thickness for major accumulation periods in Lake Melville, a large marine fjord on the coast of Labrador, Canada (see Syvitski and Lee, 1997, for details).

Stratigraphic unit	Area	Volume		Maximum thickness	Time
	(km^2)	(km^3)	(%)	(m)	(ka)
Ice contact	597	7.3	10	65	?
Ice proximal	173	9.8	14	238	10—9
Ice distal	1161	27.8	40	290	10—9
Paraglacial	937	9	13	57	9—6
Postglacial	1066	15.9	23	44	6—0

Table 3
Late Quaternary sediment accumulation rates (vertical averages in cm y^{-1}) and delivery rates (Mt y^{-1}) for four very different fjord environments (modified from Syvitski and Lee, 1997).

Stratigraphic deposit type	Lake Melville	St. Lawrence Estuary	Cambridge Fiord	Muir Inlet	Unit
Ice proximal	5.7 [15]	12 [900]	4.3 [3.4]	12 [31]	cm y^{-1} [Mt y^{-1}]
Ice distal	2.4 [42]	2.4 [183]			cm y^{-1} [Mt y^{-1}]
Paraglacial	0.3 [4.5]	0.8 [51]	0	0	cm y^{-1} [Mt y^{-1}]
Postglacial	0.3 [3.9]	0.4 [27]	0.1 [0.8]	0	cm y^{-1} [Mt y^{-1}]
System deposition rate[a]	8.6	38	23	33	Kt km^2 y^{-1}
Meltwater load[b]	19	347	3.8	34	Mt y^{-1}
Postglacial load[c]	4.4	31	0.4	0.0	Mt y^{-1}

[a] Total sediment volume x bulk density/basin area/time.
[b] (volume of ice-proximal + ice-distal + paraglacial sediment) × bulk density/time.
[c] Postglacial sediment volume × bulk density/time.

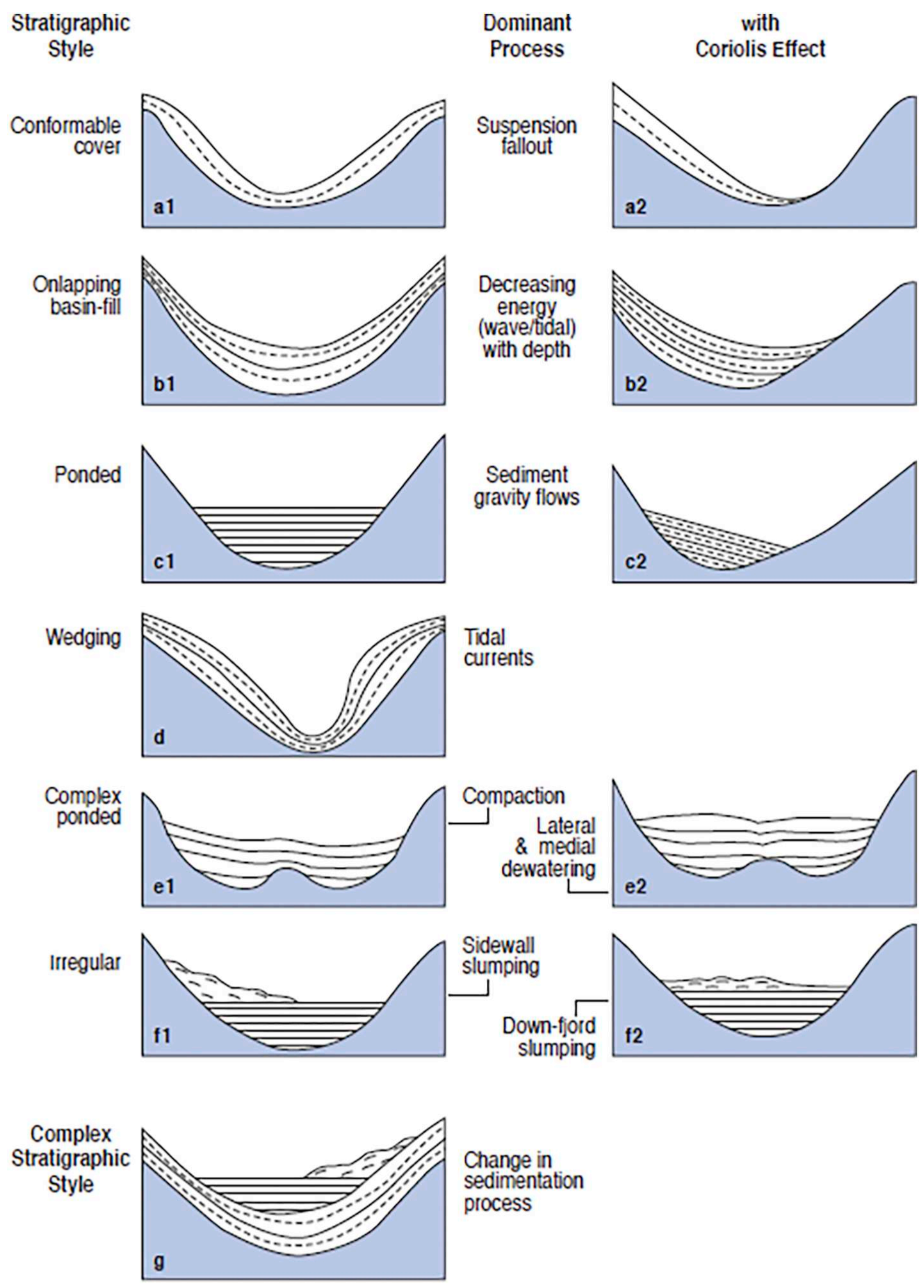

Fig. 4. Fjord lateral cross-sections showing idealized styles of basin filling representing different dominant sedimentation processes and the influence of the Coriolis force (a2, b2, c2). Also shown are some post-depositional disturbances to basin layers, including compaction and dewatering. (From Syvitski et al., 1987).

fjord and continuing down-fjord as a surface or hypopycnal plume. Freshwater conservatively mixes with seawater; suspended particle concentration is non-conservative and exponentially decreases with distance down-fjord (Syvitski et al., 1985). Within the marine layer, particles settle as floccules (marine snow), and ride the weaker deep-water currents onto the seafloor. Particle tracking studies suggest that particles settle, on average, vertical to the point where they exit the surface freshwater layer (Syvitski and MacDonald, 1982). The deposit from such a plume thins exponentially down-fjord, with a length depending on fjord geometry and associated discharge magnitude. The final deposit is conformable to (drapes) the bottom topography (Fig. 4a1: Syvitski et al., 1987). River plumes commonly hug the right-hand side of a northern hemisphere fjord due to the Coriolis influence (Fig. 4a2), and the resulting downstream deposit has its center to the right of the fjord's thalweg. As more sediment is deposited on the steep and rocky sidewall environments, slope failure becomes likely, with the sediment moved downslope or onto the basin floor (Fig. 4f1: Farrow et al., 1983).

Underflows, i.e., bottom currents, are common in some fjords and generally shape their morphology, at least in the most proximal basins. Theoretically, forming underflows in fjords requires suspended sediment concentrations of 30–40 g L^{-1} at the active river plume (Syvitski, 1989; Syvitski and Shaw, 1995) to overcome the density contrasts between river water and seawater. Sediment concentrations are rarely this high however, but flocculation within the brackish water layer at the river mouth has been suggested to enhance particle settling and to favor the formation of dense underflows indirectly at sediment concentrations as low as 1 g L^{-1} (Parsons et al., 2001). High discharge of sediment-laden river waters can create turbidity currents in fjords either directly (plunging of river waters; Mulder and Syvitski, 1995; Mulder et al., 2003) or indirectly (rapid sediment accumulation at the delta-lip) resulting in slope instability and eventually submarine slides (Clare et al., 2016). Turbidity currents resulting from high-suspended sediment loads can also be triggered by sediment settling from the river plume (Parsons et al., 2001; Hizzett et al., 2018). Turbidity currents formed by such plume-triggered events are more dilute compared to slope failures and are able to maintain turbulence for longer periods, eventually leading to long runouts (Hizzett et al., 2018). Recent observations at the Squamish delta, British Columbia, suggest that these plume-triggered events can be produced at sediment concentrations as low as 0.07 g L^{-1}, especially if they coincide with low tides (Hage et al., 2019). These bottom currents have the ability to carve deep subaqautic channels and form elongated channel-levee systems on distances that can cover several tens of kilometers (Gales et al., 2019).

Turbidity current channels cutting into the seafloor fronting fjord head deltas are common to British Columbian, Alaskan, Patagonian, Baffin Island and some Norwegian fjords, and can carry coarser sediment to the deeper parts of the fjord, sometimes bypassing large lengths of the seafloor before depositing their load (Syvitski and Farrow, 1983; Hein and Syvitski, 1992). These channels have channel depths of 1 to 40 m, and widths up to 100 m (Syvitski and Shaw, 1995; Gales et al., 2019; Vandekerkhove et al., 2020). Their lengths are highly variable, even in settings fed by rivers with similar discharges (Gales et al., 2019). While such channels are not generally sinuous, they may converge with one another or even truncate one another (Syvitski et al., 1987); channels often have their widths and depths decrease downslope. Because of the ubiquitous nature of turbidity currents in fjords, the deep basin of some fjords is comprised of an extraordinary amount of sand deposits, in environments where hemipelagic sedimentation would predict the deposition of mud.

Many fjords have multiple points of freshwater and sediment entry. Itirbilung Fiord, Baffin Island has 15 major entry points in addition to its fjord head sandur that delivers 92% of the sediment load and is only 55 km long (Syvitski and Hein, 1991). In non-temperate fjords, the amount of sediment blown into the fjord may be three times greater than the total fluvial load (Syvitski and Hein, 1991). There are still few studies on the aeolian transport of sediment into fjords (e.g., McKenna-Neuman and Gilbert, 1986), even though large sand dunes occupy many arctic fjord valleys. Thus, there are highly variable amounts of suspended solids moving through the water column of fjords (González et al., 2013; Marin et al., 2013; Quiroga et al., 2016).

Tidal current and wave reworking of the shallower seafloor portions of the fjord will leave on-lapping basin fill patterns (Fig. 4b1,2: Carter, 1976; Piper et al., 1983). Ocean swells can commonly enter the outer portion of fjords and may propagate up-fjord for some distance. Wind speeds generated from either katabatic or regional fronts, commonly exceed 100 km h^{-1}, and exceed 250 km h^{-1} in Baffin and Greenland fjords (Syvitski et al., 1987). Tidal currents are particularly important in forming lags on shallow sills (Schafer et al., 1989), and in creating and maintaining tidal channels (Fig. 4d: Syvitski and Lee, 1997).

Sediment ponding (flat lying or tilted under the Coriolis effect: Fig. 4 (1c,2c) is a common sedimentation pattern, and highlights the large number of fjords that experience turbidity currents (Syvitski et al., 1987). Likewise, bottom currents may redistribute the sediment, just like in the deep ocean, resulting in important lateral variations in sediment thickness (Vandekerkhove et al., 2020). Few fjords do not contain slump, slide, and debris flow deposits (e.g., Syvitski et al., 1987; Bellwald et al., 2016, 2019). Rotational slides are common, as are retrogressive mass flow such as from the failure of fjord head quick clays. Debris flows are a signature deposit of side-entry rivers that attempt to build out a delta on fjord wall slopes of between 5° and 30°. Failure can occur annually with each new freshet of the river. In some fjords, earthquakes shake a sediment column with very high excess pore pressure - entire portions of the fjord mass may liquify down to depths 30 to 40 m below the seafloor (Syvitski and Schafer, 1996). Fjord sediments are also commonly deformed by mass flows originating from onshore mass movements (i.e. debris flows, rockslides and avalanches) propagating into the fjord (e.g., Bornhold et al., 2007; Van Daele et al., 2013). The development of high-resolution imaging technologies in the last decades has allowed mapping such subaquatic features in detail at water depths of tens to thousands of meters (e.g., Dowdeswell et al., 2016).

In general, fjords offer model environments to conduct gradient analysis, or conservation of mass studies, or the influence of process interactions. As a result, many fjords have complex stratigraphic patterns (Fig. 4g), associated with both the modern dominant processes, and processes that no longer are present. Today's modern sediment supply is often predictable with knowledge of the size and morphological relief of the surrounding drainage basins, climate and its impacts on sediment yield (e.g., rock weathering, vegetation cover, snow and ice melt, rainfall intensity, soil development, permafrost). The ensuing fjord processes can be modeled to get the various grain sizes of the fluvial load distributed across the fjord's seafloor (Morehead et al., 2001). Humans have had a large impact on this natural sediment delivery whether from accelerating erosion (e.g. mining, deforestation, road building, agriculture) or from sequestration of fluvial sediment behind dams. Fjords with seasonal ice-cover, magnify the seasonality of deep-basin sediment flux, by limiting the wintertime sediment delivery from rivers and aeolian transport, and wind-wave resuspension transport (Skei, 1983; Syvitski et al., 1987).

2.2. Water column stratification and biogeochemical properties

Fjord water columns are typically highly stratified, with an outward-flowing surface layer of brackish or fresh water and deeper salt-rich water flowing inward to compensate for the loss of water entrained offshore (Fig. 2). The degree of stratification and residence time of the freshwater, which is typically in the order of days, is essentially related to freshwater discharge (Gillibrand et al., 2005; Cage et al., 2006). Equivalent heights of freshwater supply from river discharge typically reach several meters (e.g., Calvete and Sobarzo, 2011) and the balance between buoyancy of the upper freshwater mass and processes such as tides and wind that effectively mix the freshwater with the denser and saltier seawater below (Syvitski et al., 1987) controls the stability of the stratification. Fjord stratification is generally highly seasonal with most fjords displaying a strong stratification and a relatively deep halocline during spring and summer due to the increased input of snowmelt and ice melt in glaciated regions or precipitation in temperate regions. Winter conditions are generally much more vertically homogeneous since the surface freshwater layer is not able to sustain with limited freshwater supply modulated by strong wind mixing.

Well-stratified fjords are characterized by remarkable changes in physical (temperature, density) and biogeochemical (oxygen, chlorophyll) variables (Syvitski et al., 1987). Under stratification in spring and summer, for example, primary productivity can be restricted to the upper few meters of the water column. Similarly, chromophoric dissolved organic matter (CDOM) from runoff of humic-rich terrestrial matter can limit light penetration and primary productivity to the surface waters of fjords (Gonsior et al., 2008). Conversely, in conditions with a deep euphotic zone and nutrient availability at depth, such as fjords with marine-terminating glaciers and upwelling from subsurface meltwater discharge, primary production in summer can extend to at least 30 m (Meire et al., 2017). The degradation of sinking organic matter consumes oxygen in the underneath saline water, of which the replenishment may be limited by weak mixing (Calvete and Sobarzo, 2011) due to silled entrances, and potentially leading to suboxic or even anoxic conditions below the redox cline (Friedrich et al., 2014). Under such conditions, sulfate in the deeper saline water is reduced chemically or biologically to sulfide. When sulfide in the saline water penetrates into the photic zone or when the chemocline is shallow enough, photic zone euxinia (PZE) occurs (Anderson et al., 1988). Euxinic conditions do not permit oxygenic photosynthesis and anoxygenic photosynthesisers may outcompete other oxygen-demanding organisms. For example, sulfur oxidizing bacteria live under euxinic conditions, harvesting light and oxidizing sulfide to sustain life (Fallesen et al., 2000). So far, PZE in fjords have only been investigated in Scandinavia, such as Framvaren Fjord and Mariager Fjord, and have been proposed as modern analogs for ancient PZE events over geological timescales (Meyer and Kump, 2008). However, while clearly related to stratification, it is still unclear whether their occurrence in fjords is a global feature or local phenomenon driven by regional factors. Because fjords are often stratified and receive large stores of fresh carbon, intermittent PZE and potentially rapid water column sulfurization (Raven et al., 2016) may be important drivers facilitating carbon storage in fjords, which clearly requires further investigation, at least on regional scales, in the future (Canfield, 1989).

2.3. Fjord sediments as high-resolution archives of climate and environmental change

Due to high accumulation rates and their location at the land-ocean interface, fjord sediments are ideal archives for high-resolution records of past climate and environmental change. Multiple proxies can be applied to fjord sediments that focus on either marine (e.g. Cage and Austin, 2010) or terrestrial-derived (e.g. Cundill et al., 2006; Faust et al., 2014b) components, which can ultimately provide a broader perspective of regional change than could be obtained from terrestrial or marine environments alone. Fjord sediment core chronologies are generally based on a combination of radiocarbon dating and radionuclide (^{210}Pb, ^{137}Cs) analysis (e.g., Faust et al., 2014; Koziorowska et al., 2018; Winkelmann and Knies, 2005; Zaborska et al., 2017). The high accumulation rates frequently encountered in fjords tend to result in a significant dilution of the radionuclide concentrations, but they limit the influence of bioturbation on downcore radionuclide profiles. In ice-proximal environments, very low organic matter concentrations often result in a lack of material available for radiocarbon dating, and therefore in relatively poorly constrained chronologies. In addition, reconstruction of past climate and environmental change from fjord sediments requires core collection from appropriate basins where sediment transport mechanisms, fjord hydrography and bottom water oxygen concentrations are reasonably well constrained. Such an understanding is increasingly based on the monitoring of modern fjord physico-chemical properties either during repeated ship-based surveys or using moored instruments, including sediment traps. Although coring artifacts may disturb sediment records, especially in environments with sharp lithological variations or those rich in gas, these issues are limited for soft sediments deposited during the Holocene (Lebel et al., 1982). Obtaining multiple cores within the same sub-basin is generally recommended to account for spatial variations in sediment transport and deposition processes.

In the past, much work based on fjord sediment cores has been carried out to reconstruct river discharge (Faust et al., 2014b; Bertrand et al., 2014; Rebolledo et al., 2015), regional atmospheric circulation (Faust et al., 2014, 2016; Gillibrand et al., 2005; Hinojosa et al., 2017), coastal ocean temperature (Sepúlveda et al., 2009; Cage and Austin, 2010; Caniupán et al., 2014), marine productivity (Rebolledo et al., 2008; Mayr et al., 2014; Aracena et al., 2015; Faust and Knies, 2019), glacier dynamics (Howe et al., 2010; Bertrand et al., 2012a, 2017), volcanic activity (Cage et al., 2011; Kilian et al., 2013; Wils et al., 2018), timing of sea level rise (Nørgaard-Pedersen et al., 2006; Dlabola et al., 2015), and earthquakes (St-Onge et al., 2004; Wils et al., 2018; Piret et al., 2017), with sensitivity or temporal resolution similar to hydrologic records derived from tree-rings, corals, and varved lake sediments (e.g., Howe et al., 2010).

2.3.1. High-resolution archives of climate and environmental change from temperate fjords

Temperate fjords in British Columbia, Chile, Norway, New Zealand and Scotland feature present-day or formerly glaciated mountains, with drainage basins dominated by temperate rainforest. Orographic precipitation in these regions is generally high ($>$ 6 m annually) due to the westerly atmospheric circulation encountering topography (Garreaud et al., 2013), which results in high volumes of freshwater discharging at the head of the fjord. Typical for temperate fjords, sediment, including chemical weathering products, are delivered to the fjord by fluvial and mass wasting transport mechanisms (Howe et al., 2010). At the heads of fjords, fluvial processes commonly lead to the development of deltas composed of bedload sediments. Inner sub-basins located near the head of the fjord generally contain sediments largely composed of terrestrial organic fragments and lithogenic material, with variable concentrations of organic matter (Smeaton and Austin, 2019). In middle or outer fjord basins close to the primary sill, sediments generally contain lower concentrations of terrestrial organic matter and are composed of biogenic carbonate (e.g. bivalves and foraminifera), fecal pellets, phytoplanktonic debris, and lithogenic components (Faust et al., 2014; Hinojosa et al., 2014; Smeaton and Austin, 2017).

Because the nature of sediment accumulating in different basins is ultimately influenced by the two-layer fjord circulation driven by freshwater supply (Section 2.2), down core variations in terrestrial vs. marine components have been used to reconstruct changes in the westerly winds (Knudson et al., 2011; Bertrand et al., 2014), regional precipitation and fjord circulation (Lamy et al., 2010; Cui et al., 2016c; Hinojosa et al., 2017), aquatic productivity (Aracena et al., 2015; Bertrand et al., 2017), and vegetation history (Pickrill et al., 1992). Paleoclimate studies that investigate variations in organic matter provenance driven by precipitation and fjord circulation in all temperate settings require well-constrained marine and terrestrial-derived end members, including a comprehensive understanding of the variables that affect the composition of sediment and associated proxies (e.g. Bertrand et al., 2012a, 2012b; Faust et al., 2014, 2017; Rebolledo et al., 2019; Harland et al., 2019). The proportion of freshwater diatoms, pollen assemblages, the stable carbon isotopic composition of sedimentary organic matter ($\delta^{13}C$), and biomarkers, such as branched isoprenoid tetraethers (BIT) and the *n*-alkane-based terrestrial/aquatic

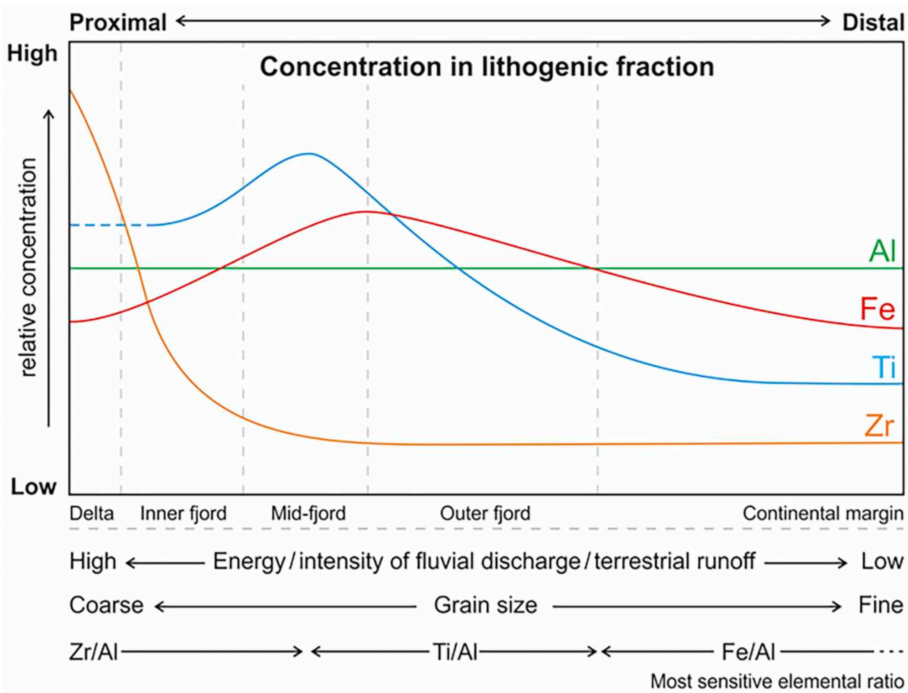

Fig. 5. Schematic representation of the distribution of Al, Fe, Ti and Zr in the lithogenic fraction of the sediment, in relation to distance to the tributaries and energy of the river supply (modified from Bertrand et al., 2012b). This illustration demonstrates that not all elemental ratios are sensitive in all types of fjord basins. Zr/Al is the most sensitive near fjord heads, whereas Fe/Al is best suited in distal environments.

ratio (e.g., Smith et al., 2010; Bertrand et al., 2014; Hinojosa et al., 2014; Bianchi et al., 2016; Smeaton and Austin, 2017; Prebble et al., 2018; Rebolledo et al., 2019), are well-constrained organic proxies that track changes in the delivery of terrestrial organic matter to fjord basins. Other organic geochemical approaches been used to evaluate water hydrodynamics (Browne et al., 2017; Cui et al., 2016a), mass-wasting events (Cui et al., 2016a), and bedrock erosion (Walinsky et al., 2009).

Another approach involves monitoring catchment erosion using major and trace element concentrations and ratios. With the advent of XRF core scanners (Croudace and Rothwell, 2015), sediment geochemistry is increasingly used to reconstruct hydrological variability (i.e., river discharge) at high resolution (mm to cm scale); the concentrations of Zr, Ti, and Fe are particularly sensitive to discharge in inner, mid and outer fjords, respectively (Bertrand et al., 2012b) (Fig. 5). Other commonly used proxies that reflect catchment inputs include sediment grain size, which can be measured directly or derived from high-resolution XRF core scanner measurements (Liu et al., 2019), and ice-rafted debris (e.g., Vermassen et al., 2019).

Sediment elemental and isotopic composition can be used to reconstruct past changes in redox conditions that are related to the rate of fjord estuarine circulation. Sub-oxic or anoxic conditions in the water column can develop in fjord basins where the renewal rate of deep marine waters slows. Basins located far from the sea, and/or are separated by multiple bathymetric sills, have relatively low deep-water renewal rates. Redox changes associated with low oxygen conditions will influence the concentration of redox-sensitive elements in the sediment. For instance, when oxygen depletion is severe and conditions become euxinic (i.e., negligible concentrations of oxygen and significant concentrations of hydrogen sulfide), aqueous Fe re-precipitates as Fe sulfides, such as pyrite (Hinojosa et al., 2016). In Fiordland, data obtained from the modern water column and underlying sediments provide evidence for an increase in authigenic Fe and other redox-sensitive trace metals (e.g., Mo, U, Mn) in surface sediments under anoxic/euxinic conditions (Hinojosa et al., 2014, 2016).

Temperate fjord basins, constrained by an outer sill near fjord mouths, were flooded by seawater incursion, a consequence of post-glacial sea level rise following the LGM (Kilian et al., 2013; Dlabola et al., 2015). These basins provide a valuable record of regional environments once sea level reached the level of the outer sill. Records of sea-level change from the Southern Hemisphere are greatly outnumbered by the Northern Hemisphere, leaving a gap in global sea-level reconstructions. Additional high-resolution records of paleo sea-level from the Southern Hemisphere can be gathered by utilizing fjord sediments, which further facilitates our understanding of non-eustatic and glacio-eustatic components of global sea-level variations (Milne and Mitrovica, 2008). Additionally, well-dated mid-latitude Southern Hemisphere records can also be used to evaluate the Antarctic contribution to sea-level rise following the LGM (Bamber et al., 2018). Because the sill depth controls the timing of marine incursion, obtaining multiple cores from several basins, and at the same time constraining regional uplift rates, can ultimately be used to develop a comprehensive sea level curve (Dlabola et al., 2015).

2.3.2. High-resolution archives of climate and environmental change from high latitude fjords

Fjords located at higher latitudes, such as in the Arctic, sub-Arctic and southern Chile, have varying degrees of vegetation coverage in their drainage basin due to the large impact of oceanic and atmospheric heat transport on regional scales, leading to deglaciation over the Holocene (e.g., Seager et al., 2002). Sub-Polar fjord regions characterized by summer mean air temperatures of above 0 °C exist in west Greenland, Svalbard, and parts of the Canadian Arctic (Gilbert, 2000). Typical for these regions is the presence of glaciers and winter sea ice, which usually breaks up during summer. The main sediment sources are sub-glacially derived material and sub-glacial meltwater runoff, icebergs and terrestrial rivers. East and north Greenland and Canadian Arctic fjords are categorized as Polar fjords, almost permanently covered by sea ice and glaciated in the drainage area (Howe et al., 2010; Bjørk et al., 2012). Sediment supply in these fjords occur mainly from the glacier bed, as well as from subglacial rivers and icebergs. Sediment delivery to such fjords is mainly through rafting by icebergs and sea ice (Syvitski, 1989). It is worth noting that fjords currently in Antarctica, although fully covered by glaciers similar to Polar fjords in Greenland and Canada, have been rarely studied in terms of their particle sources, biogeochemical processes, and long-term records. Additionally, records of westerly winds reconstructed on sediment cores from Antarctica and Patagonia may shed light on their latitudinal shifts. Chemical weathering is limited in high-latitude fjords, and since particles are mainly derived from the terrestrial hinterland, the sedimentary inorganic geochemical composition mostly reflects authigenic formation of source bedrocks or eroded soils in the drainage basin. Accordingly, fjord sediment deposits allow for high-resolution, continuous reconstruction of past glacier dynamics, an optimal way to compare with traditional geomorphic evidence and exposure dating studies which are notoriously discontinuous (e.g., moraines only represent glacier extent). However, the relationship between glacial movements and fjord sediment properties is not straightforward (Love et al., 2016), and there have been conflicting interpretations recently in the scientific literature. For example, increased clastic sedimentation has been interpreted as evidence for both glacial advance and recession. Decreasing sediment grain-size has been interpreted as representing increasing distance to the ice front (Bertrand et al., 2012a; Bakke et al., 2013), or decreasing meltwater discharge (Ariztegui et al., 1997; Cowan et al., 1999).

3. 3. Organic matter cycling

3.1. Sources and transport dynamics

In general, organic carbon in fjords is classified into two main categories: autochthonous and allochthonous. Autochthonous carbon refers to organic carbon produced in situ in the fjord ecosystem by local primary producers, including pelagic phytoplankton, macroalgae, and sea-ice algae, the latter of which is only found in (seasonally) ice-covered fjords. In contrast, allochthonous carbon refers to organic carbon derived from external sources, such as, terrestrial hinterlands, the coastal ocean or glaciers.

The nature and distribution of sedimentary organic carbon is dependent on latitude, land cover and bedrock type and, thus, particularly vulnerable to climate change. Moreover, the oceanographic setting influences the autochthonous and allochthonous carbon content of fjords Faust and Knies (2019). Based on the relative contribution of freshwater versus saline seawater, fjord systems can be subdivided into three categories:

1) Fjords with low marine water inflow and variable terrestrial runoff are generally characterized by a predominance of terrestrially derived organic matter (Fig. 6a, b). Examples for this setting include fjords in east Greenland and in NW Europe (Smeaton and Austin, 2017) and in New Zealand (Cui et al., 2016a,c; Hinojosa et al., 2014; Smith et al., 2010);
2) Fjords with high marine inflow and high freshwater runoff (Fig. 6c) reveal a substantial land-sea gradient of terrigenous versus marine organic matter, such as the Trondheimsfjord (Faust et al., 2014) or Patagonian fjords (Sepúlveda et al., 2011).
3) Fjords with high marine inflow and low river runoff is low (Fig. 6d) are dominated by marine organic matter and the contribution of terrestrial organic carbon to total organic carbon quickly decreases in seaward direction (Duffield et al., 2017; Cui et al., 2016b).

3.1.1. Autochthonous: algal-derived sources and productivity

In the euphotic zone of fjords, primary producers fix CO_2 dissolved in seawater into organic carbon. For example, the average annual CO_2 uptake within Greenland fjords is estimated to be 65–110 g C m^{-2} y^{-1} (Rysgaard et al., 2012; Meire et al., 2015) and 60 g C m^{-2} y^{-1} during the spring-summer seasons in Patagonia fjords (Chile; Torres et al., 2011). Fjord primary productivity is generally low close to the terrestrial boundary and tends to significantly increase once surface salinity exceeds the 15 PSU threshold - where growth conditions for phytoplankton become more favorable (Hendry et al., 2019; Hopwood et al., 2019). Major factors controlling primary productivity are nutrients and photosynthetically-available radiation. Light availability in fjords is inversely correlated with suspended sediment concentrations and is severely limited in areas that are subject to high glacial freshwater inputs. Moreover, in high latitudes light availability is highly seasonal. Furthermore primary production can also be reduced by topographic shading from the steep-sided walls (Wing et al., 2007), as well as by high inputs of terrestrial CDOM that reduce the depth of the photic zone (Gonsior et al., 2008; Yamashita et al., 2015). Nutrient availability has also been recognized as a limiting factor for primary production. For instance, Öztürk et al. (2002) showed that Fe limitation inhibits primary production in Norwegian fjords. Additionally, high precipitation in temperate fjords can create a persistent low salinity layer in surface

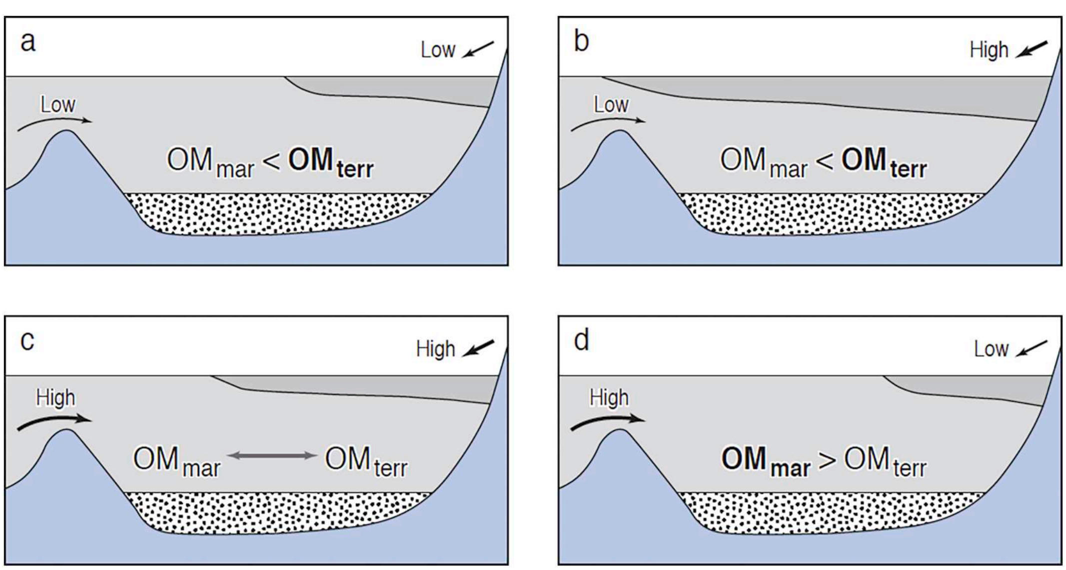

Fig. 6. Typical bathymetry and estuarine circulation pattern within fjords where oceanic water enters the fjord across an entrance sill (left) and the freshwater input in the inner part (right) creates a brackish surface water layer. In fjords with low marine and low freshwater inflow as well as in fjords with high river runoff but relatively low marine inflow (a and b) are dominated by terrigenous organic matter (OM_{terr}). Fjords were both, marine inflow and freshwater runoff are high (c) have a substantial inside-outside gradient of terrigenous versus marine organic matter. And if the marine inflow is high and river runoff is low (d) fjord sediments are dominated by marine organic matter (OM_{mar}). Adapted from Faust and Knies (2019).

waters (Gillibrand et al., 1995; Gibbs, 2001) that accentuates salinity stratification and limits phytoplankton access to nutrient-rich saline waters, except during wind-induced mixing episodes (Sakshaug and Myklestad, 1973; Goebel et al., 2005).

Regionally, primary productivity reveals strong interannual variability, which is linked to the supply of freshwater and the inflow of saline seawater (Hegseth and Tverberg, 2013). For example, some of Greenland's fjords experience pronounced summer phytoplankton blooms that are driven by nutrient inputs from upwelling plumes forming at the grounding line of Greenland's marine-terminating glaciers and mixing glacial nutrient with deep marine nutrient inputs (Meire et al., 2017; Kanna et al., 2018). Based on field observations and estimates from a hydrodynamic model of upwelling plumes in 12 Greenland fjords, Hopwood et al. (2018) showed that this deep nutrient 'pump' represents the main pathway of Greenland Ice Sheet (GrIS) nutrient fluxes to coastal waters, and that the depth of the grounding line controls the importance of glacial nutrient fluxes for the production of the fjord ecosystem.

Phytoplankton composition varies with distance from the fjord head. Carbonate-producing organisms such as foraminifera and coccolithophores are limited in some fjords to outer fjord environments where salinity is high year-round. Diatoms are abundant in some fjords (Wassmann, 1983; Waite et al., 2005; Schuller and Savage, 2011), presumably because they can take advantage of the buoyant conditions and the high silica concentrations in low salinity layers. A relatively little known and often overlooked primary producer in fjords can be macroalgae. Macroalgal nutrient assimilation, high influenced gradients in irradiance, salinity, and water motion, has a large influence on their isotopic signatures ($\delta^{15}N$ and $\delta^{13}C$) (Cornelissen et al., 2007). For example, the availability of nutrient forms can change with salinity gradients, with the proportion of HCO_3^- to $CO_{2(aq)}$ increasing with salinity, and NH_4^+ and NO_3^- increasing from both freshwater (terrestrial) and oceanic inputs. Similarly, the types of phytoplankton and particle flux in fjords can be governed by both autochthonous within the estuary proper, and allochthonous sources from the coast, depending upon seasonal shifts in coastal currents (Wassmann et al., 1996). Sea-ice algae can be an important component of the ecosystem in glaciated fjords located in Polar Regions (Carroll and Carroll, 2003; Wassmann and Reigstad, 2011). However, with climate change induced declines in sea-ice thickness and extended durations of open water (Comiso, 2006), a decrease in sea-ice algae production is observed with concurrent increase in pelagic primary production colonized by small size species (Li et al., 2009; Fujiwara et al., 2011).

The depositional flux of *autochthonous* carbon is mainly driven by primary producers- although zooplankton, as the secondary producer, can also contribute to the flux of labile organic matter (Wexels et al., 2001). The produced organic matter is partially consumed by pelagic biota in the water column, especially in regions where steep salinity gradients and associated water density differences can enhance the buoyancy of plankton and the residence times of organic carbon in the low salinity layer. The residual flux of *autochthonous* carbon that survives water column degradation is deposited on to sediments. Its distribution on sediment surface thus reflects the patchy distributions of phytoplankton that is driven by the pronounced physicochemical gradients in fjords (Schuller and Savage, 2011; Schüller et al., 2013; Schuller et al., 2015).

3.1.2. Allochthonous sources

Allochthonous inputs to fjords include organic carbon produced by primary producers in the adjacent coastal ocean, as well as terrestrial biospheric carbon, petrogenic carbon, aeolian sourced black carbon, and potentially petroleum contamination. Terrestrial biospheric OC is a heterogeneous mixture of fresh OC ($OC_{bio\text{-}terr}$) and soil OC. Fresh terrestrial OC consists of woody biomass, leaves, grasses and moss, and is the dominant contributor to temperate fjords due to dense vegetation coverage in the drainage basins (Olson et al., 1985; McLeod and Wing, 2009). Additionally, the dissolved phase can be an important component of terrestrial biospheric OC in fjords with vegetated catchments and extreme rainfall (Stanton and Pickard, 1981; Gonsior et al., 2008). Soil OC consists primarily of the altered remains of vascular land plants and degraded humic substances (Hedges, 1992). In most regions, soil development in fjord catchments is poor due to high elevations, steep slopes, and large rainfall rates, all of which can promote mass wasting events and shorten soil residence time in catchments. The residence time of weathered particles from bedrock, which essentially are the major inorganic component of soil, is short and does not favor the development of a thick soil layer. Similarly, based on compound specific radiocarbon analysis, the age of soil OC in New Zealand fjords ranges from modern to a few hundred years, with vascular plant debris having even younger ages, suggestive of fast soil turnover (Cui et al., 2017a). Radiocarbon dating in fjord sediments from Svalbard, Norway, has shown that soil-derived material may have a residence time of thousands of years (Kim et al., 2011). In some areas, soil OC from permafrost areas can be distinguished, especially in circumpolar catchments. This carbon is still relatively labile once exposed (Zimov et al., 2006; Schirrmeister et al., 2011), and can result in a substantial flux of CO_2 during transport (Anderson et al., 2009; Serikova et al., 2018).

Petrogenic carbon refers to carbon originally of biological origin that became trapped in sedimentary or metamorphic rocks (Blattmann et al., 2018). Galy et al. (2015) estimated that, globally, 18–104 (avg. = 43) megatonnes (Mt) of petrogenic POC are discharged from land to the ocean annually, corresponding to approximately 20% of total global OC export to the ocean. The significance of petrogenic carbon erosion in fjords is strongly correlated with the catchment bedrock type. For example, the influence of petrogenic rock sources is minimal in New Zealand fjords due to the dominance of igneous rocks in the catchments (Cui et al., 2017a); in contrast, SE Alaskan fjords may host the largest pool of petrogenic carbon remobilization in North America (Cui et al., 2016b). Petrogenic carbon erosion in SE Alaska is promoted by two factors: 1) the rock type of Cenozoic trench filling sediments, and 2) the physical impact of glaciers. Theoretically, reburial of OC_{petro} from bedrock to marine sediments does not represent a source of CO_2 to the atmosphere; however, some OC_{petro} can be degraded by microbes during transport, becoming a temporal CO_2 source to the atmosphere (Galy et al., 2015; Cui et al., 2016a; Blattmann et al., 2018).

Several methods, including bulk and molecular level measurement, have been applied to unravel petrogenic carbon inputs in coastal settings, such as fjords. For example, hopanes and PAHs have been applied as biomarkers indicative of sedimentary rock erosion. Variable concentrations of biomarkers relative to bedrock OC content makes it impossible to estimate petrogenic carbon inputs quantitatively. Instead, radiocarbon measurements of sedimentary OC are applied for a quantitative estimation of biospheric versus petrogenic carbon. This is based on the fact that petrogenic carbon has a $\Delta^{14}C$ value of −1000‰, or a fraction modern (Fm) value of 0. By assuming a Fm or a $\Delta^{14}C$ value for biospheric OC (Galy et al., 2015), including marine and terrestrial sourced, the content of petrogenic carbon in sediments can be estimated quantitatively by measuring the radiocarbon content of bulk OC.

Point sources such as rivers and landslides (mass wasting events), and non-point sources such as overland runoff, are the major pathways of terrestrial inputs to fjords, with fjord head rivers playing a major role in the upper reaches of fjord systems, and non-point sources evenly distributed along fjords. Landslides are unevenly distributed spatially and temporally, being a function of topography, rainfall and seismic activity (Hungr et al., 2014; Meunier et al., 2008). The majority of organic matter is associated with finer, but denser clay minerals in the middle reaches of New Zealand fjords, where the oldest carbon is commonly found (Cui et al., 2016a, 2017a). Along fjords, topography and climate conditions affect the properties of OM being eroded from mountainous banks. Due to the steep topography of mountainous slopes along fjords, landslides can be evident by the observations of exposed bedrock and successional stage of vegetation colonization (Mark et al., 1964). Toward the fjord mouths, allochthonous carbon sources may be re-worked by winnowing and stripping of pre-deposited material from the sill tops (Ramirez et al., 2016; Cui et al., 2017a).

3.2. Carbon degradation, burial/sequestration, and budgets

The importance of fjords as a carbon sink versus source, depending on hydrodynamics and climate zone, was first suggested by Pearson (1980). Later work indicated that burial of OC in fjords was important globally (Nuwer and Keil, 2005). Using Holocene sediment fill data from Syvitski et al. (1987), Nuwer and Keil (2005) estimated that over the last 100,000 years, 12% of continental margin sediments have been stored in fjords, and likely have a nearly equal contribution to total marine OC burial. Smith et al. (2015) examined modern OC burial rates using two distinct methods. The first mimicked the deltaic and non-deltaic estimation methods of Berner (1989) and Hedges and Keil (1995), by re-proportioning 813 Mt. yr^{-1} of terrestrial sediments to fjords (Durr et al., 2011) and applying an average fjord surface sediment OC value of 2.6%, which is nearly four times as large as that of deltaic shelf sediments. For the second, using a similar method as for the calculation of biogenous sediments in Berner (1982), Smith et al. (2015) scaled OC accumulation rates derived from core data published from fjords in several systems throughout the globe to total fjord surface area published in Durr et al. (2011). The estimates of fjord burial using the two methods were very similar (17 and 20 Mt., respectively), showing that fjords account for 11% of marine OC burial.

While these models constrain the inputs of OC to fjord sediments relatively well, the preservation of OC during burial at depth is less certain. An 80% deep burial efficiency was chosen by Smith et al. (2015) for comparison with Berner (1982) and Hedges and Keil (1995), yet OC burial efficiencies in fjords have been found to vary, with estimated values ranging from 28% to 90% (Koziorowska et al., 2018; Zaborska et al., 2018). Some of this variation can be attributed to differences in calculation methods, which include comparing surface and deep sediments or measuring carbon inputs and losses, although they are also related to differences in the composition of sedimentary OC, with terrestrial OM being preferentially preserved. The high linear accumulation rates (LAR) and MARs such as those found in fjords have been found to quickly bury accumulated OC below the aerobic sediment layer, reducing the oxygen exposure time and enhancing preservation (Berner, 1989). Tables 4 and 5 illustrate the latitudinal variability with LAR and MAR, without information on specific fjords. Suboxic or anoxic/euxinic bottom water conditions that become established in some fjords would be expected to further increase OC preservation (Bianchi et al., 2016). In addition, high glacial iron fluxes to fjords might play an important, yet overlooked role in OM preservation. Fe and Mn-phases known to adsorb or to co-precipitate efficiently with dissolved organic compounds. A recent study revealed that 23–27% of total OC is bound to iron suggesting that the OC-Fe associations enhance long-term burial (e.g. Lalonde et al., 2012; Salvado et al., 2015; Shields et al., 2017). Additionally, sulfurization can be important in binding and preserving OC in euxinic and sulfide rich fjords (Canfield, 1989). Therefore, the range of burial efficiencies observed are likely a function of the different OC sources, MARs, and bottom water redox conditions of fjords in different regions (Tables 4 and 5). Overall, most estimates of the OC burial efficiency of fjords are within the ranges published for other marine regions that experience suboxic or anoxic conditions, and higher than typical continental shelf sediments (Burdige, 2005).

Fjords receive relatively fresh organic material and many do not have persistent or seasonally suboxic/anoxic bottom waters (Cui et al., 2017a; Hinojosa et al., 2016), which suggests the presence of other unique features that enhance OC burial efficiencies in these systems. For example, the high OC burial rates found in New Zealand fjords are directly linked to numerous processes that result in the rapid transport and burial of large volumes of terrestrially-derived material. As a

Table 4
Sedimentation rates (SR), mass accumulation rates (MAR), OC content, and organic carbon accumulation rates (OCAR) in fjords on a regional scale. See further details in Cui et al. (2016c).

Regions	SR	MAR	OC%	OCAR	OC_{Terr} AR	%Terr	References
Units	mm/yr	$kg/m^2/yr$	(%)	$gC/m^2/yr$	$gC/m^2/yr$		
Patagonia	3.1	1.27 ± 0.60	1.9 ± 0.8	24.0 ± 16.3	10.2 ± 10.7	42.3	Aracena et al., 2011; Mayr et al., 2014; Sepúlveda et al., 2005; Sepúlveda et al., 2011; Silva et al., 2011
West Canada	3.0	1.75 ± 1.87	1.6 ± 3.6	28.0 ± 3.1	13.3 ± 4.0	47.5	Brown et al., 1972; Ingall et al., 2005; Nuwer and Keil, 2005; Smittenberg et al., 2004a; Walsh et al., 2008
NW. Europe	3.5	0.70 ± 0.71	4.2 ± 4.2	29.3 ± 17.3	14.3 ± 8.6	76.5	Faust et al., 2014; Huguet et al., 2007; Loh et al., 2008; Muller, 2001; Nordberg et al., 2001; Nordberg et al., 2009; Smittenberg et al., 2005; Smittenberg et al., 2004b; Velinsky and Fogel, 1999
New Zealand	1.4	0.88 ± 0.32	3.8 ± 1.9	33.8 ± 23.0	24.8 ± 20.9	73.4	Cui et al., 2016c; Knudson et al., 2011; Smith et al., 2015; Smith et al., 2010
East Canada	7.0	4.77 ± 5.44	0.7 ± 0.9	34.8 ± 71.6	24.4 ± 73.8	70.1	Louchouarn et al., 1997; St-Onge and Hillaire-Marcel, 2001; Syvitski et al., 1990
Svalbard	11.0	3.15 ± 3.83	1.2 ± 0.8	38.8 ± 47.4	27.7 ± 32.9	71.2	Koziorowska et al., 2016; Wehrmann et al., 2014; Winkelmann and Knies, 2005; Zaborska et al., 2006; Zajaczkowski et al., 2004
Antarctica	1.8	6.60 ± 3.59	1.1 ± 3.7	73.4 ± 80.6	39.7 ± 36.3	54.1	Burkins et al., 2001; Damsté et al., 2007; Li et al., 2000; McMinn et al., 2001
Alaska	NA	36.21 ± 72.34	0.4 ± 2.9	146.9 ± 211.8	70.3 ± 153.5	47.9	Cui et al., 2016a; Jaeger et al., 1998; Walinsky et al., 2009
Greenland	19.7	26.64 ± 59.26	1.3 ± 0.9	356.6 ± 849.4	250.2	70.0	Gilbert et al., 1998; Gilbert et al., 2002; Glud et al., 2000; Møller et al., 2006; Rysgaard et al., 1996; Smith et al., 2002; Smith and Andrews, 2000
Average	6.3 ± 6.2	9.11 ± 13.02	0.93 ± 1.32	85.08 ± 109.0	52.77 ± 76.2	61.4 ± 13.2	

Table 5
Linear accumulation rate (LAR) and mass accumulation rate (MAR) in fjords, modified from Faust et al. (2019), Koziorowska et al. (2018) and Smeaton et al. (2016).

Region	LAR [cm y^{-1}]	MAR [g m^{-2} y^{-1}]	Reference
Arctic region			
Kongsfjorden	0.13–0.41	1350–6279	Kuliński et al. (2014)
	0.22–0.47	1270–5490	Zaborska et al. (2017)
Hornsund	0.12–0.19	1310–2330	Koziorowska et al. (2018)
	0.17–0.66	1800–6250	Zaborska et al. (2017)
Storfjorden	0.18	570–2240	Winkelmann and Knies (2005)
Barents Sea	0.03–0.4	320–650	Carroll et al. (2008)
Young Sund (Greenland Sea)	0.04–0.23	–	Rysgaard and Nielsen (2006)
Scoresby Sund (E Greenland)	0.02–0.03	85.1–127.7	Marienfeld (1992)
Kangerlussuaq Fjord (E Greenland)	0.12–0.83	510.6–3531.7	Smith et al. (2002)
Canada and Alaska			
Glaciated fiord (SE Alaska)	–	90,000–3,300,000	Cui et al. (2016a,b,c)
Saguenay fjord (Canada)	0.2–1.5	–	Smith and Walton (1980); St-Onge and Hillaire-Marcel (2001)
Gulf of St. Lawrence (Canada)	0.08	~ 285	Silverberg et al. (2000)
	1.0–1.5	–	Muzuka and Hillaire-Marcel (1999)
Labrador Sea	0.2–2.8	–	Muzuka and Hillaire-Marcel (1999)
Other regions			
Nordåsvannet fjord (Norway)	0.04–0.22	44.6–261.5	Muller (2001)
Trondheimsfjord (Norway)	0.03–0.49	127.7–2085.0	Faust et al. (2014)
Lofoten Fjords (Norway)	0.01–0.78	42.6–3318.9	Faust and Knies (2019)
Loch Sunart (Scotland)	0.02–0.09	–	Smeaton et al. (2016)
Patagonia fjords (Chile)	0.14–0.47	–	Sepúlveda et al. (2011)
Fiorland (New Zeland)	0.06–0.38	51–1140	Smith et al. (2015)
			Knudson et al. (2011)
			Pickrill (1993)

National Park, Fiordland is a nearly 100% pristine temperate rainforest ecosystem, with abundant vegetation that can enter fjords from the watershed through mass-wasting events, overland runoff, and headwater streams (Smith et al., 2010). The steep slopes, enhanced direct contact between land and the estuary, abundant rainfall (7 m of annual rainfall, Hicks et al., 1996), and seismic activity drive the mass-wasting events on surrounding slopes (Whitehouse, 1988; Keefer, 1994; Bellwald et al., 2019), which can be identified by large scars of missing forest or vast areas with early successional stages of vegetation. After such an event, the forest can become re-established on the order of < 100 years. These processes result in an efficient mechanism where large amounts of stable terrestrially-derived OM are continually produced and cycled directly into fjord sediments on relatively short (decadal to centennial) timescales, and also contribute to high MARs that increase OC preservation. Nevertheless, concerns may arise that such event of paused particle input to fjords through mass wasting events may complicate our interpretation of paleoclimate based on core record. In New Zealand, these terrestrial OC fluxes can also help to sustain benthic ecosystems (McLeod and Wing, 2009) (e.g., Table 4). Since organic carbon involved in mass wasting events has minimal oxygen exposure time in the water column, it is preserved efficiently in fjord sediments. Therefore, mass wasting events are a predominant driver of terrestrial inputs and burial, especially in the lower reaches of fjords where riverine disturbance is negligible. As terrestrially-derived particles sink through the water column, they undergo microbial reworking so that the dissolved organic carbon (DOC) in deep basins is enriched in humic-like components that are distinct from surface DOC (Yamashita et al., 2015). This DOC generated through microbial transformations saturates the water column and pore water, preventing further degradation of particulate OC in the deeper part of fjords (Yamashita et al., 2015).

Fjords are also efficient sediment traps, retaining the vast majority of material that enters from the watershed. Fjords are often the deepest settings along continental shelves, and are able to protect sedimentary OC from the impacts of large storms, which promote OC remineralization through sediment resuspension in estuaries (Paerl et al., 2018) and on continental shelves (Bianchi et al., 2018; Bianucci et al., 2018). In combination with the deep basins, the shallow sills at the fjord mouths or throughout the fjords efficiently prevent the mobilization of bedload sediments. Glacial-interglacial cycles may determine the residence time of sediments in fjords, with the possibility of fjords being "re-carved" during glacial advances (Cowan et al., 2010), and ultimately control the timescales over which fjord OC storage impacts the global C cycle. Therefore, more work needs to be done to determine sediment fluxes to fjords over glacial-interglacial cycles (Andrews and Syvitski, 1994).

It is estimated that between 55 and 62% of OC buried in fjords is terrestrially-derived and fjords have been found to account for 17 ± 12% of all terrestrial OC burial in the global ocean (Cui et al., 2016c). Thus, fjords may represent a previously unconstrained sink that can help to close the geochemical "conundrum" of missing terrestrial OC in the ocean (Hedges et al., 1997). The presence of this terrestrial material also increases the overall OC burial efficiency of these systems (Hedges, 1992). Lignin, similar to carbohydrates and proteins, is one of the most abundant biopolymers on Earth (Parsons et al., 1984; Tissot and Welte, 1978; Bianchi and Canuel, 2011; Jex et al., 2014) and also one of the most stable components of vascular plants (Hedges et al., 1985), found to be preserved for tens of millions of years (Obst et al., 1991; Grimes et al., 2001). Thus, the production, transport, and preservation of lignin play an important role in affecting OC burial. Systems that accumulate a lot of lignin-rich OM typically have high OC burial rates. Lignin is produced nearly exclusively by vascular plants on land (Sarkanen and Ludwig, 1971), where fungi degrade the lignin after it enters soils by producing nonspecific enzymes (Benner et al., 1984). During transport to the coastal ocean, lignin breakdown may be dominated by photochemical oxidation (Opsahl and Benner, 1995). In marine sediments, lignin breakdown is primarily carried out by bacteria in aerobic portions of the sediment, and lignin breakdown largely stops when buried past the depth of oxygen penetration (Jex et al., 2014). Rapid transport processes in fjord watersheds and high MARs in fjords therefore quickly transport lignin to deeper sediments where it can be preserved.

Uncertainties exist in our current estimation of fjord OC burial. We lack estimates of preservation efficiency and remineralization rate from a number of regions both in bulk and at the molecular level (Koziorowska et al., 2018). For example, Hamilton and Hedges (1988) found a lack of selectivity in breakdown between lignin and carbohydrates in Saanich Inlet, while Louchouarn et al. (1997) observed slower rates of lignin breakdown relative to the labile OC fraction in the Lower St. Lawrence Estuary. Additionally, glaciated fjords in Alaska (Cui et al., 2016b) and systems that have high rates of uplift and erosion in mountainous watersheds such as Fiordland (Hilton et al., 2011) receive large volumes of petrogenic OC, and the broader study of petrogenic OC across more fjord regions, as well as its fate, is needed. Finally, the general assumption of spatial homogeneity of sedimentation in burial models contradicts with our understanding of spatial variation within fjords, which propagates errors when upscaling to a global scale (Cui et al., 2016c). Despite these uncertainties, it is clear that fjords are significant OC sinks, greatly exceeding all other sedimentary marine systems in terms of OC burial per unit area (Smith et al., 2015).

As highlighted, the over deepened glacial geomorphology and high sedimentation rates observed in fjords allow for significant quantities of C to be buried (Smith et al., 2015). Yet the total quantity of C held within fjords remain largely unknown. Already more than thirty years ago Syvitski et al. (1987) commented that "the development of a methodological approach to quantify the C in the sediment of a fjord must be a priority", yet in the subsequent years there has been relatively little progress toward this goal until recently. Smeaton et al. (2016) using Loch Sunart (Scotland) as a pilot study developed a new approach that utilized seismic geophysics to map a 3D volumetric model of the sediment. This was integrated with physical property and geochemical data collected from cores which reached back through the Holocene and into sediments derived from the last glacial period. Using this method, it was estimated that 26.9 ± 0.5 Mt. C (Postglacial: 19.9 Mt. C; Glacial: 7 Mt. C) was stored in the sediments of Loch Sunart, and this was further broken down into 11.5 Mt. OC and 15.4 Mt. inorganic carbon. The methodology developed by Smeaton et al. (2016) was designed to be applicable to any fjord where appropriate data is available.

This new approach by Smeaton et al. (2016) was subsequently applied to several other Scottish fjords with the aim of calculating the first national C stock estimation for a marine system. Using the C stock estimates from these fjords in conjunction with the physical characteristics of each fjord and its adjacent catchment, it was further estimated that the sediments held within Scotland's 111 large fjords (over 2 km long, with fjord length twice fjord width) store a total of 640.7 ± 46 Mt. C (Smeaton et al., 2017). When these results are broken down further, the postglacial sediments hold the greatest quantity of C with 467 ± 65 Mt. (OC: 252 ± 62 Mt.; IC: 215 ± 85 Mt) stored, while the glacial sediments hold significantly less (173 ± 18 Mt. C; OC: 43 ± 12 Mt.; IC: 130 ± 22 Mt), due to the decrease in terrestrial OC sources during the last glacial period. The 640.7 ± 46 Mt. of C held within the sediment of the fjords represents one of Scotland's largest C stores. For example, the fjord sediments hold a greater quantity of C than all the living vegetation in Scotland (Forestry Commission, 2015; Vanguelova et al., 2013). Scotland's soils, particularly the peatlands (Chapman et al., 2009), contain a greater total quantity of OC than the fjords. However, when the OC density is calculated (i.e. area normalized), fjordic sediments are estimated to store 0.219 Mt. OC km^{-2} (Smeaton et al., 2017) which is significantly higher than the C rich peatlands of Scotland, which only store 0.094 Mt. OC km^{-2} (Chapman et al., 2009). On an area-by-area basis, Scottish fjords are the most effective places for the long term (10^3 years) storage of C in Scotland and the UK; it is likely that this pattern will be mirrored in fjord systems globally.

3.3. Latitudinal gradients in sequestration and organic matter storage

In high latitudinal fjords where the drainage basin landscape is covered by glaciers, bedrocks are physically eroded by glacier movements, and bedrock particles are transported into fjords (Storms et al., 2012). In regions such as SE Alaska, the bedrock is mainly composed of sedimentary rocks (Cui et al., 2016b) (Table 4). The petrogenic carbon stored in sedimentary rocks has been preserved in rocks for millions of years and the erosion of which is a significant contributor to petrogenic carbon recycling (Hedges, 1992). Once they are exposed to the atmosphere or water body, they will be remineralized partially. The CO_2 generated through petrogenic carbon remineralization will contribute significantly to the atmospheric CO_2 pool, serving as a net source of CO_2 temporally (Galy et al., 2015). In contrast, in regions where the bedrock is composed of igneous, volcanic, and metamorphic rocks, such processes can be ignored due to the absence of petrogenic carbon. In general, the significance of petrogenic carbon recycling is dependent on the dissolved oxygen concentration in the water column, sedimentation rates, and oxygen exposure time (Hemingway et al., 2018).

Moving from high latitudes toward low latitudes, the glacial ice extent diminishes due to the rise in mean annual temperature and glacier melting. Consequently, bedrock erosion rates and sedimentation rates decrease by orders of magnitudes (Cui et al., 2017b). In this setting, the drainage basin landscape is minimally colonized by vegetation. Therefore, without physical forcing by glaciers, chemical weathering is the primary driver of bedrock erosion, and is potentially a source of atmospheric CO_2 through petrogenic OC oxidation (Amiotte Suchet et al., 2003). Commonly, terrestrial biospheric carbon input is minimal during this time. In Sitka Sound (SE Alaska) and Elefantes Gulf (Patagonia), for example, the sedimentary OC is dominated by marine sources, both supported by bulk OC $\delta^{13}C$ measurements and biomarkers (Cui et al., 2016b) (Table 4). Interestingly, new work has shown that inputs of continentally-derived organic matter of pedogenic origin vary in terms of their potential reactivity and their binding to organic matter in surface waters (Blattmann et al., 2019). For example, organic matter associated with smectite mineral surfaces was released to the water upon discharge, dispersal, and/or sedimentation in oceanic settings. Conversely, organic matter derived from petrogenic sources remained tighly bound to minerals composed of mica and chlorite upon entering the marine environment. Thus, while burial may be higher in regions receiving significant inputs of petrogenic compared to pedogenic material, there will be more decoupling from any water column processes associated with CO_2 air-water exchange. Shifts from petrogenic carbon erosion and remineralization to burial of marine phytoplankton derived OC signify the switch from fjords potentially releasing CO_2 to sequestering CO_2. In regions dominated by marine OC, the oxygen levels in bottom waters is commonly low, slowing down remineralization of OC over short term. Cases of substantial terrestrial erosion exist in regions where soil was well-developed pre-glaciers (Kim et al., 2011). For example, soil erosion following glacier retreat is prevalent in Svalbard, Norway, corroborated by biomarkers indicative of vascular plants and grasses (Kim et al., 2011). Since Svalbard is currently only colonized by low-level plants, the discovery of vascular plant biomarkers points to their potential synthesis before glacier advancing, which is further supported based on ^{14}C analysis (Kim et al., 2011). Since the respiration of this component of terrestrial OC has been inhibited by glacier capping, the re-exposure of aged soil carbon to microbes post-glacial retreat can potentially release respired CO_2, which requires further investigation (Vonk et al., 2012).

In mid latitudes, vegetation colonization is prevalent in fjord drainage basins and along slopes. Depending on locations, terrestrially-derived biospheric carbon may be the dominant type of OC in fjord sediments. A typical example is New Zealand fjords, where terrestrial OC dominance is indicated by depleted ^{13}C and high concentrations of lignin and long-chain fatty acids. Downcore analysis in sediment cores evenly collected along fjord basins, reveal undetectable degradation of OC with time (Cui et al., 2016c; Hinojosa et al., 2014). This is in contrast to the fact that most fjords are well oxygenated in the bottom water (Silva and Vargas, 2014). In fact, sediments deposited in these fjords, rich in organic carbon and oxygen, are consumed quickly in sediments. Short oxygen-exposure time of organic carbon in temperate fjords is comparable to upwelling regions where organic carbon is well

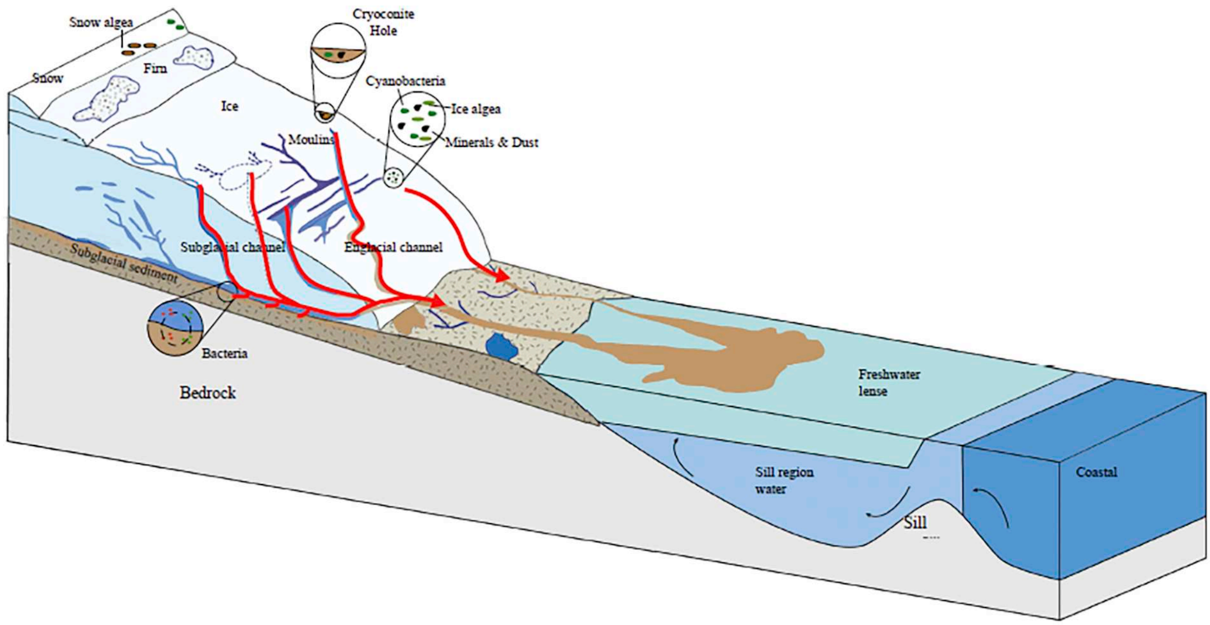

Fig. 7. Glacial nutrient and carbon factories. Sources (magnifying glass) and transport pathways (red) of carbon and nutrient inputs from land-terminating glaciers to fjords (modified from Chu, 2014 and Boetius et al., 2015).

preserved even with slow sedimentation rates.

In general, regions with glacier movement has the largest potential of burying organic carbon due to petrogenic carbon erosion. In fact, burial of petrogenic carbon does not interact with modern carbon cycling and biospheric carbon sequestration. In contrast, fjords located in relatively lower latitudes have a larger potential of interacting with contemporary carbon cycle by burying newly synthesized organic carbon through photosynthesis (Cui et al., 2016b).

3.4. Nutrient fluxes from glaciers

Along glaciated coasts, fjord and adjacent coastal ocean ecosystems are characterized by a complex interplay of physical and biogeochemical processes that create sharp, but dynamic environmental gradients (Fig. 7). Once thought devoid of life, glaciers and ice sheets are now recognized as complex ecosystems characterized by hotspots of biogeochemical activity that accumulate and store organic carbon and nutrients (e.g., Anesio and Laybourn-Parry, 2012; Hood et al., 2015; Renaud et al., 2015). Carbon and nutrients are released when glaciers melt and exert an important, yet poorly quantified influence on downstream ecosystems. Glacial carbon and nutrient export is mainly derived from geochemical interactions and microbial activity in glacial environments that are connected by a seasonally evolving hydrological system (Bartholomew et al., 2010, 2011; Sole et al., 2013; Chandler et al., 2013; Cowton et al., 2013; Chu, 2014).

On the glacier surface, heavily pigmented and actively photosynthesizing microalgae and cyanobacteria that live in snow, on the ice or in the surface layers of cryoconite holes (Yallop et al., 2012), fix carbon and nitrogen from the atmosphere. They do not only enrich surface meltwaters in dissolved organic carbon, phosphorus and nitrogen (Boetius et al., 2015), but also enhance ice melting rates through surface darkening (Stibal et al., 2017). Although all major groups of heterotrophic bacteria and many fungal groups are found in supraglacial environments (Boetius et al., 2015), heterotrophic activity is often low. It has been suggested that, unlike other freshwater systems, glaciers and ice sheets are net autotrophic. Anesio et al. (2009) estimated that cryoconite holes alone, may fix as much as 64 Gt C y^{-1}. However, these estimates are based on a limited number of local studies and thus are associated with large uncertainties. Past work has indicated that the balance between autotrophic and heterotrophic processes is spatially and temporally variable (e.g. Stibal et al., 2012). They define glacier surfaces as “factories” that fix carbon from the atmosphere and recycle recalcitrant organic carbon from various sources into more labile carbon substrates, highlighting the importance of both autotrophic and heterotrophic processes in accumulating carbon and nutrients on the surface. The supraglacial carbon and nutrient enriched meltwaters descend to the glacier bed where they transit permanently dark, debris-rich and potentially anoxic subglacial environments. Here, water residence times on the order of days to weeks, intense physical erosion by glacier sliding over the bedrock, high water-rock ratios and microbially-mediated chemical weathering of ground bedrock promote further enrichment of meltwaters with carbon, nutrients and fine suspended particulate matter (e.g. Tranter et al., 1996; Sharp and Tranter, 2017; Wadham et al., 2019). In addition, microorganisms may fix inorganic carbon via chemolithoautotrophy or degrade organic carbon sourced from overridden bedrock, sediments, soils, vegetation and exported from the glacier surface (Skidmore et al., 2005; Stibal and Tranter, 2007; Bhatia et al., 2010; Lawson et al., 2014).

Most of the dissolved nutrients are delivered to fjords during the peak glacial-melt periods when the drainage system has evolved from a slow inefficient system to a faster, more efficient channelized system (Chandler et al., 2013). Although the seasonal evolution of glacier hydrology is increasingly well characterized (e.g., Nienow et al., 2017), the way in which subglacial hydrological and biogeochemical processes interact to control the export of dissolved and particulate carbon and nutrients over a melt season, as well as its response to projected climate change remains poorly understood. A recent study highlights the key role of water residence time (daily to seasonal) in controlling mineral weathering reactions in subglacial systems and therefore that hydrological information is key to the interpretation of radiogenic and stable isotope data in subglacial runoff (Linhoff et al., 2017). In addition, periodic flushing of concentrated stored waters by supraglacial lake drainage events has been observed (Bartholomew et al., 2010). Furthermore, Lamarche-Gagnon et al. (2019) report a continuous export of methane-superated waters from the Greenland ice sheet. Their measurements show that the exported methane is of microbial origion and that the magnitude of the export flux is strongly linked to the efficiency of the subglacial drainage system. On the other hand, observations suggest that the limitation of supraglacial production controls dissolved organic carbon concentrations in the runoff (Lawson et al., 2014).

Additionally, fluxes of particle-bound nutrients reveal more complex controls. For instance, labile phosphorus fractions appear sensitive to changes in pH and hydrological water sources, thus illustrating the strong connectivity and complexity of the glacial bioreactor. Finally, high freshwater inputs in a Patagonian fjord resulted in seasonally higher CH_4 concentrations, mostly in the cold and brackish nutrient-depleted surface waters, were largely derived from runoff waters and microbial decay that occurred where seston and/or plankton accumulate near the pycnocline (Farias et al., 2017).

Based on a recent compilation of organic carbon concentrations measured in more than 300 of glacier and ice-sheet surface samples from around the world, Hood et al. (2015) estimate that glaciers and ice sheets release ~3 Tg OC y^{-1}, including ~1 Tg C y^{-1} as DOC. The Greenland ice sheet is a large contributor to those OC fluxes, with estimated fluxes of 0.36–1.54 Tg C y^{-1} (POC) and 0.13–0.17 Tg C y^{-1} (DOC). In addition, first, large-scale estimates indicate that nutrient input from GrIS rivals that from some of the largest rivers in the world. For instance, bioavailable iron input from the GrIS (0.3–0.7 Tg, Hawkings et al., 2014, Bhatia et al., 2013) exceeds aeolian dust inputs to the North Atlantic (0.040–0.160 Tg y^{-1}). It should be noted that while Fe GrIS is more point-sourced than the overall broader dust deposition pathways across high latitudes (Bullard et al., 2016). In addition, observed soluble reactive phosphorous concentrations in ice sheet meltwaters (up to 0.35 μM) are comparable to those found in major Arctic rivers. Estimations of total GrIS phosphorous yields, on the basis of these limited data, exceeds published riverine yields reported by an order of magnitude (Hawkings et al., 2014). Estimated dissolved and amorphous silica fluxes (0.20 Tmol y^{-1}) represent roughly ~50% of the Si input from Arctic rivers. Hydrogeochemical observations from four melt seasons (Hawkings, 2015; Hawkings et al., 2016) indicate that increasing melt rates will likely increase the subglacial export of carbon and nutrients. Hood et al. (2015) predict that by 2050, the annual DOC and POC release will accelerate to reach a cumulated 48 and 78 Tg C respectively (~4 times the annual OC discharge of the Amazon River). In addition, enhanced glacier melt rates cause prolonged melt seasons and higher discharge rates, which in turn erode and thus mobilize potentially large, yet poorly quantified amounts of permafrost organic carbon into proglacial rivers and fjords (Bendixen et al., 2017; Rudy et al., 2017).

The bulk of this meltwater is either channeled from land-terminating glaciers through proglacial rivers into fjords or, directly flows from marine-terminating (tidewater) glaciers into the fjords. Fjords are thus important routes through which glacially-derived carbon and nutrients reach the global coastal ocean. Similar to estuaries, fjords are not simple conduits of meltwater fluxes. Fjords are active bioreactors that act as important modulators (filters) of terrestrial carbon and nutrient fluxes. High primary production rates, high sedimentation rates, strong salinity gradients, pronounced redox zonation and long residence times, in combination with highly dynamic and complex circulation patterns play an important, yet poorly quantified role in transforming, storing and delaying glacial carbon and nutrient delivery to the global ocean. So far, little is known about the exact fate of glacial OC inputs. Typically, supraglacial DOC is characterized by a microbial signature with up to 62% of DOC represented by low molecular weight compounds. On the other hand, high glacial SPM and iron loads might favor the formation of OC mineral associations and, thus, decrease the bioavailability of OC exported from the cryosphere. How much of this material is readily metabolized, or is deposited in fjord sediment, remains essentially unknown.

Much of the current scientific debate with respect to the biogeochemical influence of glacial meltwater on fjords has focused on the role of glacial meltwater fluxes for the productivity of fjord ecosystems. Studies from Alaskan and Svalbard fjords have shown that environmental gradients caused by glacial runoff control community structure (e.g., Renner et al., 2012; Lydersen et al., 2014; Dalpadado et al., 2016). It has been proposed that glacial carbon and nutrient fluxes exert a fertilizing effect on downstream ecosystems (e.g., Wadham et al., 2016; Hawkings, 2015). However, variable nutrient ratios and resulting nutrient limitations (Meire et al., 2016), high sediment loads and resulting light-limitation (Murray et al., 2015), limit the direct effect of glacial runoff on fjord primary productivity. Recent research shows that direct fertilization of the fjord ecosystem by glacial nutrients might, in most cases, be secondary to their fertilization by meltwater-driven upwelling of deep, nutrient-rich marine waters (e.g. Macdonald et al., 2010; Hopwood et al., 2019; Cape et al., 2019). A notable exception might be glacially-derived silica (Hendry et al., 2019), which has been directly linked to altering the relative abundance of diatoms and their respective blooms in Godthåbsfjord (Meire et al., 2016).

The physical and chemical weathering of bedrock in high latitudes provide important sources of trace elements to fjords. For example, in Svalbard fjord sediments much of the particulate iron and manganese oxyhyroxides are delivered by glacial meltwaters (Kostka et al., 1999; Nickel et al., 2008; Wehrmann et al., 2014). More recent work has shown significant differences in the amounts and composition of trace elements based on whether they are delivered by tidewater glaciers or meltwater streams in Svalbard (Herbert et al., 2020).

In related work, while enhanced iron inputs at these caused enhanced primary production, it was also found that microbial clades dominated with iron reduction processes in sediments closer to glacier with lower salinities, compared to more sulfate reducing clades farther offshore in more saline waters (Buongiorno et al., 2019). Thus, greater inputs of glacially-derived meltwaters (and their associated trace elements) to fjords in a warming climate, will vary spatially as tidewater glaciers retreat into meltwater stream valleys (Bamber et al., 2018).

The way glacial meltwaters mix with marine waters thus plays a crucial role for fjord productivity. For instance, phytoplankton productivity in Kongsfjorden typically peaks in spring after the onset of meltwater-induced stratification and declines as primary producers deplete macronutrient stocks in the stratified water column throughout the summer (Iversen and Seuthe, 2011). Buoyant meltwater plumes also impact foodchain dynamics by creating biologic 'hotspots'. High seasonal inputs massive discharge from glacial waters has been shown to cause mass mortality of surface zooplankton (Weslawski and Legezynska, 1998), something that could also lead to the accumulation of OC near the pycnocline - if much of this material were to sink. For a time, these dead zooplankton can remain in low salinity surface waters for a period of time and provide easy prey to predators such as kittiwakes (*Rissa tridactyla)* and ringed seals (*Pusa hispida*) (Urbanski et al., 2017; Everett et al., 2018).

In summary, microbial activity at the ice sheet surface and bed (e.g., Boetius et al., 2015) fix and accumulate critical amounts of bioavailable carbon and nutrients (N, P, Fe, Si) that are ultimately exported in meltwater runoff to downstream ecosystems (Hood et al., 2015; Hawkings, 2015; Hawkings et al., 2016), where they mix with fjord and marine waters and fuel intense, yet poorly quantified biogeochemical dynamics (Sørensen et al., 2015; Meire et al., 2016, Meire et al., 2017; Hopwood et al., 2018, 2019; Hendry et al., 2019, Wadham et al., 2019).

4. Human influence on biogeochemical dynamics

4.1. Impacts of global warming and land-use change

Impacts of global warming and land-use change in coastal catchments will vary across latitudinal gradients from temperate fjords with forested catchments and relatively higher human population densities to Polar Regions where glaciated fjords are sparsely populated but undergoing dramatic and rapid climate change.

Glaciated high latitude fjords are the 'canary in the coalmine' that are particularly prone to climate change since the rate of warming is three times faster in the Arctic than the global average (ACIA 2004). One-quarter of fjords worldwide are glaciated with marine-terminating outlets (Syvitski and Shaw, 1995) with these outlet glaciers undergoing rapid change due to global warming. In northern Greenland 18 major outlet glaciers have exhibited retreat since 1948 with the rate of retreat higher since the mid-1990s (Hill et al., 2018). This climate-mediated glacier retreat is accelerated by warming ocean waters that melt glaciers from below (Lu et al., 2019), and lead to increased influx of meltwater into polar fjords. The increased meltwater enhances turbidity and can decrease marine primary production, as evidenced by multi-proxy paleorecords from Kongsfjorden, Svalbard Islands, over the last two centuries (Kumar et al., 2018). Sediment records have also shown decreases in primary production in Storfjord in Spitsbergen since the 1960s with increasing air temperature records, which the authors attribute to a reduction in the marginal ice zone from global warming (Winkelmann and Knies, 2005). Increasing water temperatures also affect microbial communities, with warming stimulating heterotrophic microbial biomass and activity over phototrophs (Lara et al., 2013). Further complicating predictions about the impacts on productivity in fjords are documented range extensions of species in response to warming seas (Węsławski et al., 2010), which can alter trophic relationships and the amount of productivity that is incorporated into higher trophic levels or settles to the seabed.

Atmospheric warming has increased ocean temperatures in the Arctic and altered sea ice cover, with sea ice extent now decreasing at a rate of 10% per decade (Stroeve et al., 2007). Alterations in sea ice extent and thickness can induce photochemical decay of POC, which would affect the biological carbon pump and have important implications for carbon turnover and nutrient cycling in polar coastal margins including fjords. Sedimentation in polar fjords is mainly controlled by meltwater dynamics and erosion by sea ice and glaciers, resulting in high supply of terrigenous OC (Winkelmann and Knies, 2005). This has been verified by 6-years of continuous monitoring of particle fluxes in Kongsfjorden, Svalbard, that has undergone rapid sea ice loss and glacier retreat in recent decades. Particle fluxes in Kongsfjorden recorded a predominance of glacier carbonate and siliclastic fluxes with a 1 to 2-month lag following glacier melting, with addition of marine inputs during solar maxima (D'Angelo et al., 2018). The results suggest that land-derived OC will dramatically increase under a future warming scenario. Further, permafrost degradation from climate warming releases previously-stored detritus into coastal waters (Wassmann, 2011) and may augment terrestrial OC inputs to coastal regions in high latitudes. For example, the North Pacific warm water anomaly, commonly known as the Blob, when present, has been shown to increase rainfall in fjords of British Columbia, Canada, resulting in high flues of particulates and nutirents, with strong evidence of silica being exportd from fjords to the shelf (Johannessen et al., 2019). Accordingly, climate-mediated changes in glacier melt dynamics and sea ice cover will lead to changes in inorganic supply and physical conditions in fjords (Piwosz et al., 2009; Juul-Pedersen et al., 2015) that will influence productivity and carbon cycling in polar fjords.

Climatic-oceanographic changes that dominate impacts in the high latitude fjords typically have no humans or negligible human population densities and anthropogenic land-use changes are therefore unlikely to affect them to the same extent than in temperate fjords. By contrast, cultural eutrophication associated with intensification of land-use for agriculture or deforestation in watersheds of some temperate fjords is likely to increase autochthonous productivity and enhance carbon recycling (Smittenberg et al., 2004a). Increased marine production and enhanced biological consumption in combination with decreases in solubility of dissolved oxygen concentrations from warming seas (Keller et al., 2016) may change oxygen content in fjord bottom waters, which could influence OC mineralization. For instance, models demonstrate that temporal fluctuations in oxic-anoxic conditions in sediments can switch major pathways of OM mineralization between aerobic respiration in winter and spring and sulfate reduction in summer and autumn (Friedrich et al., 2014). In the Odense Fjord in Denmark, models of future agriculture scenarios in the watershed demonstrate that nitrate loads will interact with climate-mediated changes in freshwater discharge rates, highlighting the importance of considering multiple stressors to achieve environmental goals (Molina-Navarro et al., 2018). Similarly, in Patagonia's fjord systems regional patterns in climatic-oceanographic events like El Niño Southern Oscillation and large-scale climatic forcings are anticipated to interact with local anthropogenic activities including forestry and aquaculture to influence biogeochemical processes (Iriarte, 2018). Reduced precipitation due to global warming results in an increased influence of oceanic water and reduced water turnover time in Patagonian fjords (León-Muñoz et al., 2013). Around New Zealand, shifts in the Southern Hemisphere westerly wind patterns are strongly linked to regional precipitation in Fiordland (Hinojosa et al., 2017), with anticipated strengthening of westerly winds bringing higher orographic rainfall and potentially increased incidence of mass wasting events. In temperate fjords with vegetated watersheds like Chilean Patagonia and New Zealand, allochthonous subsidies dominate OM inputs to fjords (Vargas et al., 2010; Smith et al., 2015; Cui et al., 2016a,b,c). In these systems, management of human pressures that modify the terrestrial habitat is crucial to maintain these forest—fjord interactions, placing particular importance on maintaining protection like the Fiordland National Park in New Zealand that prevents land-use change.

Predicted changes in atmospheric circulation will also likely impact fjord systems in the future. For example, the strength and latitudinal position of the southern hemisphere westerly winds control the amount and distribution of precipitation in New Zealand and southern Chile (Garreaud, 2007). When the core of the strongest winds shift to the south or weaken, rainfall throughout these regions is reduced due to a displacement of the primary storm tracks. Global climate models predict that southward displacement of the winds will be a key feature of late 21st century circulation, coincident with a more frequent occurrence of the positive phase of the Southern Annular Mode, which strengthens and shifts the westerlies poleward (Eun-Pa et al., 2016; Yin, 2005). The reduction of rainfall and primary river discharge into fjords within these regions will likely impact the thickness and extent of the low-salinity layer in the upper reaches of the fjord, which will ultimately slow the rate of the overturning circulation and deep water renewal. These changes will likely impact bottom water oxygen concentrations ultimately impacting carbon burial rates and benthic ecology. In fact, warming in fjords of the Antarctic Peninsula have resulted in hotspots and shifts in benthic communities (Grange and Smith, 2013; Sahade et al., 2015; Grange et al., 2017).

A key challenge remains to predict whether global climate change and land-use change will act synergistically or antagonistically to influence allochthonous subsidies, marine productivity and biogeochemical processes in fjords and how this will vary across latitudinal gradients.

4.2. Management of fjords in the future

The vicinity of these marine environments to humans has led to calls for fjords to be used for the economic benefits of local and national populations. The clearest sign of this is the significant expansion of both shell and finfish aquaculture sites within the fjords of Norway, Scotland, Chile, and British Columbia. Fjords are the ideal location for this activity as the geomorphology shelters the cages and the tidal forces disperse pollutants (fecal waste, food, antibiotics, heavy metals, etc), however the siting of marine farms needs to be carefully considered alongside circulation models (Levings et al., 1995; Foreman et al., 2009). In 2017 the Scottish aquaculture sector was valued at £1.8 Billion which is expected to double by 2030 and support over 18,000 jobs (Burnett, 2016); this is a pattern mirrored globally (EY Group, 2017; Niklitschek et al., 2013). Aquaculture does have issues ranging from habitat loss, increased nutrient loading, marine litter and disturbance of marine food webs (Niklitschek et al., 2013; Skaala et al., 2014), therefore to allow unhindered expansion of the industry will come with environmental effects and impacts that must be managed.

A recent suggestion is to use the fjords ability to trap and store C to reduce CO_2 released from commercial forestry. Zimmerman and Cornelissen (2018) suggest using deep anoxic fjord basins as dumping grounds for fresh forestry waste. They argue the deep low oxygen conditions will prevent the breakdown of the waste and reduce the quantity of CO_2 released to the atmosphere. This suggestion is essentially "light" geoengineering where the potential wins (i.e. atmospheric CO_2 reductions) are largely offset by large unknowns. Dumping significant quantities of largely acidic coniferous forest waste into the fjords has a high potential to disrupt the specific conditions needed to store C (e.g. water column and sediment pH, oxygen conditions). Additionally, seabed sediments will be disturbed, suspending the sediment allowing further remineralization potentially offsetting any gains in CO_2 trapping due to the dumping of the forestry material. The geomorphological and biogeochemical nature of fjords provide a significant ecosystem service through the burial (Smith et al., 2015) and storage of C from throughout the Holocene (Smeaton et al., 2016, 2017), thus any future geoengineering and disturbance of these sediment stores will require careful consideration. Management focus should be on maintaining these systems' natural ability to trap C and preventing the disturbance of the significant quantities of C already stored in these systems, for example through the creation of Marine Protected Areas which recognize the value of sedimentary carbon stores alongside other ecosystem services (e.g. Burrows et al., 2014).

Dumping waste in fjords is not uncommon, northern Norway has been dumping and discharging mining waste/tailings since at least the 1970's into the fjords as a low cost alternative to transporting and land-based disposal (Andersson et al., 2018; Brooks et al., 2018; Sternal et al., 2017). Though Norway has the longest history of waste disposal, fjords in British Colombia (Odhiambo et al., 1996; Petticrew et al., 2015) and Greenland (Loring and Asmund, 1989) have also received mining tailings. These sites become heavily contaminated with metals which damage benthic communities (Trannum et al., 2018). Further the fate of much of this waste is unknown as the tailings are known to be transported within fjords (Andersson et al., 2018). Though this approach to disposal of mine waste is relatively new, sediment records from Loch Sunart in Scotland show that in-wash from Lead mining within the catchment during the Napoleonic wars likely caused the same problems with large inputs of metals (Cage and Austin, 2010).

The thick accumulation of sediments in these unique continental margin settings often requires drilling technology to obtain records that span the full range of climate conditions, including conditions that may represent analogues for what is projected for our future. International drilling programs such as the International Continental Scientific Drilling Program (ICDP) and the International Ocean Discovery Program (IODP) have largely targeted terrestrial and marine basins of sediment accumulation, but continental margins, including fjord systems, remain largely unexplored (Huntley et al., 2001).

Today and in the future, fjords are and will be under pressure from climate and environmental change alongside the need for them to be economically productive (i.e. aquaculture, mining). Going forward we must remember that what make these environments productive and useful for aquaculture or enhanced carbon capture is their unique geomorphology and biogeochemistry; therefore, the management of these often remote and iconic systems should focus on retaining and protecting these attributes.

Declaration of Competing Interest

The authors declare that they have no known competing financial interests or personal relationships that could have appeared to influence the work reported in this paper.

Acknowledgments

The Jon and Beverly Thompson Endowed Chair in Geological Sciences at the University of Florida supported T. Bianchi's time and effort in writing this manuscript. Katarzyna Koziorowska-Makuch's participation in this study was supported by the Foundation for Polish Science (FNP). X. Cui would like to acknowledge Simons Foundation collaboration on the origins of life at Massachusetts Institute of Technology. W. Austin and C. Smeaton are funded by Marine Scotland through the Scottish Blue Carbon Forum.S. Arndt acknowledges funding from the European Union's Horizon 2020 research and innovation programme under the Marie Skłodowska-Curie grant agreement no.643052 (C-CASCADES project). J. Faust would like to acknowledge the ChAOS project (NE/P006493/1), part of the Changing Arctic Ocean programme and funded by the UKRI Natural Environment Research Council (NERC).All authors would like to thank Graeme Sandeman (University of St Andrews) for his assistance in (re-)drafting the figures for this manuscript.

References

Aarseth, I., 1997. Western Norwegian fjord sediments: age, volume, stratigraphy, and role as temporary depository during glacial cycles. Mar. Geol. 143 (1–4), 39–53.

Amiotte Suchet, P., Probst, J.L., Ludwig, W., 2003. Worldwide distribution of continental rock lithology: implications for the atmospheric/soil CO_2 uptake by continental weathering and alkalinity river transport to the oceans. Glob. Biogeochem. Cycles 17 (2), 1038. https://doi.org/10.1029/2002GB00189.

Anderson, L.G., Dyrssen, D., Hall, P.O.J., 1988. On the sulfur chemistry of a super-anoxic fjord, Framvaren, South Norway. Mar. Chem. 23, 283–293.

Anderson, L.G., Jutterstro, S., Hjalmarsson, S., Wåhlstrom, I., Semiletov, I.P., 2009. Outgassing of CO_2 from Siberian Shelf seas by terrestrial organic matter decomposition. Geophys. Res. Lett. 36, L20601. https://doi.org/10.1029/2009GL040046.

Andersson, M., Finne, T.E., Jensen, L.K., Eggen, O.A., 2018. Geochemistry of a copper mine tailings deposit in Repparfjorden, northern Norway. Sci. Total Environ. 644, 1219–1231.

Andrews, J.T., Principato, S.M., 2002. Grain-size characteristics and provenance of ice-proximal glacial marine sediments. Geol. Soc. Lond. Spec. Publ. 203 (1), 305–324.

Andrews, J.T., Syvitski, J.P.M., 1994. Sediment fluxes along high-latitude glaciated continental margins: Northeast Canada and eastern Greenland. In: Hay, W. (Ed.), Global Sedimentary Geofluxes. Nat. Acad. Sci. Press, Washington, pp. 99–115.

Andrews, J.T., Smith, L.M., Preston, R., Cooper, T., Jennings, A.E., 1997. Spatial and temporal patterns of iceberg rafting (IRD) along the East Greenland margin, ca. 68 N, over the last 14 cal. ka. J. Quat. Sci. 12, 1–13.

Anesio, A.M., Laybourn-Parry, J., 2012. Glaciers and ice sheets as a biome. Trends Ecol. Evol. 27, 219–225.

Anesio, A.M., Hodson, A.J., Fritz, A., Psenner, R., Sattler, B., 2009. High microbial activity on glaciers: Importance to the global carbon cycle. Glob. Chang. Biol. 15, 955–960. https://doi.org/10.1111/j.1365-2486.2008.01758.x.

Aracena, C., Lange, C.B., Iriarte, J.L., Rebolledo, L., Pantoja, S., 2011. Latitudinal patterns of export production recorded in surface sediments of the Chilean Patagonian fjords (41–55 S) as a response to water column productivity. Cont. Shelf Res. 31, 340–355.

Aracena, C., Kilian, R., Lange, C.B., Bertrand, S., Lamy, F., Arz, H.W., De Pol-Holz, R., Baeza, O., Pantoja, S., Kissel, C., 2015. Holocene variations in productivity associated with changes in glacier activity and freshwater flux in the central basin of the Strait of Magellan. Palaeogeogr. Palaeoclimatol. Palaeoecol. 436, 112–122.

Ariztegui, D., Bianchi, M.M., Masaferro, J., Lafargue, E., Niessen, F., 1997. Interhemispheric synchrony of Late-glacial climatic instability as recorded in proglacial Lake Mascardi, Argentina. J. Quat. Sci. 12, 333–338.

Austin, W.E., Inall, M.E., 2002. Deep-water renewal in a Scottish fjord: temperature, salinity and oxygen isotopes. Polar Res. 21 (2), 251–257.

Azetsu-Scott, K., Syvitski, J.P.M., 1999. Influence of melting icebergs on distribution, characteristics and transport of marine particles in an East Greenland fjord. J. Geophys. Res. 104, 5321–5328.

Bakke, J., Trachsel, M., Kvisvik, B.C., Nesje, A., Lyså, A., 2013. Numerical analyses of a multi-proxy data set from a distal glacier-fed lake, Sørsendalsvatn, Western Norway. Quat. Sci. Rev. 73, 182–195.

Baltzer, A., Bates, C.R., Mokeddem, Z., Clet-Pellerin, M., Walter Simonnet, A.V., Bonnot Courtois, C., Austin, W.E.N., 2010. Using seismic facies and pollen analyses to evaluate climatically driven change in a Scottish Sea loch (fjord) over the last 20 ka. Geol. Soc. Lond. Spec. Publ. 344, 355–369.

Bamber, J.L., Westaway, R.M., Marzeion, B., Wouters, B., 2018. A new synthesis of annual land ice mass trends 1992 to 2016. Pangea. https://doi.org/10.1594/PANGAEA.890030.

Bartholomaus, T.C., Larsen, C.F., O'Neel, S., 2013. Does calving matter? Evidence for significant submarine melt. Earth Planet. Sci. Lett. 380, 21–30.

Bartholomew, I.D., Nienow, P., Mair, D., Hubbard, A., King, M.A., Sole, A.J., 2010. Seasonal evolution of subglacial drainage and acceleration in a Greenland outlet glacier. Nat. Geosci. 3, 408–411. https://doi.org/10.1038/ngeo863.

Bartholomew, I., Nienow, P., Sole, A., Mair, D., Cowton, T., Palmer, S., Wadham, J., 2011. Supraglacial forcing of subglacial drainage in the ablation zone of the Greenland ice sheet. Geophys. Res. Lett. 85, L08502.

Bellwald, B., Hjelstuen, B.O., Sejrup, H.P., Haflidason, H., 2016. Postglacial mass movements and depositional environments in a high-latitude fjord system–Hardangerfjorden, Western Norway. Mar. Geol. 379, 157–175.

Bellwald, B., Hjelstuen, B.O., Sejrup, H.P., Stokowy, T., Kuvås, J., 2019. Holocene mass movements in west and mid-Norwegian fjords and lakes. Mar. Geol. 407, 192–212.
Bendixen, M., Iversen, L.L., Bjork, A.A., Elberling, B., Westergaard-Nielsen, A., Overeem, I., Barnhart, K.R., Kahn, S.A., Box, J.E., Abermann, J., Langlen, K., Kroom, A., 2017. Delta progradation in Greenland driven by increasing glacial mass loss. Nature 550, 101–106.
Benn, D.I., Evans, D.J.A., 2010. Glaciers and Glaciation, 2nd ed. Hodder, London.
Benn, D.I., Åström, J.A., 2018. Calving glaciers and ice shelves. Adv. Phys. 3 (1), 1513819.
Benn, D.I., Warren, C.R., Mottram, R.H., 2007. Calving processes and the dynamics of calving glaciers. Earth Sci. Rev. 82 (3–4), 143–179.
Benner, R., Newell, S.Y., Maccubbin, A.E., Hodson, R.E., 1984. Relative contribution of bacteria and fungi to rates of degradation of lignocellulosic detritus in salt-marsh sediment. Appl. Environ. Microbiol. 48, 3640.
Berger, W.H., Heath, R.G., 1968. Vertical mixing in pelagic sediments. J. Mar. Res. 26, 134–143.
Berner, R.A., 1982. Burial of organic carbon and pyrite sulfur in the modern ocean: its geochemical and environmental significance. Am. J. Sci. 282, 451–473.
Berner, R.A., 1989. Biogeochemical cycles of carbon and sulfur and their effect on atmospheric oxygen over Phanerozoic time. Palaeogeogr. Palaeoclimatol. Palaeoecol. 75, 97–122.
Bertrand, S., Hughen, K.A., Lamy, F., Stuut, J.B.W., Torrejón, F., Lange, C.B., 2012a. Precipitation as the main driver of Neoglacial fluctuations of Gualas glacier, Northern Patagonian Ice field. Clim. Past 8, 519–534.
Bertrand, S., Hughen, K.A., Sepulveda, J., Pantoja, S., 2012b. Geochemistry of surface sediments from the fjords of Northern Chilean Patagonia (44–47°S): Spatial variability and implications for paleoclimate reconstructions. Geochim. Cosmochim. Acta 76, 125–146.
Bertrand, S., Hughen, K., Sepúlveda, J., Pantoja, S., 2014. Late Holocene covariability of the southern westerlies and sea surface temperature in northern Chilean Patagonia. Quat. Sci. Rev. 105, 195–208.
Bertrand, S., Lange, C.B., Pantoja, S., Hughen, K., Van Tornhout, E., Wellner, J.L., 2017. Postglacial fluctuations of Cordillera Darwin glaciers (southernmost Patagonia) reconstructed from Almirantazgo fjord sediments. Quat. Sci. Rev. 177, 265–275.
Bhatia, M., Das, S.B., Longnecker, K., Charette, M.A., Kujawinski, E.B., 2010. Molecular characterization of dissolved organic matter associated with the Greenland ice sheet. Geochim. Cosmochim. Acta 74, 3768–3784.
Bhatia, M.P., Das, S.B., Xu, L., Charette, M.A., Wadham, J.L., Kujawinski, E.B., 2013. Organic carbon export from the Greenland ice sheet. Geochim. Cosmochim. Acta 109, 329–344.
Bianchi, T.S., Canuel, E.A., 2011. Chemical Biomarkers in Aquatic Ecosystems. Princeton University Press 396 pp.
Bianchi, T.S., Morrison, E., 2018. Human activities create corridors of change in aquatic zones. EOS 99 (11), 13–15. https://doi.org/10.1029/2018EO104743.
Bianchi, T.S., Schreiner, K.M., Smith, R.W., Burdige, D.J., Woodard, S., Conley, D.J., 2016. Redox effects on organic matter storage in coastal sediments during the Holocene: a biomarker/proxy perspective. Annu. Rev. Earth Planet. Sci. 44, 295–319.
Bianchi, T.S., Cui, X.Q., Blair, N.E., Burdige, D.J., Eglinton, T.I., Galy, V., 2018. Centers of organic carbon burial and oxidation at the land-ocean interface. Org. Geochem. 115, 138–155.
Bianucci, L., Balaguru, K., Smith, R.W., Moriarty, J.M., 2018. Sci. Rep. 8, 15740. https://doi.org/10.1038/s41598-018-33640-3.
Bjørk, A.A., Kjær, K.H., Korsgaard, N.J., Khan, S.A., Kjeldsen, K.K., Andresen, C.S., Box, J.E., Larsen, N.K., Funder, S., 2012. An aerial view of 80 years of climate-related glacier fluctuations in Southeast Greenland. Nat. Geosci. 5, 427–432.
Blattmann, T.M., Zhang, Y., Zhao, Y., Wen, K., Lin, S., Li, J., Wacker, L., Haghipour, N., Plötze, M., Liu, Z., Eglinton, T.I., 2018. Contrasting fates of petrogenic and biospheric carbon in the South China Sea. Geophys. Res. Lett. 45. https://doi.org/10.1029/2018GL079222.
Blattmann, T.M., Liu, Z., Zhang, Y., Zhao, Y., Haghipour, N., Montluçon, D.B., Plötze, M., Eglinton, T.I., 2019. Mineralogical control on the fate of continentally derived organic matter in the ocean. Science 366, 742–745.
Boetius, A., Anesio, A.M., Deming, J.W., Mikucki, J.A., Rapp, J.Z., 2015. Microbial ecology of the cryosphere: sea ice and glacial habitats. Nat. Rev. Microbiol. 13, 677–690.
Boldt, K.V., 2014. Fjord sedimentation during the rapid retreat of tidewater glaciers: observations and modelling. In: PhD thesis in Geological Oceanography. University of Washington (162 pp).
Bornhold, B.D., Harper, J.R., McLaren, D., Thomson, R.E., 2007. Destruction of the First Nations Village of Kwalate by a rock avalanchegenerated tsunami. Atmosphere-Ocean 45, 123–128.
Boudreau, B.P., 1998. Mean mixed depth of sediments: the wherefore and the why. Limnol. Oceanogr. 43, 524–526.
Brooks, S.J., Escudero-Oñate, C., Gomes, T., Ferrando-Climent, L., 2018. An integrative biological effects assessment of a mine discharge into a Norwegian fjord using field transplanted mussels. Sci. Total Environ. 644, 1056–1069.
Brown, F.S., Baedecker, M.J., Nissenbaum, A., Kaplan, I.R., 1972. Early diagenesis in a reducing fjord, Saanich Inlet, British Columbia—III. Changes in organic constituents of sediment. Geochim. Cosmochim. Acta 36, 1185–1203.
Browne, I.M., Moy, C.M., Riesselman, C.R., Neil, H.L., Curtin, L.G., Gorman, A.R., Wilson, G.S., 2017. Late Holocene intensification of the westerly winds at the sub Antarctic Auckland Islands (51°S), New Zealand. Clim. Past 1–37.
Bullard, J.E., Baddock, M., Bradwell, T., Crusius, J., Darlington, E., Gaiero, D., Gassó, S., Gisladottir, G., Hodgkins, R., McCulloch, R., McKenna-Neuman, C., Mockford, T., Stewart, H., Thorsteinsson, T., 2016. High-latitude dust in the Earth system. Rev. Geophys. 54, 447–485. https://doi.org/10.1002/2016RG000518.
Buongiorno, J., Herbert, L.C., Wehrmann, L.M., Michaud, A.B., Laufer, K., Røy, H., Jørgensen, B.B., Szynkiewicz, A., Faiia, A., Yeager, K.M., Schindler, K., Lloyd, K.G., 2019. Complex microbial communities drive iron and sulfur cycling in Arctic fjord sediments. Appl. Environ. Microbiol. 85https://doi.org/10.1128/AEM.00949-19. (e00949–19).
Burdige, D.J., 2005. Burial of terrestrial organic matter in marine sediments: a re-assessment. Glob. Biogeochem. Cycles 19, GB4011.
Burkins, M.B., Virginia, R.A., Wall, D.H., 2001. Organic carbon cycling in Taylor Valley, Antarctica: quantifying soil reservoirs and soil respiration. Glob. Chang. Biol. 7, 113–125.
Burnett, S., 2016. A Strategic Plan for Farming Scotland's Seas: Aquaculture Growth to 2030. Accessible from. http://scottishsalmon.co.uk/wp-content/uploads/2016/10/aquaculture-growth-to-2030.pdf.
Burrell, D.C., 1988. Carbon flow in fjords. Oceanogr. Mar. Biol. 26, 143–226.
Burrows, M.T., Schoeman, D.S., Richardson, A.J., García Molinos, J., Hoffmann, A., Buckley, L.B., Moore, P.J., Brown, C.J., Bruno, J.F., Duarte, C.M., Halpern, B.S., Hoegh-Guldberg, O., Kappel, C.V., Kiessling, W., O'Connor, M.I., Pandolfi, J.M., Parmesan, C., Sydeman, W.J., Ferrier, S., Williams, K.J., Poloczanska, E.S., 2014. Geographical limits to species-range shifts are suggested by climate velocity. Nature 507, 492–495.
Cage, A.G., Austin, W.E.N., 2010. Marine climate variability during the last millennium: the Loch Sunart record, Scotland, UK. Quat. Sci. Rev. 29, 1633–1647.
Cage, A.G., Heinemeier, J., Austin, W.E.N., 2006. Marine radiocarbon reservoir ages in Scottish coastal and fjordic waters. Radiocarbon 48 (31–43), 2006.
Cage, A.G., Davies, S.M., Wastegard, S., Austin, W.E.N., 2011. Identification of the Icelandic Landnam tephra (AD 871 +/− 2) in Scottish fjordic sediment. Quat. Int. 246, 168–176.
Calvete, C., Sobarzo, M., 2011. Quantification of the surface brackish water layer and frontal zones in southern Chilean fjords between Boca del Guafo (43°30'S) and Estero Elefantes (46°30'S). Cont. Shelf Res. 31, 162–171. https://doi.org/10.1016/j.csr.2010.09.013.
Canfield, D.E., 1989. Sulfate reduction and oxic respiration in marine sediments: implications for organic carbon preservation in euxinic environments. Deep-Sea Res. 36 (1), 121–138.
Caniupán, M., Lamy, F., Lange, C.B., Kaiser, J., Kilian, R., Arz, H.W., León, T., Mollenhauer, G., Sandoval, S., De Pol-Holz, R., Pantoja, S., Wellner, J., Tiedemann, R., 2014. Holocene sea-surface temperature variability in the. Chilean fjord region Quaternary Research 82 (2), 342–353.
Cape, M.R., Straneo, F., Beaird, N., Bundy, R.M., Charette, M.A., 2019. Nutrient release to oceans from buoyancy-driven upwelling at Greenland tidewater glaciers. Nat. Geosci. 12, 34–39.
Carr, J.R., Stokes, C., Vieli, A., 2014. Recent retreat of major outlet glaciers on Novaya Zemlya, Russian Arctic, influenced by fjord geometry and sea-ice conditions. J. Glaciol. 60 (219), 155–170. https://doi.org/10.3189/2014JoG13J122.
Carrington, D., 2016. The Anthropocene epoch: scientists declare dawn of human influenced age. In: The Guardian (April 19), Retrieved from. http://www.theguardian.com.
Carroll, M.L., Carroll, J., 2003. The Arctic Seas. In: Shimmield, G.B., Black, K.D. (Eds.), Biogeochemistry of Marine Systems. Blackwell Publishing, pp. 127–156.
Carroll, J., Zaborska, A., Papucci, C., Schirone, A., Carroll, M.L., Pempkowiak, J., 2008. Accumulation of organic carbon in western Barents Sea sediments. Deep-Sea Res. II 55 (20 − 21), 2361–2371. https://doi.org/10.1016/j.dsr2.2008.05.005.
Carter, L., 1976. Seston transport and deposition in Pelorus Sound, South Island, New Zealand. NZ J. Mar. Freshwat. Res. 10, 263–282.
Chandler, D.M., Wadham, J.L., Lis, G.P., Cowton, T., Sole, A., Bartholomew, I., 2013. Evolution of the subglacial drainage system beneath the Greenland Ice Sheet revealed by tracers. Nat. Geosci. 6, 195–198. https://doi.org/10.1038/ngeo1737.
Chapman, S.J., Bell, J., Donnelly, D., Lilly, A., 2009. Carbon stocks in Scottish peatlands. Soil Use Manag. 25, 105–112. https://doi.org/10.1111/j.1475-2743.2009.00219.x.
Christoffersen, P., O'Leary, M., van Angelen, J.H., van den Broeke, M., 2012. Partitioning effects from ocean and atmosphere on the calving stability of Kangerdlugssuaq Glacier, East Greenland. Ann. Glaciol. 53 (60), 249–256.
Chu, V.W., 2014. Greenland Ice Sheet hydrology: a review. Prog. Phys. Geogr. 38 (1), 19–54. https://doi.org/10.1177/0309133313507075.
Clare, M.A., Hughes Clarke, J.E., Talling, P.J., Cartigny, M.J.B., Pratomo, D.G., 2016. Preconditioning and triggering of offshore slope failures and turbidity currents revealed by most detailed monitoring yet at a fjord-head delta. Earth Planet. Sci. Lett. 450, 208–220.
Comiso, J.C., 2006. Abrupt decline in the Arctic winter sea ice cover. Geophys. Res. Lett. 33, L18504. https://doi.org/10.1029/2006GL027341.
Cornelissen, A.D., Wing, S.R., Clark, K.L., Bowman, M.H., Frew, R.D., Hurd, C.L., 2007. Patterns in the $\delta^{13}C$ and $\delta^{15}N$ signature of *Ulva pertusa*: Interaction between physical gradients and nutrient source pools. Limnol. Oceanogr. 52, 820–832.
Cottier, F.R., Nilsen, F., Skogseth, R., Tverberg, V., Skarthhamar, J., Svendsen, H., 2010. Arctic fjords: a review of the oceanographic environment and dominant physical processes. Geol. Soc. Lond. Spec. Publ. 344 (1), 35–50. https://doi.org/10.1144/SP344.4.
Cowan, E.A., Powell, R.D., 1991. Ice-proximal sediment accumulation rates in a temperate glacial fjord, southeastern Alaska. In: Anderson, J.B., Ashley, G.M. (Eds.), Glacial Marine Sedimentation: Paleoclimatic Significance, pp. 61–73 Boulder Co., Geol. Society America Spec. Paper 261.
Cowan, E.A., Seramur, K.C., Cai, J., Powell, R.D., 1999. Cyclic sedimentation produced by fluctuations in meltwater discharge, tides and marine productivity in an Alaskan fjord. Sedimentol. 46, 1109–1126.
Cowan, E.A., Seramur, K.C., Powell, R.D., Willems, B.A., Bulick, S.P.S., Jaeger, J.M., 2010. Fjords as temporary sediment traps: history of glacial erosion and deposition in

Muir Inlet, Glacier Bay National Park, southeastern Alaska. Geol. Soc. Am. Bull. 122, 1067–1080.
Cowton, T., Nienow, P., Sole, A., Wadham, J., Lis, G., Bartholomew, I., Mair, D., Chandler, D., 2013. Evolution of drainage system morphology at a land-terminating Greenlandic outlet glacier. J. Geophys. Res. Earth Surf. 118 (1), 29–41.
Cowton, T., Slater, D., Sole, A., Goldberg, D., Nienow, P., 2015. Modeling the impact of glacial runoff on fjord circulation and submarine melt rate using a new subgrid-scale parameterization for glacial plumes. J. Geophys. Res. Oceans 120 (2), 796–812.
Croudace, I.W., Rothwell, R.G. (Eds.), 2015. Micro-XRF Studies of Sediment Cores: Applications of a Non-Destructive Tool for the Environmental Sciences. Vol. 17 Springer.
Crutzen, P.J., Stoermer, E.E., 2000. The 'Anthropocene'. IGBP Newsl. 41, 17–18.
Cui, X., Bianchi, T.S., Hutchings, J.A., Savage, C., Curtis, J.H., 2016a. Partitioning of organic carbon among density fractions in surface sediments of Fiordland, New Zealand. J. Geophys. Res. Biogeosci. 121, 1016–1031.
Cui, X., Bianchi, T.S., Jaeger, J.M., Smith, R.W., 2016b. Biospheric and petrogenic organic carbon flux along Southeast Alaska. Earth Planet. Sci. Lett. 452, 238–246.
Cui, X., Bianchi, T.S., Savage, C., Smith, R.W., 2016c. Organic carbon burial in fjords: terrestrial versus marine inputs. Earth Planet. Sci. Lett. 451, 41–50.
Cui, X., Bianchi, T.S., Savage, C., 2017a. Erosion of modern terrestrial organic matter as a major component of sediments in fjords. Geophys. Res. Lett. 44, 1457–1465.
Cui, X., Bianchi, T.S., Kenney, W.F., Wang, J., Curtis, J.H., Xu, K., 2017b. Carbon dynamics along a temperate fjord-head delta: linkages with carbon burial in fjords. J. Geophys. Res. - Biogeo. 122 (12), 3419–3430.
Cundill, P.R., Austin, W.E.N., Davies, S.E., 2006. Modern pollen from the catchment and surficial sediments of a Scottish Sea loch (fjord). Grana 45 (3), 230–238. https://doi.org/10.1080/00173130600873919.
Curran, K.J., Hill, P.S., Milligan, T.G., Cowan, E.A., Syvitski, J.P.M., Konings, S.M., 2004. Fine-grained sediment flocculation below the Hubbard Glacier meltwater plume, Disenchantment Bay, Alaska. Mar. Geol. 203, 83–94.
Dalpadado, P., Hop, H., Rønning, J., Pavlov, V., Sperfeld, E., Buchholz, F., Rey, A., Wold, A., 2016. Distribution and abundance of euphausiids and pelagic amphipods in Kongsfjorden, Isfjorden and Rijpfjorden (Svalbard) and changes in their relative importance as key prey in a warming marine ecosystem. Polar Biol. https://doi.org/10.1007/s00300-015-1874-x.
Damsté, J.S.S., Rijpstra, W.I.C., Coolen, M.J., Schouten, S., Volkman, J.K., 2007. Rapid sulfurisation of highly branched isoprenoid (HBI) alkenes in sulfidic Holocene sediments from Ellis Fjord, Antarctica. Org. Geochem. 38, 128–139.
D'Angelo, A., Giglio, F., Miserocchi, S., Sanchez-Vidal, A., Aliani, S., Tesi, T., Viola, A., Mazzola, M., Langone, L., 2018. Multi-year particle fluxes in Kingsfjorden, Svalbard. Biogeosc. 15, 5343–5363.
Dlabola, E.K., Wilson, G.S., Gorman, A.R., Riesselman, C.R., Moy, C.M., 2015. A post-glacial relative sea-level curve from Fiordland, New Zealand. Global Planet. Chang. 131, 104–114.
Domack, E.W., Foss, D., Syvitski, J.P.M., McClennen, C.E., 1994. Transport of suspended particulate matter in an Antarctic fjord. Mar. Geol. 121, 161–170.
Dowdeswell, J.A., Evans, J., Cofaigh, C., 2010. Submarine landforms and shallow acoustic stratigraphy of a 400 km-long fjord-shelf-slope transect, Kangerlussuaq margin, East Greenland. Quat. Sci. Rev. 29 (25–26), 3359–3369.
Dowdeswell, J.A., Canals, M., Jakobsson, M., Todd, B.J., Dowdeswell, E.K., Hogan, E.K. (Eds.), 2016. Atlas of Submarine Glacial Landforms: Modern, Quaternary and Ancient. Geological Society, London, pp. 65–66 Memoirs 46.
Duffield, C.J., Alve, E., Andersen, N., Andersen, T.J., Hess, S., Strohmeier, T., 2017. Spatial and temporal organic carbon burial along a fjord to coast transect: a case study from Western Norway. The Holocene 27, 1325–1339.
Durr, H.H., Laruelle, G.G., van Kempen, C.M., Slomp, C.P., Meybeck, M., Middelkoop, H., 2011. Worldwide typology of nearshore coastal systems: defining the estuarine filter of river inputs to the oceans. Estuar. Coasts 34, 441–458.
Engstrom, 1975 ld,',tjord Report i-Il (Report No. 192 and 193, Havsfiskelaboratoriet, Lysekil, Sweden.
Eun-Pa, L., Hendon, H.H., Arblaster, J.M., Delage, F., Nguyen, H., Ki Min, S., Wheeler, M.C., 2016. The impact of the Southern Annular Mode on future changes in Southern Hemisphere rainfall. Geophys. Res. Lett. 43, 7160–7167.
Everett, A., Kohler, J., Sundfjord, A., Kovacs, K.M., Torsvik, T., Pramanik, A., Boehme, L., Lydersen, C., 2018. Subglacial discharge plume behaviour revealed by CTD-instrumented ringed seals. Sci. Report. 8 (1), 13467.
EY Group, 2017. The Norwegian Aquaculture Analysis 2017. Accessible from: https://www.ey.com/Publication/vwLUAssets/EY_-The_Norwegian_Aquaculture_Analysis_2017/$FILE/EY-Norwegian-Aquaculture-Analysis-2017.pdf.
Fallesen, G., Andersen, F., Larsen, B., 2000. Life, death and revival of the hypertrophic Mariager Fjord, Denmark. J. Mar. Syst. 25, 313–321.
Farias, L., Sanzana, K., Sanhueza-Guevara, S., Yevenes, M.A., 2017. Dissolved methane distribution in the Reloncaví Fjord and adjacent marine system during Austral Winter (41°–43° S). Estuar. Coasts 40 (6), 592–1606.
Farmer, D.M., Freeland, H.J., 1983. The Physical oceanography of fjords. Prog. Oceanogr. 12 (2).
Farrow, G.E., Syvitski, J.P.M., Tunnicliffe, V., 1983. Suspended particulate loading on the macrobenthos in a highly turbid fjord; Knight Inlet, British Columbia, Canada. Fish. Aquat. Sci. 40, 100–116.
Faust, J.C., Knies, J., 2019. Organic matter sources in North Atlantic fjord sediments. Geochem. Geophys. Geosyst. 20, 2872–2885. https://doi.org/10.1029/2019GC008382.
Faust, J.C., Knies, J., Slagstad, T., Vogt, C., Milzer, G., Giraudeau, J., 2014. Geochemical composition of Trondheimsfjord surface sediments: sources and spatial variability of marine and terrigenous components. Cont. Shelf Res. 88, 61–71.
Faust, J.C., Knies, J., Milzer, G., Giraudeau, J., 2014b. Terrigenous input to a fjord in Central Norway records the environmental response to the North Atlantic Oscillation over the past 50 years. The Holocene 24, 1411–1418. https://doi.org/10.1177/0959683614544052.
Faust, J.C., Fabian, K., Milzer, G., Giraudeau, J., Knies, J., 2016. Norwegian fjord sediments reveal NAO related winter temperature and precipitation changes of the past 2800 years. Earth Planet. Sci. Lett. 435, 84–93.
Faust, J.C., Scheiber, T., Fabian, K., Vogt, C., Knies, J., 2017. Geochemical characterisation of northern Norwegian fjord surface sediments: a baseline for further paleo-environmental investigations. Cont. Shelf Res. 148, 104–115. https://doi.org/10.1016/j.csr.2017.08.015.
Forbes, D., Syvitski, J.P.M., 1995. Paraglacial Coasts. In: Woodruffe, C., Carter, R.W.G. (Eds.), Coastal Evolution. Cambridge University of Press, Cambridge, UK, pp. 373–424 Chapter 10.
Foreman, M.G.G., Czajko, P., Stucchi, D.J., Guo, M., 2009. A finite volume model simulation for the Broughton Archipelago, Canada. Ocean Model 30 (1), 29–43.
Forestry Commission, 2015. Carbon in Living Woodland Trees in Britain: A National Forestry Inventory Report. available at: http://www.forestry.gov.uk/pdf/FCNFI113.pdf/$FILE/FCNFI113.pdf.
Fraser, N.J., Skogseth, R., Nilsen, F., Inall, M.E., 2018. Circulation and exchange in a broad Arctic fjord using glider-based observations. Polar Res. 37 (1), 1485417. https://doi.org/10.1080/17518369.2018.1485417.
Freeland, H.J., Farmer, D.M., Levings, C.D., 1980. Fjord Oceanography. Plenum Press, New York (715 pp).
Friedrich, J., Janssen, F., Aleynik, D., et al., 2014. Investigating hypoxia in aquatic environments: diverse approaches to addressing a complex phenomenon. Biogeosciences 11, 1215–1259. https://doi.org/10.5194/bg-11-1215-2014.
Fujiwara, A., Hirawake, T., Suzuki, K., Saitoh, S.I., 2011. Remote sensing of size structure of phytoplankton communities using optical properties of the Chukchi and Bering Sea shelf region. Biogeosciences 8, 3567–3580. https://doi.org/10.5194/bg-8-3567-2011.
Gales, J.A., Talling, P.J., Cartigny, M.J.B., Hughes Clarke, J., Lintern, G., Stacey, C., Clare, M.A., 2019. What controls submarine channel development and the morphology of deltas entering deep-water fjords? Earth Surf. Process. Landf. 44, 535–551. https://doi.org/10.1002/esp.4515.
Galy, V., Peucker-Ehrenbrink, B., Eglinton, T., 2015. Global carbon export from the terrestrial biosphere controlled by erosion. Nature 521, 204–207.
Garreaud, R.D., 2007. Precipitation and circulation covariability in the extratropics. J. Clim. 20, 4789–4797.
Garreaud, R., Lopez, P., Minvielle, M., Rojas, M., 2013. Large-scale control on the patagonian climate. J. Clim. 26, 215–230. https://doi.org/10.1175/Jcli-D-12-00001.
Gibbs, M.T., 2001. Aspects of the structure and variability of the low-salinity-layer in Doubtful Sound, a New Zealand fiord. N. Z. J. Mar. Freshw. Res. 35 (1), 59–72.
Gilbert, R., 1983. Sedimentary processes of Canadian Arctic fjords. Sediment. Geol. 36 (2–4), 147–175.
Gilbert, R., 2000. Environmental assessment from the sedimentary record of high-latitude fiords. Geomorphology 32 (3), 295–314.
Gilbert, R., Nielsen, N., Desloges, J.R., Rasch, M., 1998. Contrasting glacimarine sedimentary environments of two arctic fiords on Disko, West Greenland. Mar. Geol. 147, 63–83.
Gilbert, R., Nielsen, N., Möller, H., Desloges, J.R., Rasch, M., 2002. Glacimarine sedimentation in Kangerdluk (Disko Fjord), West Greenland, in response to a surging glacier. Mar. Geol. 191, 1–18.
Gillibrand, P.A., Turrell, W.R., Elliott, A.J., 1995. Deep-water renewal in the upper basin of Loch Sunart, a Scottish fjord. J. Phys. Oceanogr. 25 (6), 1488–1503.
Gillibrand, P.A., Cage, A.G., Austin, W.E.N., 2005. A preliminary investigation of basin water response to climate forcing in a Scottish fjord: evaluating the influence of the NAO. Cont. Shelf Res. 25 (5–6), 571–587.
Glud, R.N., Risgaard-Petersen, N., Thamdrup, B., Fossing, H., Rysgaard, S., 2000. Benthic carbon mineralization in a high-Arctic sound (Young Sound, NE Greenland). Mar. Ecol. Prog. Ser. 206, 59–71.
Goebel, N.L., Wing, S.R., Boyd, P.W., 2005. A mechanism for onset of diatom blooms in a fjord with persistent salinity stratification. Estuar. Coast. Shelf Sci. 64 (2–3), 546–560.
Gonsior, M., Peake, B., Cooper, W., Jaffe, R., Young, H., Kahn, A., Kowalczuk, P., 2008. Spectral characterization of chromophoric dissolved organic matter (CDOM) in a fjord (Doubtful Sound, New Zealand). Aquat. Sci. 70 (4), 397–409.
González, H.E., Castro, L.R., Daneri, G., Iriarte, J.L., Silva, N., Tapia, F., Teca, E., Vargas, C.A., 2013. Land-ocean gradient in haline stratification and its effects on plankton dynamics and trophic carbon fluxes in Chilean Patagonian fjords (47 − 50°S). Prog. Oceanogr. 119, 32–47.
Grange, L.J., Smith, C.R., 2013. Megafaunal communities in rapidly warming fjords along the West Antarctic Peninsula: hotspots of abundance and beta diversity. PLoS One 8 (12), e77917. https://doi.org/10.1371/journal.pone.0077917.
Grange, L.L., Smith, C.R., Lindsay, D.J., Bentlage, B., Youngbluth, M.J., 2017. High abundance of the epibenthic trachymedusa *Ptychogastria polaris* Allman, 1878 (Hydrozoa, Trachylina) in subpolar fjords along the West Antarctic Peninsula. PLoS One 12 (1), e0168648. https://doi.org/10.1371/journal.pone.0168648.
Grimes, S.T., Brock, F., Rickard, D., Davies, K.L., Edwards, D., Briggs, D.E.G., Parkes, R.J., 2001. Understanding fossilization: experimental pyritization of plants. Geology 29, 123–126.
Hage, S., Cartigny, M.J.B., Sumner, E.J., Clare, M.A., Hughes Clarke, J.E., Talling, P.J., Lintern, D.G., Simmons, S.M., Silva Jacinto, R., Vellinga, A.J., Allin, J.R., Azpiroz-Zabala, M., Gales, J.A., Hizzett, J.L., Hunt, J.E., Mozzato, A., Parsons, D.R., Pope, E.L., Stacey, C.D., Symons, W.O., Vardy, M.E., Watts, C., 2019. Direct monitoring reveals initiation of turbidity currents from extremely dilute river plumes. Geophys. Res. Lett. 46 (20), 11310–11320.

Hamilton, S.E., Hedges, J.I., 1988. The comparative geochemistries of lignins and carbohydrates in an anoxic fjord. Geochim. Cosmochim. Acta 52, 129–142.
Hansen, D.V., Rattray Jr., M., 1966. New dimensions in estuary classification. Limnol. Oceanogr. 11, 319–326.
Harland, R., Asteman, I.P., Nordberg, K., 2019. Dinoflagellate cysts from the 'Anthropocene'of Gullmar Fjord, west coast of Sweden and their potential for monitoring climate change. Rev. Palaeobot. Palynol. 261, 31–40.
Hawkings, J., 2015. An Investigation into the Production and Export of Nutrients from Glaciers. School of Geographical Sciences, University of Bristol, Bristol (241 pp, Thesis (Ph.D.)).
Hawkings, J., Wadham, J.L., Tranter, M., Raiswell, R., Benning, L.G., Statham, P.J., Tedstone, A., Nienow, P., 2014. Ice sheets as a significant source of highly reactive nanoparticulate iron to the oceans. Nat. Commun. 5, 3929. https://doi.org/10.1038/ncomms4929.
Hawkings, J., Wadham, J.L., Tranter, M., Telling, J., Bagshaw, E.A., Beaton, A., Simmons, S.L., Tedstone, A., Nienow, P.W., 2016. The Greenland Ice Sheet as a hot spot of phosphorus weathering and export in the Arctic. Global Biogeochem. Cycles 30, 191–210.
Hay, A.E., Burling, R.W., Murray, J.W., 1982. Remote acoustic detection of a turbidity current surge. Science 217, 833–835.
Hedges, J.I., 1992. Global biogeochemical cycles: progress and problems. Mar. Chem. 39, 67–93.
Hedges, J.I., Keil, R.G., 1995. Sedimentary organic-matter preservation – an assessment and speculative synthesis. Mar. Chem. 49, 81–115.
Hedges, J.I., Cowie, G.L., Ertel, J.R., Barbour, R.J., Hatcher, P.G., 1985. Degradation of carbohydrates and lignins in buried woods. Geochim. Cosmochim. Acta 49, 701–711.
Hedges, J.I., Keil, R.G., Benner, R., 1997. What happens to terrestrial organic matter in the ocean? Org. Geochem. 27, 195–212.
Hegseth, E.N., Tverberg, V., 2013. Effect of Atlantic water inflow on timing of the phytoplankton spring bloom in a high Arctic fjord (Kongsfjorden, Svalbard). J. Mar. Syst. 113–114, 94–105.
Hein, F.J., Syvitski, J.P.M., 1992. Sedimentary environments and facies in an arctic basin, Itirbilung Fiord, Baffin Island. Can. Sed. Geol. 81, 1–29.
Hemingway, J.D., Hilton, R.G., Hovius, N., Eglinton, T.I., Haghipour, N., Wacker, L., Galy, V.V., 2018. Microbial oxidation of lithospheric organic carbon in rapidly eroding tropical mountain soils. Science 360 (6385), 209–212.
Hendry, K.R., Huvenne, V.A.I., Robinson, L.F., Annett, A., Badger, M., Jacobel, A.W., Ng, H.C., Opher, J., Pickering, R.A., Taylor, M.L., Bates, S.L., Cooper, A., Cushman, G.G., Goodwin, C., Hoy, S., Rowland, G., Samperiz, A., Williams, A., Achterberg, E.P., Arrowsmith, C., Brearley, J.A., Henley, S.F., Krause, J.W., Leng, M.J., Li, T., McManus, J.F., Meredith, M.P., Perkins, R., Woodward, E.M.S., 2019. The biogeochemical impact of glacial meltwater from Southwest Greenland. Prog. Oceanogr. 176, 102126 (01.09.2019).
Herbert, L.C., Riedinger, N., Michaud, A.B., Laufer, K., Røy, H., Jørgensen, B.B., Heilbrun, C., Aller, R.C., Cochra, J.K., Wehrmann, L.M., 2020. Glacial controls on redox-sensitive trace element cycling in Arctic fjord sediments (Spitsbergen, Svalbard). Geochimica Cosmochimica Acta 271, 33–60.
Hicks, D.M., Hill, J., Shankar, U., 1996. Variation in suspended sediment yields around New Zealand: the relative importance of rainfall and geology. In: Erosion and Sediment Yield: Global and Regional Perspectives. 236. IAHS Publishing, pp. 149–156.
Hill, P., Syvitski, J.P.M., Powell, R.D., Cowan, E.A., 1998. In situ observations of floc settling velocities in Glacier Bay, Alaska. Mar. Geol. 145 (1–2), 85–94.
Hill, E.A., Carr, J.R., Stokes, C.R., Gudmundsson, G.H., 2018. Dynamic changes in outlet glaciers in northern Greenland from 1948 to 2015. Cryosphere 12, 3243–3263.
Hilton, R.G., Galy, A., Hovius, N., Horng, M.J., 2011. Efficient transport of fossil organic carbon to the ocean by steep mountain rivers: an orogenic carbon sequestration mechanism. Geology 39, 71–74.
Hinojosa, J.L., Moy, C.M., Stirling, C.H., Wilson, G.S., Eglinton, T.I., 2014. Carbon cycling and burial in New Zealand's fjords. Geochem. Geophys. Geosyst. 15 (10), 4047–4063.
Hinojosa, J.L., Stirling, C.H., Reid, M.R., Moy, C.M., Wilson, G.S., 2016. Trace metal cycling and $^{238}U/^{235}U$ in New Zealand's fjords: Implications for reconstructing global paleoredox conditions in organic-rich sediments. Geochim. Cosmochim. Acta 179, 89–109.
Hinojosa, J.L., Moy, C.M., Stirling, C.H., Wilson, G.S., Eglinton, T.I., 2017. A New Zealand perspective on centennial-scale Southern Hemisphere westerly wind shifts during the last two millennia. Quat. Sci. Rev. 172, 32–43.
Hizzett, J.L., Hughes Clarke, J.E., Sumner, E.J., Cartigny, M.J.B., Talling, P.J., Clare, M.A., 2018. Which triggers produce the most erosive, frequent, and longest runout turbidity currents on deltas? Geophys. Res. Lett. 45 (2), 855–863.
Hood, E., Battin, T.J., Fellman, J., O'Neel, S., Spencer, R.G.M., 2015. Storage and release of organic carbon from glaciers and ice sheets. Nat. Geosci. 8 (2), 91–96.
Hopwood, M.J., Carroll, D., Browning, T.J., Meire, L., Mortensen, J., Krisch, S., Acterberg, E.T., 2018. Marine productivity to increased meltwater discharge around Greenland. Nat. Commun. 9, 3256. https://doi.org/10.1038/s41467-018-05488-8.
Hopwood, M., Carroll, D., Dunse, T., Hodson, A., Holding, J., Iriarte, J., Ribeiro, S., Achterberg, E., Cantoni, C., Carlson, D., Chierici, M., Clarke, J., Cozzi, S., Fransson, A., Juul-Pedersen, T.S., Winding, M., Meire, L., 2019. Review Article: How does glacier discharge affect marine biogeochemistry and primary production in the Arctic? Cryosphere Discuss. https://doi.org/10.5194/tc-2019-136.
How, P., Schild, K.M., Benn, D.I., Noormets, R., Kirchner, N., Luckman, A., Vallot, D., Hulton, N.R., Borstad, C., 2019. Calving controlled by melt-under-cutting: detailed calving styles revealed through time-lapse observations. Ann. Glaciol. 60 (78), 20–31.
Howat, I.M., Joughin, I., Tulaczyk, S., Gogineni, S., 2005. Rapid retreat and acceleration of Helheim Glacier, East Greenland. Geophys. Res. Lett. 32 (22), L22502. https://doi.org/10.1029/2005GL024737.
Howe, J.A., Shimmield, T., Austin, W.E., Longva, O., 2002. Post-glacial depositional environments in a mid-high latitude glacially-overdeepened sea loch, inner loch Etive, western Scotland. Mar. Geol. 185 (3–4), 417–433.
Howe, J.A., Austin, W.E.N., Forwick, M., Paetzel, M., Harland, R., Cage, A.G., 2010. Fjord systems and archives: a review. Geol. Soc. Lond. Spec. Publ. 344 (1), 5–15.
Huguet, C., Smittenberg, R.H., Boer, W., Damsté, J.S.S., Schouten, S., 2007. Twentieth century proxy records of temperature and soil organic matter input in the Drammensfjord, southern Norway. Org. Geochem. 38, 1838–1849.
Hungr, O., Leroueil, S., Picarelli, L., 2014. The Varnes classification of landslide types, an update. Landslides 11 (2), 167–194.
Huntley, D.H., Bobrowsky, P.T., Clague, J.J., 2001. Ocean drilling program leg 169S: surficial geology, stratigraphy and geomorphology of the Saanich Inlet area, southeastern Vancouver island, British Columbia. Mar. Geol. 174 (1–4), 27–41.
Inall, M.E., Nilsen, F., Cottier, F.R., Daae, R., 2015. Shelf/fjord exchange driven by coastal-trapped waves in the Arctic. J. Geophys. Res. Oceans 120 (12), 8283–8303.
Ingall, E., Kolowith, L., Lyons, T., Hurtgen, M., 2005. Sediment carbon, nitrogen and phosphorus cycling in an anoxic fjord, Effingham Inlet, British Columbia. Am. J. Sci. 305, 240–258.
Iriarte, J.L., 2018. Natural and human influences on marine processes in Patagonian Subantarctic coastal waters. Front. Mar. Sci. 5, 360. https://doi.org/10.3389/fmars.2018.00360.
Iriarte, J.L., González, H.E., Nahuelhual, L., 2010. Patagonian fjord ecosystems in southern chile as a highly vulnerable region: problems and needs. Ambio 39, 463–466. https://doi.org/10.1007/s13280-010-0049-9.
Iversen, K.R., Seuthe, L., 2011. Seasonal microbial processes in a high-latitude fjord (Kongsfjorden, Svalbard): I. Heterotrophic bacteria, picoplankton and nano flagellates. Polar Biol. 34, 731–749. https://doi.org/10.1007/s00300-010-0929-2.
Jaeger, J.M., Nittrouer, C.A., Scott, N.D., Milliman, J.D., 1998. Sediment accumulation along a glacially impacted mountainous coastline: north-east Gulf of Alaska. Basin Res. 10, 155–173.
Jenkins, A., 2011. Convection-driven melting near the grounding lines of ice shelves and tidewater glaciers. J. Phys. Oceanogr. 41 (12), 2279–2294.
Jex, C.N., Pate, G.H., Blyth, A.J., Spencer, R.G.M., Hernes, P.J., Khan, S.J., Baker, A., 2014. Lignin biogeochemistry: from modern processes to Quaternary archives. Quat. Sci. Rev. 87, 46–59. https://doi.org/10.1016/j.quascirev.2013.12.028.
Johannessen, S.C., Macdonal, R.W., Wright, C.A., 2019. Rain, runoff and diatoms: the effects of the North Pacific 2014-2015 warm anomaly on particle flux in a Canadian west coast fjord. Estuar. Coasts 42, 1052–1065.
Joughin, I., Smith, B.E., Shean, D.E., Floricioiu, D., 2014. Brief communication: further summer speedup of Jakobshavn Isbræ. Cryosphere 8 (1), 209–214.
Juul-Pedersen, T., Arendt, K.E., Mortensen, J., Blicher, M.E., Sogaard, D.H., Rysgaard, S., 2015. Seasonal and interannual phytoplankton production in a sub-Arctic tidewater outlet glacier fjord., SW Greenland. Mar. Ecol. Prog. Ser. 524, 27–38.
Kanna, N., Sugiyama, S., Ohashi, Y., Sakakibara, D., Fukamachi, Y., Nomura, D., 2018. Upwelling of macronutrients and dissolved inorganic carbon by a subglacial freshwater driven plume in Bowdoin Fjord, northwestern Greenland. J. Geophys. Res. Biogeosci. 123, 1666–1682.
Keefer, D.K., 1994. The importance of earthquake-induced landslides to long-term slope erosion and slope-failure hazards in seismically active regions. Geomorphology 10, 265–284.
Keller, D.P., Kriest, I., Koeve, W., Oschlies, A., 2016. Southern Ocean biological impacts on global ocean oxygen. Geophys. Res. Lett. 43, 6469–6477.
Khazendar, A., Fenty, I.G., Carroll, D., Gardner, A., Lee, C.M., Fukumori, I., Wang, O., Zhang, H., Seroussi, H., Moller, D., Noël, B.P.Y., van den Broeke, M.R., Dinardo, S., Willis, J., 2019. Interruption of two decades of Jakobshavn Isbrae acceleration and thinning as regional ocean cools. Nat. Geosci. 12, 277–283. https://doi.org/10.1038/s41561-019-0329-3.
Kilian, R., Baeza, O., Breuer, S., Ríos, F., Arz, H., Lamy, L., Wirtz, J., Baque, D., Korf, P., Kremer, K., Ríos, C., Mutschke, E., Michels, S., DePohl-Holz, R., Arevalo, M., Wörner, G., Schneider, C., Casassa, G., 2013. Late Glacial and Holocene paleogeographical and paleoecological evolution of the Seno Skyring and Otway fjord systems in the Magellan region. Anales del Instituto de la Patagonia. 1 (2), 5–26.
Kim, J.H., Peterse, F., Willmott, V., Klitgaard Kristensen, D., Baas, M., Schouten, S., Sinninghe Damsté, J.S., 2011. Large ancient organic matter contributions to Arctic marine sediments (Svalbard). Limnol. Oceanogr. 56 (4), 1463–1474. https://doi.org/10.4319/10.2011.56.4.1463.
Knudson, K.P., Hendy, I.L., Neil, H.L., 2011. Re-examining Southern Hemisphere westerly wind behavior: insights from a late Holocene precipitation reconstruction using New Zealand fjord sediments. Quat. Sci. Rev. 30 (21 − 22), 3124–3138.
Koppes, M., Hallet, B., Anderson, J., 2009. Synchronous acceleration of ice loss and glacial erosion, Glaciar Marinelli, Chilean Tierra del Fuego. J. Glaciol. 55, 207–220.
Kostka, J.E., Thamdrup, B., Glud, R.N., Canfield, D., 1999. Rates and pathways of carbon oxidation in permanently cold Arctic sediments. Mar. Ecol. Prog. Ser. 180, 7–21.
Koziorowska, K., Kuliński, K., Pempkowiak, J., 2016. Sedimentary organic matter in two Spitsbergen fjords: Terrestrial and marine contributions based on carbon and nitrogen contents and stable isotopes composition. Cont. Shelf Res. 113, 38–46.
Koziorowska, K., Kulinski, K., Pempkowiak, J., 2018. Comparison of the burial rate estimation methods of organic and inorganic carbon and quantification of carbon burial in two high Arctic fjords. Oceanologia 60, 405–418.
Kuliński, K., Kędra, M., Legeżyńska, J., Głuchowska, M., Zaborska, A., 2014. Particulate organic matter sinks and sources in high Arctic fjord. J. Mar. Syst. 139, 27–37. https://doi.org/10.1016/j.jmarsys.2014.04.018.
Kumar, V., Tiwari, M., Rengarajan, R., 2018. Warming in the Arctic captured by productivity variability at an Arctic fjord over the past two centuries. PLoS One 13 (8), e0201456.
Lalonde, K., Mucci, A., Ouellet, A., Gelinas, Y., 2012. Preservation of organic matter in

sediments promoted by iron. Nature 483, 198–200.
Lamarche-Gagnon, G., Wadham, J.L., Lollar, B.S., Arndt, S., Fietzek, P., Beaton, A.D., Tedstone, A.J., Telling, J., Bagshaw, E.A., Hawkings, J.R., 2019. Greenland melt drives continuous export of methane from the ice-sheet bed. Nature 565 (73), 2019. https://doi.org/10.1038/s41586-018-0800-0.
Lamy, F., Kilian, R., Arz, H.W., Francois, J.P., Kaiser, J., Prange, M., Steinke, T., 2010. Holocene changes in the position and intensity of the southern westerly wind belt. Nat. Geosci. 3, 695–699.
Lara, E., Arrieta, J.M., Garcia-Zarandona, I., Boras, J.A., Duarte, C.M., Agustí, S., Wassmann, P.F., Vaqué, D., 2013. Experimental evaluation of the warming effect on viral, bacterial and protistan communities in two contrasting arctic systems. Aquat. Microb. Ecol. 70, 17–32. https://doi.org/10.3354/ame01636.
Larsen, S.H., Khan, S.A., Ahlstrøm, A.P., Hvidberg, C.S., Willis, M.J., Andersen, S.B., 2016. Increased mass loss and asynchronous behavior of marine-terminating outlet glaciers at Upernavik Isstrøm, NW Greenland. J. Geophys. Res. Earth Surf. 121 (2), 241–256.
Lawson, E.C., Wadham, J.L., Tranter, M., Stibal, M., Lis, G.P., Butler, C.E.H., Laybourn-Parry, J., Nienow, P., Chandler, D., Dewsbury, P., 2014. Greenland Ice Sheet exports labile organic carbon to the Arctic oceans. Biogeosciences 11, 4015–4028. https://doi.org/10.5194/bg-114015-2014.
Lebel, J., Silverberg, N., Sundby, B., 1982. Gravity core shortening and pore water chemical gradients. Deep-Sea Res. 29, 1365–1372.
León-Muñoz, J., Marcé, R., Iriarte, J.L., 2013. Influence of hydrological regime of an Andean river on salinity, temperature and oxygen in a Patagonian fjord, Chile. NZ J. Mar. Freshwat. Res. 47, 515–528. https://doi.org/10.1080/00288330.2013.802700.
Levings, C.D., Ervik, A., Johannessen, P., Aure, J., 1995. Ecological criteria to help site farms in fjords. Estuaries 18 (1A), 81–90.
Li, B., Yoon, H.-I., Park, B.-K., 2000. Foraminiferal assemblages and CaCO3 dissolution since the last deglaciation in the Maxwell Bay, King George Island, Antarctica. Mar. Geol. 169, 239–257.
Li, W.K.W., McLaughlin, F.A., Lovejoy, C., Carmack, E.C., 2009. Smallest algae thrive as the Arctic Ocean freshens. Science 326, 539.
Linhoff, B.S., Charette, M.A., Nienow, P.W., Wadham, J.L., Tedstone, A.J., Cowton, T., 2017. Utility of ^{222}Rn as a passive tracer of subglacial distributed system drainage. Earth Planet. Sci. Lett. 462, 180–188.
Liu, D., Bertrand, S., Weltje, G.J., 2019. An empirical method to predict sediment grain size from inorganic geochemical measurements. Geochem. Geophys. Geosyst. 20.
Loh, P., Reeves, A., Harvey, S., Overnell, J., Miller, A., 2008. The fate of terrestrial organic matter in two Scottish Sea lochs. Estuar. Coast. Shelf Sci. 76, 566–579.
Loring, D.H., Asmund, G., 1989. Heavy metal contamination of a Greenland fjord system by mine wastes. Environ. Geol. Water Sci. 14 (1), 61–71.
Louchouarn, P., Lucotte, M., Canuel, R., Gagne, J.P., Richard, L.F., 1997. Sources and early diagenesis of lignin and bulk organic matter in the sediments of the lower St. Lawrence Estuary and the Saguenay Fjord. Mar. Chem. 58, 3–26.
Love, K.B., Hallet, B., Pratt, T.L., O'neel, S.H.A.D., 2016. Observations and modeling of fjord sedimentation during the 30 year retreat of Columbia Glacier, AK. J. Glaciol. 62 (234), 778–793.
Lu, A., Rignot, E., Millan, R., Tinto, K., Willis, J., 2019. Bathymetry of northwest Greenland using “Ocean Melting Greenland” (OMG) high-resolution airborne gravity and other data. Remote Sens. 11, 131.
Luckman, A., Benn, D.I., Cottier, F., Bevan, S., Nilsen, F., Inall, M., 2015. Calving rates at tidewater glaciers vary strongly with ocean temperature. Nat. Commun. 6, 8566.
Lydersen, C., Assmy, P., Falk-Petersen, S., Kohler, J., Kovacs, K.M., Reigstad, M., Steen, H., Strøm, H., Sundfjord, A., Varpe, Ø., Walczowski, W., Weslawski, J.M., Zajaczkowski, M., 2014. The importance of tidewater glaciers for marine mammals and seabirds in Svalbard, Norway. J. Mar. Syst. 129, 452–471.
Macdonald, R.W., Anderson, L.G., Christensen, J., Miller, L.A., Semiletov, I.P., Steinet, R., 2010. The Arctic Ocean: budgets and fluxes. In: Liu, K.K., Atkinson, L., Quinones, R., Talaue-McManus, L. (Eds.), Carbon and Nutrient Fluxes in Continental Margins: A Global Synthesis. Springer, Berlin, pp. 290–303.
Marienfeld, P., 1992. Recent sedimentary processes in Scoresby Sund, East Greenland. Boreas 21 (2), 169–186. https://doi.org/10.1111/j.1502-3885.1992.tb00024.x.
Marin, V.H., Tironi, A., Alejandra Paredes, M., Contreras, M., 2013. Modeling suspended solids in a Northern Chilean Patagonia glacier-fed fjord: GLOF scenarios under climate change conditions. Ecol. Model. 264, 7–16. https://doi.org/10.1016/j.ecolmodel.2012.06.017.
Mark, A.F., Scott, G.A.M., Sanderson, F.R., James, P.W., 1964. Forest succession on landslides above Lake Thomson, Fiordland. N. Z. J. Bot. 2, 60–89.
Mayr, C.C., Rebolledo, L., Schulte, K., Schuster, A., Zolitschka, B., Fösterra, G., Häusserman, V., 2014. Responses of nitrogen and carbon deposition rates in Comau Fjord (42°S, Southern Chile) to natural and anthropogenic impacts during the last century. Cont. Shelf Res. 78, 29–38.
McIntyre, K.L., Howe, J.A., 2010. Scottish west coast fjords since the last glaciation: a review. Geol. Soc. Lond. Spec. Publ. 344 (1), 305–329.
McKenna-Neuman, C., Gilbert, R., 1986. Aeolian processes and landforms in glacifluvial environments in southeastern Baffin Island, N.W.T., Canada. In: Nickling, W.G. (Ed.), Aeolian Geomorphology. Proceedings of the Seventeenth Annual Binghamton Geomorphology Symposia. Geo Books, Norwich, Ch. 12. pp. 213–235.
McLeod, R.J., Wing, S.R., 2009. Strong pathways for incorporation of terrestrially derived organic matter into benthic communities. Estuar. Coast. Shelf Sci. 82 (4), 645–653.
McMinn, A., Heijnisj, H., Harle, K., McOrist, G., 2001. Late-Holocene climatic change recorded in sediment cores from Ellis Fjord, eastern Antarctica. The Holocene 11, 291–300.
Medrzycka, D., Benn, D.I., Box, J.E., Copland, L., Balog, J., 2016. Calving behavior at Rink Isbræ, West Greenland, from time-lapse photos. Arct. Antarct. Alp. Res. 48 (2), 263–277.
Meire, L., Søgaard, D.H., Mortensen, J., Meysman, F.J.R., Soetaert, K., Arendt, K.E., Juul-Pedersen, T., Blicher, M.E., Rysgaard, S., 2015. Glacial meltwater and primary production are drivers of strong CO_2 uptake in fjord and coastal waters adjacent to the Greenland Ice Sheet. Biogeosciences 12, 2347–2363. https://doi.org/10.5194/bg-12-2347-2015.
Meire, L., Meire, P., Struyf, E., Krawczyk, D.W., Arendt, K.E., Yde, J.C., Pedersen, juul, Hopwood, M.J., Rysgaard, S., Meysman, F.J.R., 2016. High export of dissolved silica from the Greenland Ice Sheet. Geophys. Res. Lett. 43, 9173–9182.
Meire, L., Mortensen, J., Meire, P., Juul-Pedersen, T., Sejr, M.K., Rysgaard, S., Nygaard, R., Huybrechts, P., Meysman, F.J.R., 2017. Marine-terminating glaciers sustain high productivity in Greenland fjords. Glob. Chang. Biol. 23, 5344–5357. https://doi.org/10.1111/gcb.1380.
Meunier, P., Hovius, N., Haines, A.J., 2008. Topographic site effects and the location of earthquake induced landslides. Earth Planet. Sci. Lett. 275 (3–4), 221–232.
Meyer, K.M., Kump, L.R., 2008. Oceanic euxinia in Earth history: causes and consequences. Annu. Rev. Earth Planet. Sci. 36, 251–288.
Mikalsen, G., Sejrup, H.P., Aarseth, I., 2001. Late-Holocene changes in ocean circulation and climate: foraminiferal and isotopic evidence from Sulafjord, western Norway. The Holocene 11, 437–446.
Milne, G., Mitrovica, J., 2008. Searching for eustasy in deglacial sea-level histories. Quat. Sci. Rev. 27, 2292–2302.
Moffat, C., 2014. Wind-driven modulation of warm supply to a proglacial fjord, Jorge Montt Glacier, Patagonia. Geophys. Res. Lett. 41, 3943–3950.
Molina-Navarro, E., Andersen, H.E., Nielsen, A., Thodsen, H., Trolle, D., 2018. Quantifying the combined effects of land use and climate changes on stream flow and nutrient loads: a modelling approach in the Odense Fjord catchment (Denmark). Sci. Total Environ. 621, 253–264.
Møller, H.S., Jensen, K.G., Kuijpers, A., Aagaard-Sørensen, S., Seidenkrantz, M.-S., Prins, M., Endler, R., Mikkelsen, N., 2006. Late-Holocene environment and climatic changes in Ameralik Fjord, southwest Greenland: evidence from the sedimentary record. The Holocene 16, 685–695.
Morehead, M., Syvitski, J.P.M., Hutton, E.W.H., 2001. The link between abrupt climate change and basin stratigraphy: a numerical approach. Glob. Planet. Chang. 28, 107–127.
Motyka, R.J., Dryer, W.P., Amundson, J., Truffer, M., Fahnestock, M., 2013. Rapid submarine melting driven by subglacial discharge, LeConte Glacier, Alaska. Geophys. Res. Lett. 40 (19), 5153–5158.
Motyka, R.J., Cassotto, R., Truffer, M., Kjeldsen, K.K., Van As, D., Korsgaard, N.J., Fahnestock, M., Howat, I., Langen, P.L., Mortensen, J., Lennert, K., 2017. Asynchronous behavior of outlet glaciers feeding Godthåbsfjord (Nuup Kangerlua) and the triggering of Narsap Sermia's retreat in SW Greenland. J. Glaciol. 63 (238), 288–308.
Mulder, T., Syvitski, J.P.M., 1995. Turbidity currents generated at river mouths during exceptional discharges to the world oceans. J. Geol. 103, 285–299.
Mulder, T., Syvitski, J.P.M., Migeon, S., Faugères, J.-C., Savoye, B., 2003. Marine hyperpycnal flows: initiation, behavior and related deposits. A review. Mar. Pet. Geol. 20, 861–882.
Muller, A., 2001. Geochemical expressions of anoxic conditions in Nordasvannet, a land-locked fjord in western Norway. Appl. Geochem. 16 (3), 363–374. https://doi.org/10.1016/s0883-2927(00)00024-x.
Murray, C., Markager, S., Stedmon, C.A., Juul-Pedersen, T., Sejr, M.K., Bruhn, A., 2015. The influence of glacial melt water on bio-optical properties in two contrasting Greenlandic fjords. Estuar. Coast. Shelf Sci. 163, 72–83.
Muzuka, A.N.N., Hillaire-Marcel, C., 1999. Burial rates of organic matter along the eastern Canadian margin and stable isotope constraints on its origin and diagenetic evolution. Mar. Geol. 160 (3–4), 251–270. https://doi.org/10.1016/s0025-3227(99)00022-5.
Nickel, M., Vandieken, V., Brüchert, V., Jørgensen, B.B., 2008. Microbial Mn(IV) and Fe(III) reduction in northern Barents Sea sediments under different conditions of ice cover and organic carbon deposition. Deep-Sea Res. II 55, 2390–2398. https://doi.org/10.1016/j.dsr2.2008.05.003.
Nienow, P.W., Sole, A.J., Slater, D.A., Cowton, T.R., 2017. Recent advances in our Understanding of the Role of Meltwater in the Greenland Ice Sheet System. Curr. Clim. Chang. Rep. 3, 330–344.
Niklitschek, E.J., Soto, D., Lafon, A., Molinet, C., Toledo, P., 2013. Southward expansion of the Chilean salmon industry in the Patagonian Fjords: main environmental challenges. Rev. Aquac. 5, 172–195. https://doi.org/10.1111/raq.12012.
Nordberg, K., Filipsson, H.L., Gustafsson, M., Harland, R., Roos, P., 2001. Climate, hydrographic variations and marine benthic hypoxia in Koljö Fjord, Sweden. J. Sea Res. 46, 187–200.
Nordberg, K., Filipsson, H.L., Linné, P., Gustafsson, M., 2009. Stable oxygen and carbon isotope information on the establishment of a new, opportunistic foraminiferal fauna in a Swedish Skagerrak fjord basin, in 1979/1980. Mar. Micropaleontol. 73, 117–128.
Nørgaard-Pedersen, N., Austin, W.E.N., Howe, J.A., Shimmield, T., 2006. The Holocene record of Loch Etive, western Scotland: Influence of catchment and relative sea level changes. Mar. Geol. 228 (1–4), 55–71.
Nuwer, J.M., Keil, R.G., 2005. Sedimentary organic matter geochemistry of Clayoquot Sound, Vancouver Island, British Columbia. Limnol. Oceanogr. 50 (4), 1119–1128.
Obst, J.R., McMillan, N.J., Blanchette, R.A., Christensen, D.J., Faix, O., Han, J.S., Kuster, T.A., Landucci, L.L., Newman, R.H., Pettersen, R.C., Schwandt, V.H., Wesolowski, M.F., 1991. Characterization of Canadian Arctic fossil woods. Geol. Surv. Can. 403, 123–146.
Odhiambo, B.K., Macdonald, R.W., O'Brien, M.C., Harper, J.R., Yunker, M.B., 1996. Transport and fate of mine tailings in a coastal fjord of British Columbia as inferred from the sediment record. Sci. Total Environ. 191 (1–2), 77–94.
O'Leary, M., Christoffersen, P., 2013. Calving on tidewater glaciers amplified by

submarine frontal melting. Cryosphere 7 (1), 119–128.
Olson, J.S., Garrels, R.M., Berner, R.A., Armentano, T.V., Dyer, M.I., Taalon, D.H., 1985. The natural carbon cycle. In: Trabalka, J.R. (Ed.), Atmospheric Carbon Dioxide and the Global Carbon Cycle. US Department of Energy, Washington, DC, pp. 175–213.
O'Neel, S., Pfeffer, W.T., Krimmel, R., Meier, M., 2005. Evolving force balance at Columbia Glacier, Alaska, during its rapid retreat. J. Geophys. Res. 110, F03012. https://doi.org/10.1029/2005JF000292.
Opsahl, S., Benner, R., 1995. Early diagenesis of vascular plant tissues: lignin and cutin decomposition and biogeochemical implications. Geochim. Cosmochim. Acta 59, 4889–4904.
Overeem, I., Syvitski, J.P.M., 2010. Experimental exploration of the stratigraphy of fjords fed by glaciofluvial systems. In: Howe, J.A., Austin, W.E.N., Forwick, M., Paetzel, M. (Eds.), Fjord Systems and Archives, pp. 125–142. https://doi.org/10.1144/SP344.11. Geological Society, London, Special Publications, 344.
Overeem, I., Hudson, B.D., Syvitski, J.P.M., Mikkelsen, A.B., Hasholt, B., van den Broeke, M.R., Noël, B.P.Y., Morlighem, M., 2017. Substantial export of suspended sediment to the global oceans from glacial erosion in Greenland. Nat. Geosci. 10, 859–863.
Öztürk, M., Steinnes, E., Sakshaug, E., 2002. Iron speciation in the Trondheim fjord from the perspective of iron limitation for phytoplankton. Estuar. Coast. Shelf Sci. 55 (2), 197–212.
Paerl, H.W., Crosswell, J.R., Van Dam, B., Hall, N.S., Rossignol, K.L., Osburn, C.L., Hounshell, A.G., Sloup, R.S., Harding Jr., L.W., 2018. Two decades of tropical cyclone impacts on North Carolina's estuarine carbon, nutrient and phytoplankton dynamics: implications for biogeochemical cycling and water quality in a stormier world. Biogeochem. https://doi.org/10.1007/s10533-018-0438-x.
Parsons, T.R., Takahashi, M., Hargrave, B., 1984. Biological Oceanographic Processes. Pergamon Press (330 pp).
Parsons, J.D., Bush, J.W.M., Syvitski, J.P.M., 2001. Hyperpycnal plume formation from riverine outflows with small sediment concentrations. Sedimentol. 48, 465–478.
Pearson, T.H., 1980. The macrobenthos of fjords. In: Freeland, H.J., Farmer, D.M., Levings, C.D. (Eds.), Fjord Oceanography. Plenum Press, New York, pp. 569–603.
Peng, T.H., Broecker, W.S., Kipphut, G., Shackleton, N., 1977. Benthic mixing in deep sea cores as determined by 14C dating and its implications regarding climate stratigraphy and the fate of fossil fuel CO2. In: Andersen, N.R., Malahoff, A. (Eds.), The Fate of Fossil Fuel in the Oceans. Plenum Press, New York, pp. 355–373.
Perillo, G.M.E., 1995. Definitions and geomorphic classifications of estuaries. In: Perillo, G.M.E. (Ed.), Geomorphology and Sedimentology of Estuaries. Elsevier Science, New York, pp. 17–47 Developments in Sedimentology 53.
Petticrew, E.L., Alber, S.J., Baldwin, S.A., Carmack, E.C., Déry, S.J., Gantner, N., Graves, K.E., Laval, B., Morrison, J., Owens, P.J., Selbie, D.T., Vagle, S., 2015. The impact of a catastrophic mine tailings impoundment spill into one of North America's largest fjord lakes: Quesnel Lake, British Columbia, Canada. Geophys. Res. Lett. 42, 3347–3355. https://doi.org/10.1002/2015GL063345.
Pfeffer, W.T., 2007. A simple mechanism for irreversible tidewater glacier retreat. J. Geophys. Res. 112, F03S25. https://doi.org/10.1029/2006JF000590.
Pickrill, R.A., 1987. Circulation and sedimentation of suspended particulate matter in New Zealand fjords. Mar. Geol. 74 (1–2), 21–39.
Pickrill, R.A., 1993. Sediment yields in Fiordland. J. Hydrol. 31 (1), 39–55.
Pickrill, R.A., Fenner, J.M., McGlone, M.S., 1992. Late Quaternary evolution of a fjord environment in Preservation Inlet, New Zealand. Quat. Res. 38 (3), 331–346.
Piper, D.J.W., Letson, J.R.J., Delure, A.M., Barrie, C.Q., 1983. Sediment accumulation in low sedimentation, wave dominated, glacial inlets. Sediment. Geol. 36, 195–215.
Piret, L., Bertrand, S., Kissel, C., De Pol-Holz, R., Tamayo Hernando, A., Van Daele, M., 2017. First evidence of a mid-Holocene earthquake-triggered megaturbidite south of the Chile Triple Junction. Sediment. Geol. 375, 120–133. https://doi.org/10.1016/j.sedgeo.2018.01.002.
Piwosz, K., Walkusz, W., Hapter, R., Wieczorek, P., Hop, H., Wiktor, J., 2009. Comparison of productivity and phytoplankton in a warm (Kongsfjorden) and a cold (Hornsund) Spitsbergen fjord in mid-summer 2002. Polar Biol. 32, 549–559.
Powell, R.D., 1990. Glacimarine processes at grounding-line fans and their growth to ice-contact deltas. In: Dowdeswell, J.A., Scorse, J.D. (Eds.), Glaciomarine Environments: Processes and Sediments, pp. 53–73 Geological Society, Special Publication 53.
Prebble, J.G., Hinojosa, J.L., Moy, C.M., 2018. Palynofacies assemblages reflect sources of organic matter in New Zealand fjords. Cont. Shelf Res. 154, 19–25.
Quiroga, E., Ortiz, P., González, R., Tapia, F., Pérez-Santos, I., Rebolledo, L., Reid, B., Mansilla, R., Pineda, C., Cari, I., Salinas, N., Montiel, A., Gerdes, D., 2016. Seasonal patterns in the benthic realm of a glacial fjord (Martinez Channel, Chilean Patagonia): the role of suspended sediment and terrestrial organic matter. Mar. Ecol. Prog. Ser. 56, 31–50.
Ramirez, M.T., Allison, M.A., Bianchi, T.S., Cui, X., Savage, C., Schuller, S.E., Smith, R.W., Vetter, L., 2016. Modern deposition rates and patterns of organic carbon burial in Fiordland, New Zealand. Geophys. Res. Lett. 43, 11,768–11,776. https://doi.org/10.1002/2016GL070021.
Raven, R.M., Sessions, A.L., Adkins, J.F., Thunell, R.C., 2016. Rapid organic matter sulfurization in sinking particles from the Cariaco Basin water column. Geochim. Cosmochim. Acta 190, 175–190.
Rebolledo, L., Sepúlveda, J., Lange, C.B., Pantoja, S., Bertrand, S., Hughen, K., Figueroa, D., 2008. Late Holocene marine productivity changes in Northern Patagonia-Chile inferred from a multi-proxy analysis of Jacaf channel sediments. Estuar. Coast. Shelf Sci. 80, 314–322.
Rebolledo, L., Lange, C.B., Bertrand, S., Muñoz, P., Salamanca, B., Lazo, P., Iriarte, J.J., Vargas, G., Pantoja, S., Dezileau, L., 2015. Late Holocene precipitation variability recorded in the sediments of Reloncaví Fjord (41°S, 72° W). Quat. Res. 84 (1), 21–36.
Rebolledo, L., Bertrand, S., Lange, C.B., Tapia, F.J., Quiroga, E., Troch, M., Silva, N., Cárdenas, P., Pantoja, S., 2019. Compositional and biogeochemical variations of sediments across the terrestrial-marine continuum of the Baker-Martínez fjord system (Chile, 48°S). Progr. Oceanogr. https://doi.org/10.1016/j.pocean.2018.12.004.
Renaud, P.E., Løkken, T.S., Jørgensen, L.L., Berge, J., Johnson, B.J., 2015. Macroalgal detritus and food-web subsidies along an Arctic fjord depth-gradient. Front. Mar. Sci. 2, 31. https://doi.org/10.3389/fmars.2015.00031.
Renner, M., Arimitsu, M.L., Piatt, J.F., 2012. Structure of marine predator and prey communities along environmental gradients in a glaciated fjord. Can. J. Fish. Aquat. Sci. 69, 2029–2045.
Rignot, E., Koppes, M., Velicogna, I., 2010. Rapid submarine melting of the calving faces of West Greenland glaciers. Nat. Geosci. 3 (3), 187–191.
Rivera, A., Koppes, M., Bravo, C., Aravena, J.C., 2012. Little Ice Age advance and retreat of Glacier Jorge Montt, Chilean Patagonia. Clim. Past 8, 403–414.
Rosenberg, R., Olsson, I., Olundh, E., 1977. Energy flow model of an oxygen-deficient estuary on the Swedish west coast. Mar. Biol. 42, 99–107.
Rudy, A.C.A., Lamoureux, S.F., Kokelj, S.V., Smith, I.R., England, J.H., 2017. Accelerating thermokarst transforms ice-cored terrain triggering a downstream cascade to the ocean. Geophys. Res. Lett. 44, 11,080–11,087.
Rysgaard, S., Nielsen, T.G., 2006. Carbon cycling in a high-arctic marine ecosystem – Young Sound, NE Greenland. Prog. Oceanogr. 71 (2–4), 426–445. https://doi.org/10.1016/j.pocean.2006.09.004.
Rysgaard, S., Finster, K., Dahlgaard, H., 1996. Primary production, nutrient dynamics and mineralisation in a northeastern Greenland fjord during the summer thaw. Polar Biol. 16, 497–506.
Rysgaard, S., Vang, T., Stjernholm, M., Rasmussen, B., Windelin, A., Kiilsholm, S., 2003. Physical conditions, carbon transport and climate change impacts in a NE Greenland fjord. Arct. Antarct. Alp. Res. 35, 301–312.
Rysgaard, S., Mortensen, J., Juul-Pedersen, T., Sørensen, L.L., Lennert, K., Søgaard, D.H., Arendt, K.E., Blicher, M.E., Sejr, M.K., Bendtsen, J., 2012. High air–sea CO_2 uptake rates in nearshore and shelf areas of Southern Greenland: temporal and spatial variability. Mar. Chem. 128–129, 26–33. https://doi.org/10.1016/j.marchem.2011.11.002.
Sahade, R., Lagger, C., Torre, L., Momo, F., Monien, P., Schloss, I., Barnes, D.K.D., Servetto, N., Tarantelli, S., Tatián, M., Zamboni, N., Abele, D., 2015. Climate change and glacier retreat drive shifts in an Antarctic benthic ecosystem. Mar. Ecol. 1 (10), e1500050. https://doi.org/10.1126/sciadv.1500050.
Sakshaug, E., Myklestad, S., 1973. Studies on the phytoplankton ecology of the trondheimsfjord. III. Dynamics of phytoplankton blooms in relation to environmental factors, bioassay experiments and parameters for the physiological state of the populations. J. Exp. Mar. Biol. Ecol. 11 (2), 157–188.
Salvado, J.A., Tesi, T., Andersson, A., Ingri, J., Dudarev, O.V., Semiletov, I.P., Gustafsson, O., 2015. Organic carbon remobilized from thawing permafrost is resequestered by reactive iron on the Eurasian Arctic Shelf. Geophys. Res. Lett. 42, 8122–8130. https://doi.org/10.1002/2015GL066058.
Sarkanen, K.V., Ludwig, C.H., 1971. Lignins. Wiley-Inter-science (916 pp).
Schafer, C.T., Cole, F.E., Syvitski, J.P.M., 1989. Bio and lithofacies of modern sediments in Knight and Bute Inlets, B.C. Palaios 4, 107–126.
Schiffelbein, P., 1984. Effect of benthic mixing on the information content of deep- sea stratigraphical signals. Nature 311, 651–653.
Schirrmeister, L., Grosse, G., Wetterich, S., Overduin, P.P., Strauss, J., Schuur, E.A., Hubberten, H.W., 2011. Fossil organic matter characteristics in permafrost deposits of the northeast Siberian Arctic. J. Geophys. Res. Biogeosci. 116, G00M02.
Schuller, S.E., Savage, C., 2011. Spatial distribution of diatom and pigment sedimentary records in surface sediments in Doubtful Sound, Fiordland, New Zealand. N. Z. J. Mar. Freshw. Res. 45 (4), 591–608.
Schüller, S.E., Allison, M.A., Bianchi, T.S., Tian, F., Savage, C., 2013. Historical variability in past phytoplankton abundance and composition in Doubtful Sound, New Zealand. Cont. Shelf Res. 69, 110–122.
Schuller, S.E., Bianchi, T.S., Li, X.X., Allison, M.A., Savage, C., 2015. Historical reconstruction of phytoplankton composition in Estuaries of Fiordland, New Zealand: the application of plant pigment biomarkers. Estuar. Coasts 38 (1), 56–71.
Seager, R., Battisti, D.S., Yin, J., Gordon, N., Naik, N., Clement, A.C., Cane, M.A., 2002. Is the Gulf Stream responsible for Europe's mild winters? Q. J. R. Meteorol. Soc. 128 (586), 2563–2586.
Sepúlveda, J., Pantoja, S., Hughen, K., Lange, C., Gonzalez, F., Muñoz, P., Rebolledo, L., Castro, R., Contreras, S., Ávila, A., 2005. Fluctuations in export productivity over the last century from sediments of a southern Chilean fjord (44 S). Estuar. Coast. Shelf Sci. 65, 587–600.
Sepúlveda, J., Pantoja, S., Hughen, K.A., Bertrand, S., Figueroa, D., Leon, T., Drenzek, N.J., Lange, C., 2009. Late Holocene Sea-surface temperature and precipitation variability in northern Patagonia, Chile (Jacaf Fjord, 44^0S). Quat. Res. 72, 400–409.
Sepúlveda, J., Pantoja, S., Hughen, K.A., 2011. Sources and distribution of organic matter in northern Patagonia fjords, Chile (~44-47°S): a multi-tracer approach for carbon cycling assessment. Cont. Shelf Res. 31 (3–4), 315–329.
Serikova, S., Pokrovsky, O.S., Ala-Aho, P., Kazantsev, V., Kirpotin, S.N., Kopysov, S.G., Krickov, I.V., Laudon, H., Manasypov, R.M., Shirokova, L.S., Soulsby, C., Tetzlaff, D., Karlsson, J., 2018. High riverine CO_2 emissions at the permafrost boundary of Western Siberia. Nat. Geosci. https://doi.org/10.1038/s41561-018-0218-1.
Sharp, M., Tranter, M., 2017. Glacier Biogeochemistry. Geochemical Perspectives 6 (2), 173–339.
Shields, M.R., Bianchi, T.S., Mohrig, D., Kenney, W.H., Kolker, A.S., Curtis, J.S., 2017. Ecosystem engineering builds coastline and stores blue carbon in the Mississippi River delta complex. Nat. Geosci. 10, 846–851.
Shindell, D.T., Miller, R.L., Schmidt, G.A., Pandolfo, L., 1999. Simulation of recent northern winter climate trends by greenhouse gas forcing. Nature 399, 452–455.
Silva, N., Vargas, C.A., 2014. Hypoxia in Chilean patagonian fjords. Prog. Oceanogr. 129, 62–74.
Silva, N., Vargas, C.A., Prego, R., 2011. Land–ocean distribution of allochthonous organic

matter in surface sediments of the Chiloé and Aysén interior seas (Chilean Northern Patagonia). Cont. Shelf Res. 31 (3–4), 330–339.
Silverberg, N., Sundby, B., Mucci, A., Zhong, S., Arakaki, T., Hall, P., LandeHn, A., Tengberg, A., 2000. Remineralization of organic carbon in eastern Canadian continental margin sediments. Deep-Sea Res. II 47 (3–4), 699–731. https://doi.org/10.1016/S0967-0645(99)00123-X.
Skaala, Ø., Sjøtun, K., Dahl, E., Vivian, H., Bjørge, A., Uiblein, F., 2014. Interactions between salmon farming and the ecosystem: l-essons from the Hardangerfjord, western Norway. Mar. Biol. Res. 10 (3), 199–202. https://doi.org/10.1080/17451000.2013.840730.
Skarðhamar, J., Svendsen, H., 2010. Short-term hydrographic variability in a stratified Arctic fjord. Geol. Soc. Lond., Spec. Publ. 344 (1), 51. https://doi.org/10.1144/SP344.5.
Skei, J., 1983. Why sedimentologists are interested in Fjords. Sediment. Geol. 36 (2–4), 75–80.
Skidmore, M., Anderson, S.P., Sharp, M.J., Foght, J.M., Lanoil, B.D., 2005. Comparison of microbial community composition in two subglacial environments reveals a possible role for microbes in chemical weathering processes. Appl. Environ. Microbiol. 71 (11), 6986–6997.
Smeaton, C., Austin, W.E.N., 2017. Sources, sinks, and subsidies: terrestrial carbon storage in mid-latitude fjords. J. Geophys. Res. Biogeosci. 122, 2754–2768. https://doi.org/10.1002/2017JG003952.
Smeaton, C., Austin, W.E.N., 2019. Where's the carbon: exploring the spatial heterogeneity of Sedimentary carbon in mid-latitude Fjords. Front. Earth Sci. 7, 269. https://doi.org/10.3389/feart.2019.00269.
Smeaton, C., Austin, W.E.N., Davies, A.L., Baltzer, A., Abell, R.E., Howe, J.A., 2016. Substantial stores of sedimentary carbon held in mid-latitude fjords. Biogeosciences 13, 5771–5787. https://doi.org/10.5194/bg-13-5771-2016.
Smeaton, C., Austin, W.E.N., Davies, A.L., Baltzer, A., Howe, J.A., Baxter, J.M., 2017. Scotland's forgotten carbon: a national assessment of mid-latitude fjord sedimentary carbon stocks. Biogeosciences 14, 5663–5674. https://doi.org/10.5194/bg-14-5663-2017.
Smith, L.M., Andrews, J.T., 2000. Sediment characteristics in iceberg dominated fjords, Kangerlussuaq region, East Greenland. Sediment. Geol. 130, 11–25.
Smith, J.N., Walton, A., 1980. Sediment accumulation rates and geochronologies measured in the Saguenay Fjord using the Pb-210 dating method. Geochim. Cosmochim. Acta 44 (2), 225–240.
Smith, L.M., Alexander, C., Jennings, A.E., 2002. Accumulation in East Greenland fjords and on the continental shelves adjacent to the Denmark strait over the last century based on Pb-210 geochronology. Arctic 55 (2), 109–122.
Smith, R.W., Bianchi, T.S., Savage, C., 2010. Comparison of lignin phenols and branched/isoprenoid tetraethers (BIT index) as indices of terrestrial organic matter in Doubtful Sound, Fiordland, New Zealand. Org. Geochem. 41 (3), 281–290.
Smith, R.W., Bianchi, T.S., Allison, M., Savage, C., Galy, V., 2015. High rates of organic carbon burial in fjord sediments globally. Nat. Geosci. 8 (6), 450–U46.
Smittenberg, R.H., Hopmans, E.C., Schouten, S., Hayes, J.M., Eglinton, T.I., Sinninghe Damste, J.S., 2004a. Compound-specific radiocarbon dating of the varved Holocene sedimentary record of Saanich Inlet, Canada. Paleoceanography 19.
Smittenberg, R.H., Pancost, R.D., Hopmans, E.C., Paetzel, M., Damste, J.S.S., 2004b. A 400-year record of environmental change in an euxinic fjord as revealed by the sedimentary biomarker record. Palaeogeogr. Palaeoclimatol. Palaeoecol. 202 (3–4), 331–351.
Smittenberg, R.H., Baas, M., Green, M.J., Hopmans, E.C., Schouten, S., Damsté, J.S., 2005. Pre-and post-industrial environmental changes as revealed by the biogeochemical sedimentary record of Drammensfjord, Norway. Mar. Geol. 214, 177–200.
Sole, A., Nienow, P., Bartholomew, I., Mair, D., Cowton, T., Tedstone, A., King, M.A., 2013. Winter motion mediates dynamic response of the Greenland Ice sheet to warmer summers. Geophys. Res. Lett. 40, 3940–3944. https://doi.org/10.1002/grl.50764.
Sørensen, H.L., Meire, L., Juul-Pedersen, T., de Stigter, H.C., Meysman, F.J.R., Rysgaard, S., Thamdrup, B., Glud, R.N., 2015. Seasonal carbon cycling in a Greenlandic fjord: an integrated pelagic and benthic study. Mar. Ecol. Prog. Ser. 539, 1–17. https://doi.org/10.3354/meps11503.
Stanton, B.R., Pickard, G.L., 1981. Physical oceanography of the New Zealand fiords. New Zealand Oceanogr. Inst. Mem. 88, 1–36.
Sternal, B., Junttila, J., Skirbekk, K., Forwick, M., Carroll, J., Pedersen, K.B., 2017. The impact of submarine copper mine tailing disposal from the 1970s on Repparfjorden, northern Norway. Mar. Pollut. Bull. 120 (1–2), 136–153.
Stibal, M., Tranter, M., 2007. Laboratory investigation of inorganic carbon uptake by cryoconite debris from Werenskioldbreen, Svalbard. J. Geophys. Res. 112, G04S33. https://doi.org/10.1029/2007JG000429.
Stibal, M., Telling, J., Cook, J., Mak, K.M., Hodson, A., Anesio, A.M., 2012. Environmental controls on microbial abundance and activity on the Greenland ice sheet: a multivariate analysis approach. Microb. Ecol. 63, 74–84.
Stibal, M., Box, J.E., Cameron, K.A., Langen, P.L., Yallop, M.L., Mottram, R.H., Khan, A.L., Molotch, N.P., Chrismas, N.A.M., Calì Quaglia, F., Remias, D., Paul Smeets, C.J.P., van den Broeke, M.R., Ryan, J.C., Hubbard, A., Tranter, M., van As, D., Ahlstrøm, A.P., 2017. Algae drive enhanced darkening of bare ice on the Greenland ice sheet. Geophys. Res. Lett. 44, 11463–411471.
St-Onge, G., Hillaire-Marcel, C., 2001. Isotopic constraints of sedimentary inputs and organic carbon burial rates in the Saguenay Fjord, Quebec. Mar. Geol. 176, 1–22.
St-Onge, G., Mulder, T., Piper, D.J., Hillaire-Marcel, C., Stoner, J.S., 2004. Earthquake and flood-induced turbidites in the Saguenay Fjord (Québec): a Holocene paleoseismicity record. Quat. Sci. Rev. 23 (3), 283–294.
Storms, J.E., de Winter, I.L., Overeem, I., Drijkoningen, G.G., Lykke-Andersen, H., 2012. The Holocene sedimentary history of the Kangerlussuaq Fjord-valley fill, West Greenland. Quat. Sci. Rev. 35, 29–50.
Straneo, F., Hamilton, G.S., Sutherland, D.A., Stearns, L.A., Davidson, F., Hammill, M.O., Stenson, G.B., Rosing-Asvid, A., 2010. Rapid circulation of warm subtropical waters in a major glacial fjord in East Greenland. Nat. Geosci. 3, 182–186. https://doi.org/10.1038/ngeo764.
Stravers, J.A., Syvitski, J.P.M., 1991. Early Holocene land-sea correlations and deglacial evolution of the Cambridge Fiord basin, Northern Baffin Island. Quat. Res. 35, 72–90.
Stroeve, J., Holland, M.M., Meier, W., Scambros, T., Serreze, M., 2007. Arctic Sea ice decline: Faster than forecast. Geophys. Res. Lett. 34 (9), L09501.
Syvitski, J.P.M., 1989. On the deposition of sediment within glacier-influenced fjords: Oceanographic controls. Mar. Geol. 85, 301–329.
Syvitski, J.P.M., 1993. Glaciomarine environments in Canada: an overview. Can. J. Earth Sci. 30, 354–371.
Syvitski, J.P.M., Farrow, G.E., 1983. Structures and processes in bayhead deltas: Knight and Bute Inlet, British Columbia. Sediment. Geol. 36, 217–244.
Syvitski, J.P.M., Hein, F.J., 1991. Sedimentology of an arctic basin: Itirbilung Fiord, Baffin Island, Northwest Territories. Geological Survey of Canada Paper 91–11, 67 pp.
Syvitski, J.P.M., Lee, H.J., 1997. Paraglacial sequence stratigraphy of Lake Melville, Labrador, during ice-sheet retreat since 10,000 years BP. Mar. Geol. 143, 55–80.
Syvitski, J.P.M., MacDonald, R.D., 1982. Sediment character and provenance in a complex fjord; Howe Sound, British Columbia. Can. J. Earth Sci. 19, 1025–1044.
Syvitski, J.P.M., Schafer, C.T., 1996. Evidence for an earthquake-triggered basin collapse in Saguenay Fjord, Canada. Sediment. Geol. 104, 127–153.
Syvitski, J.P.M., Shaw, J., 1995. Sedimentology and geomorphology of Fjords. In: Perillo, G.M.E. (Ed.), Geomorphology and Sedimentology of Estuaries. Elsevier Publ., pp. 113–178.
Syvitski, J.P.M., Asprey, K.W., Clattenburg, D.A., Hodge, G.D., 1985. The prodelta environment of a fjord: suspended particle dynamics. Sedimentol. 32, 40–65.
Syvitski, J.P.M., Burrell, D.C., Skei, J.M., 1987. Fjords: Processes and Products. Springer-Verlag, N.Y. (379 pp).
Syvitski, J.P.M., LeBlanc, K.W.G., Cranston, R.E., 1990. The flux and preservation of organic carbon in Baffin Island fjords. In: Dowdeswell, J.A., Scourse, J.D. (Eds.), Glaciomarine Environments: Processes and Sediments, pp. 217–239 Geological Society, London, Spec. Publ. 53.
Syvitski, J.P.M., Asprey, K.W., LeBlanc, K.W.G., 1995. In-situ characteristics of particles settling within a deep-water estuary. Deep-Sea Res. II 42 (1), 223–256.
Syvitski, J.P.M., Andrews, J.T., Dowdeswell, J.A., 1996. Sediment deposition in an iceberg-dominated glacimarine environment, East Greenland: basin fill implications. Glob. Planet. Chang. 12, 251–270.
Tissot, B.P., Welte, D.H., 1978. Petroleum Formation and Occurrence. Springer-Verlag (538 pp).
Torres, R., Pantoja, S., Harada, N., González, H.E., Daneri, G., Frangopulos, M., Rutllant, J.A., Duarte, C.M., Rúiz-Halpern, S., Mayol, E., Fukasawa, M., 2011. Air–sea CO_2 fluxes along the coast of Chile: from CO_2 outgassing in central northern upwelling waters to CO_2 uptake in southern Patagonian fjords. J. Geophys. Res. 116, C09006. https://doi.org/10.1029/2010JC006344.
Trannum, H.C., Gundersen, H., Escudero-Oñate, C., Johansen, J.T., Schaanning, M.T., 2018. Effects of submarine mine tailings on macrobenthic community structure and ecosystem processes. Sci. Total Environ. 630, 189–202.
Tranter, M., Brown, G.H., Hodson, A., Gurnell, A.M., 1996. Hydrochemistry as an indicator of subglacial drainage system structure: a comparison of alpine and sub-polar environments. Hydrol. Process. 10, 541–556. https://doi.org/10.1002/(SICI)1099-1085(199604)10:4 < 541::AID-HYP391 > 3.3.CO;2-0.
Truffer, M., Motyka, R.J., 2016. Where glaciers meet water: subaqueous melt and its relevance to glaciers in various settings. Rev. Geophys. 54 (1), 220–239.
Urbanski, J.A., Stempniewicz, L., Węsławski, J.M., Dragańska-Deja, K., Wochna, A., Goc, M., Iliszko, L., 2017. Subglacial discharges create fluctuating foraging hotspots for sea birds in tidewater glacier bays. Sci. Rep. 7, 43999.
Van Daele, M., Versteeg, W., Pino, M., Urrutia, R., De Batist, M., 2013. Widespread deformation of basin-plain sediments in Aysén fjord (Chile) due to impact by earthquake-triggered, onshore generated mass movements. Mar. Geol. 337, 67–79.
Vandekerkhove, E., Bertrand, S., Crescenzi Lanna, E., Reid, B., Pantoja, S., 2020. Modern sedimentary processes at the heads of Martinez Channel and Steffen fjord, Chilean Patagonia. Mar. Geol. 490. https://doi.org/10.1016/j.margeo.2019.106076.
Vanguelova, E.I., Nisbet, T.R., Moffat, A.J., Broadmeadow, S., Sanders, T.G.M., Morison, J.I.L., 2013. A new evaluation of carbon stocks in British forest soils. Soil Use Manag. 29, 169–181. https://doi.org/10.1111/sum.12025.
Vargas, A.A., Martinez, R.A., San Martin, V., Aguayo, M., Silva, N., Torres, R., 2010. Allochthonous subsidies of organic matter across a lake-river-fjord landscape in the Chilean Patagonia: Implications for marine zooplankton in inner fjord areas. Cont. Shelf Res. 31, 187–201.
Velinsky, D.J., Fogel, M.L., 1999. Cycling of dissolved and particulate nitrogen and carbon in the Framvaren Fjord, Norway: stable isotopic variations. Mar. Chem. 67, 161–180.
Vermassen, F., Wangner, D.J., Dyke, L.M., Schmidt, S., Cordua, A.E., Kjær, K.H., Haubner, K., Andresen, C.S., 2019. Evaluating ice-rafted debris as a proxy for glacier calving in Upernavik Isfjord, NW Greenland. J. Quat. Sci. 34, 258–267. https://doi.org/10.1002/jqs.3095.
Vonk, J.E., Sánchez-García, L., Van Dongen, B.E., Alling, V., Kosmach, D., Charkin, A., Eglinton, T.I., 2012. Activation of old carbon by erosion of coastal and subsea permafrost in Arctic Siberia. Nature 489 (7414), 137.
Wadham, J.L., Hawkings, J., Telling, J., Chandler, D., Alcock, J., O'Donnell, E., Kaur, P., Bagshaw, E., Tranter, M., Tedstone, A., Nienow, P., 2016. Sources, cycling and export of nitrogen on the Greenland Ice Sheet. Biogeosciences 13, 6339–6352.
Wadham, J.L., Hawkings, J.R., Tarasov, L.J Gregoire, Spencer, R.G.M., Gutjahr, M.,

Ridgwell, A., Kohfeld, K.E., 2019. Ice sheets matter for the global carbon cycle. Nat Commun 10, 3567.
Waite, A.M., Gustafsson, O., Lindahl, O., Tiselius, P., 2005. Linking ecosystem dynamics and biogeochemistry: sinking fractionation of organic carbon in a Swedish fjord. Limnol. Oceanogr. 50 (2), 658–671.
Walinsky, S.E., Prahl, F.G., Mix, A.C., Finney, B.P., Jaeger, J.M., Rosen, G.P., 2009. Distribution and composition of organic matter in surface sediments of coastal Southeast Alaska. Cont. Shelf Res. 29 (13), 1565–1579.
Walsh, E.M., Ingalls, A.E., Keil, R.G., 2008. Sources and transport of terrestrial organic matter in Vancouver Island fjords and the Vancouver-Washington margin: a multi-proxy approach using d 13Corg, lignin phenols, and the ether lipid BIT index. Limnol. Oceanogr. 53, 1054.
Wassmann, P., 1983. Sedimentation of organic and inorganic particulate material in Lindaspollene, a stratified, land-locked fjord in western Norway. Mar. Ecol. Prog. Ser. 13 (2–3), 237–248.
Wassmann, P., 2011. Arctic marine ecosystems in an era of rapid climate change. Prog. Oceanogr. 90, 1–17.
Wassmann, P., Reigstad, M., 2011. Future Arctic Ocean seasonal ice zones and implications for pelagic-benthic coupling. Oceanography 24, 220–231. https://doi.org/10.5670/oceanog.2011.74.
Wassmann, P., Svendsen, H., Keck, A., Reigstad, M., 1996. Selected aspects of the physical oceanography and particle fluxes in fjords of northern Norway. J. Mar. Syst. 8, 53–71.
Wehrmann, L.M., Formolo, M.J., Owens, J.D., Raiswell, R., Ferdelman, T.G., Riedinger, N., Lyons, T.W., 2014. Iron and manganese speciation and cycling in glacially influenced high-latitude fjord sediments (West Spitsbergen, Svalbard): evidence for a benthic recycling-transport mechanism. Geochim. Cosmochim. Acta 141, 628–655.
Weslawski, J., Legezynska, J., 1998. Glaciers caused zooplankton mortality? J. Plankton Res. 20 (7), 1233–1240.
Węsławski, J., Kendall, M.A., Włodarska-Kowalczuk, M., Iken, K., Kędra, M., Legezynska, J., Sejr, M.K., 2010. Arctic fjord and coastal macrobenthos biodiversity. Mar. Biodivers. 41, 71. https://doi.org/10.1007/s12526-010-0073-9.
Wexels, R.C., Wassmann, P., Olli, K., Arashkevich, E., 2001. Production, retention and export of zooplankton faecal pellets on and off the Iberian shelf, north-west Spain. Prog. Oceanogr. 51 (2–4), 423–442.
Whitehouse, L.E., 1988. Geomorphology of the central Southern Alps, New Zealand: the interaction of plate collision and atmospheric circulation. Geomorphology 69, 105–116.
Wils, K., Van Daele, M., Lastras, G., Kissel, C., Lamy, F., Siani, G., 2018. Holocene event record of Aysén fjord (Chilean Patagonia): an interplay of volcanic eruptions, crustal and megathrust earthquakes. J. Geophys. Res. Solid Earth 123 (1), 324–343. https://doi.org/10.1002/2017JB014573.
Wing, S.R., Leichter, J.J., Perrin, C., Rutger, S.M., Bowman, M.H., Cornelisen, C.D., 2007. Topographic shading and wave exposure influence morphology and ecophysiology of Ecklonia radiata (C. Agardh 1817) in Fiordland, New Zealand. Limnol. Oceanogr. 52 (5), 1853–1864.
Winkelmann, D., Knies, J., 2005. Recent distribution and accumulation of organic carbon on the continental margin west off Spitsbergen. Geochem. Geophys. Geosyst. 6. https://doi.org/10.1029/2005GC000916.
Winters, G.V., Syvitski, J.P.M., 1992. Suspended sediment character and distribution in McBeth Fiord, Baffin Island. Arctic 45, 25–35.
Woulds, C., Bouillon, S., Cowie, G.L., Drake, E., Middelburg, J.J., Witte, U., 2016. Patterns of carbon processing at the seafloor: the role of faunal and microbial communities in moderating carbon flows. Biogeosciences 13 (15), 4343–4357.
Yallop, M.L., Anesio, A.M., Perkins, R.G., Cook, J., Telling, J., Fagan, D., MacFarlane, J., Stibal, M., Barker, G., Bellas, C., 2012. Photophysiology and albedo-changing potentialof the ice algal community on the surface of the Greenland ice sheet. ISME J. 6, 2302–2313.
Yamashita, Y., McCallister, S.L., Koch, B.P., Gonsior, M., Jaffe, R., 2015. Dynamics of dissolved organic matter in fjord ecosystems: Contributions of terrestrial dissolved organic matter in the deep layer. Estuar. Coast. Shelf Sci. 159, 37–49.
Yin, J.H., 2005. A consistent poleward shift of the storm tracks in simulations of 21st century climate. Geophys. Res. Lett. 32, L18701. https://doi.org/10.1029/2005GL023684.
Zaborska, A., Pempkowiak, J., Papucci, C., 2006. Some sediment characteristics and sedimentation rates in an Arctic Fjord (Kongsfjorden, Svalbard). Annu. Environ. Prot. 8, 79–96.
Zaborska, A., Beszczynska-Moller, A., Włodarska-Kowalczuk, M., 2017. History of heavy metal accumulation in the Svalbard area: distribution, origin and transport pathways. Environ. Pollut. 231 (1), 437–450. https://doi.org/10.1016/j.envpol.2017.08.042.
Zaborska, A., Wlodarska-Kowalczuk, M., Legeżyńska, J., Jankowska, E., Winogradow, A., Deja, K., 2018. Sedimentary organic matter sources, benthic consumption and burial in West Spitsbergen fjords – signs of maturing of Arctic fjordic systems? J. Mar. Syst. 180, 112–123. https://doi.org/10.1016/j.jmarsys.2016.11.005.
Zajaczkowski, M., Szczucinski, W., Bojanowski, R., 2004. Recent changes in sediment accumulation rates in Adventfjorden, Svalbard. Oceanologia 46.
Zalasiewicz, J., Waters, C.N., Williams, M., 2014. Human bioturbation, and the subterranean landscape of the Anthropocene. Anthropocene 6, 3–9.
Zimmerman, A.R., Cornelissen, G., 2018. Consider Fjord-assisted carbon storage. Environ. Sci. Technol. 52 (19), 10911–10913. https://doi.org/10.1021/acs.est.8b04854.
Zimov, S., Davydov, S., Zimova, G., Davydova, A., Schuur, E., Dutta, K., Chapin, F., 2006. Permafrost carbon: stock and decomposability of a globally significant carbon pool. Geophys. Res. Lett. 33, L20502.